Gems & Gemology

The quarterly journal of the Gemological Institute of America

Gems & Gemology

CONTENTS

ABOUT THE COVER: The varieties of corundum, especially ruby and sapphire, are among the most highly prized gemstones in the world. The 17.22-ct Sri Lankan blue sapphire illustrated here is a particularly fine example of the material found in nature. Yet the popularity of these stones has also generated many attempts to synthesize them. Two such efforts are described in this issue: the Chatham flux-grown synthetic orange sapphire and synthetic blue sapphire, and Professor P. O. Knischka's synthetic ruby.

The classic baroque-inspired necklace pictured on the cover is accented with 12 brilliant-cut diamonds totaling 2.37 ct. Designed and fabricated (in 18-ct yellow gold) by Kim E. Lilot of St. Eligius European Goldsmiths and Gemologists of San Francisco, it is now in the collection of Kenneth S. Cousens, Inc. Photograph © 1981 Harold and Erica Van Pelt—Photographers, Los Angeles, CA.

Gems&Gemology

GEMSTONES OF PAKISTAN: EMERALD, RUBY, AND SPINEL

By E. J. Gübelin

Only during the last few years have the gem riches of Pakistan become known to the rest of the world. This article reports on three gem materials currently being mined: emerald, corundum (most importantly, ruby), and spinel. Intensely colored emerald crystals occur in dolomitic talc schists in the Swat Valley. Unusually high optical properties and density serve to distinguish these emeralds from those found elsewhere. Numerous gas-liquid inclusions are also typical. In the Hunza Valley, specimen- and gem-quality crystals of corundum and spinel occur in beds of marble enclosed in gneisses and mica schists. The gemological properties of the Pakistan rubies and sapphires vary only slightly within normal limits.

ABOUT THE AUTHOR

Dr. Gübelin is a certified gemologist in Meggen, Switzerland, and honorary professor at the University of Stellenbosch, South Africa.

The gem industry of Pakistan is still in its infancy and contributes less than 1% to the national product, with a total annual production reported in the late 1970s to be just over one million dollars. However, much progress has been made recently, and the geology of the country is now known and has been mapped in great detail. Whereas in 1948 only five resource minerals were known to exist in any quantity, today at least 16 minerals, including some gem materials, are known to occur in large reserves and are under production. Even the most cautious experts concede that with more intensive exploration the gem industry will improve greatly.

A remarkable variety of gemstones occur in Pakistan; the most important are emerald from the Swat Valley (Northwest Frontier Province) and ruby and spinel from the Hunza Valley (northeast of the Swat area). Also notable are pink topaz from Katlang near Mardan, a city north of Peshawar, and aquamarine from Dassu near Skardu, the capital of Baltistan Province. Sapphire, jade, quartz (including amethyst), lapis lazuli, and some ornamental stones have also been found. This report, however, will focus on the emeralds, rubies, and spinels that occur in Pakistan, particularly the major deposits and geology, current mining and cutting operations, and the properties of the Pakistan stones. Figure 1 provides a locality map for this area; the reader is referred to Qasim and Khan Tahirkheli (1969) for a detailed geological map of the region.

PART I
THE SWAT VALLEY EMERALDS

In 1958, goatherds found a few green crystals on the slopes of a hill north of Mingora and brought them to their reigning sovereign, Prince Miamgul Jahanzeb. Not recognizing the stones, the prince showed them to some visitors from Bombay, who promptly identified them as

Figure 1. Location map for the Swat Valley emerald deposits (green) and the Hunza Valley ruby and spinel deposits (red) in northern Pakistan. Map drawn by Peter Johnston.

emeralds. At once the prince declared the hill forbidden territory and engaged workmen to search the surface for more crystals. It is unlikely that the prince gained much wealth from these amateurish efforts, which continued until Pakistan abolished its feudal system in 1968. For the next several years, mining was placed under the charge of the Industrial Development Corporation of Pakistan. The latter then relinquished this responsibility to the Mineral Development Corporation of Pakistan, which operated the mines—still small in scope and with little professional guidance—for two more years. In February 1979, however, the Gemstone Corporation of Pakistan was formed and immediately began to reorganize mining according to modern principles, with professional engineers and geologists placed on the permanent staff. All of the mines currently are owned by the state. A special permit is required to visit them.

The deposits that have been prospected and worked to date lie in an emerald-bearing belt of rocks bordering the Swat Valley on the east, along the flanks of the Hindu Kush foothills. This belt stretches from the town of Mingora northeast through Charbagh, Makhad, Malam, Gujar Kili,

and Bazarkot to Bar Kotkai, for a distance of about 32 km. The area is covered by a broad amphibolitic green-schist outcrop that extends from the Afghanistan border in a northerly direction to the bend of the Indus River.

Mines are now being worked near Mingora (Saidu) as well as near Gujar Kili and Makhad on both sides of the Shangla Pass. The first-named area, the largest of the three, is located about 1.5 km north of Mingora (34°47'N, 72°22'E). The 180 acres that it covers are enclosed by barbed-wire fencing and controlled by seven watchtowers. Three large mines are being worked within the compound; figure 2 shows the view of Swat Valley from Mine 1.

GEOLOGY
The emerald-bearing rocks overlie a dark mica schist and are covered by a lighter, green chlorite-tremolite schist; the latter is further overlain by amphibolites along a tectonic shear zone (see figure 3). The emerald-bearing formation consists of dolomitic talc schist that normally reaches a thickness of about 50 m. Strongly folded and fractured lenses of ultramafic and talc-carbonate rocks are intercalated in the shear zone.
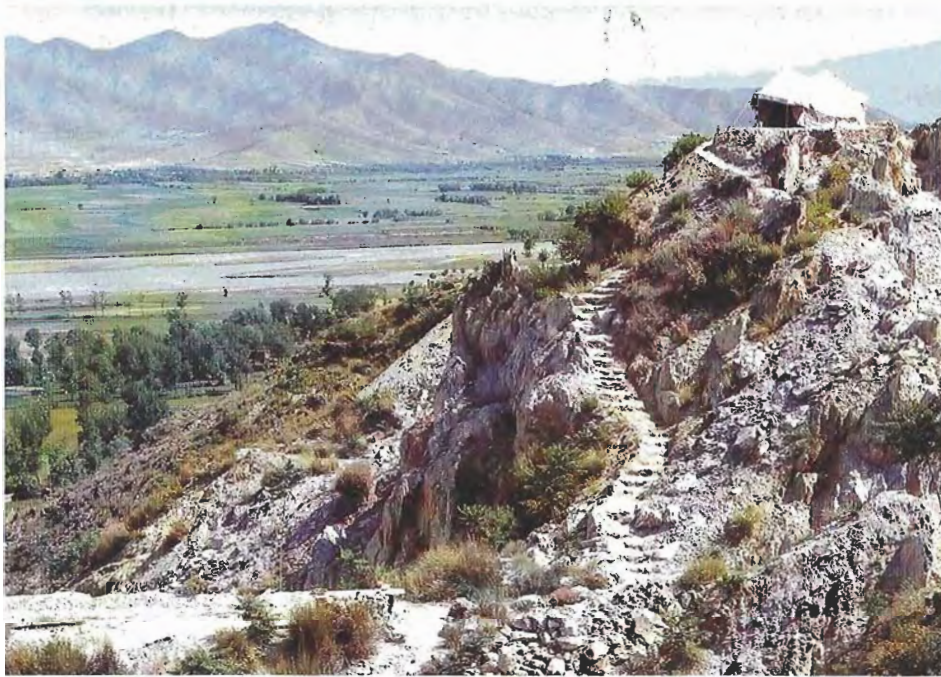
Figure 2. View across the Swat Valley from one of the dumps of emerald mine no. 1. The mountains in the background are the eastern foothills of the Hindu Kush Range.
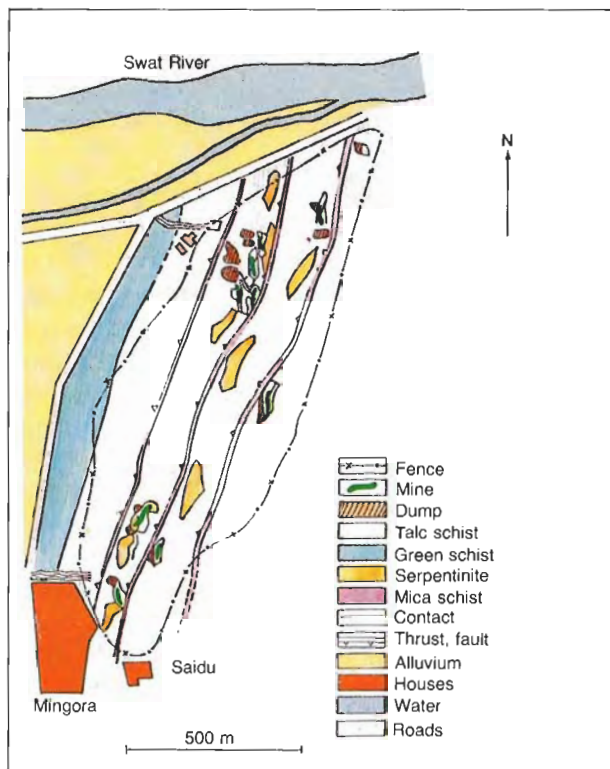
Figure 3. Geology and location of mines in the well-guarded emerald-mining area to the north of Mingora. The map shows that the three separate mining complexes now under operation are situated within the dolomitic talc-schist belt, which itself is sporadically penetrated by serpentinites.

The green chlorite-tremolite schist grades into the talc schist beneath. The thickness of the talc schist has been affected by rock movements such that some portions are considerably thinner than others. An abrupt break is noted between this formation and the underlying dark mica schist, which consists primarily of a dark gray mica containing layers of quartz and some dark gray limestone. Farther below appear arenaceous, argillaceous, and calcareous sedimentary rocks, then older ultramafic dikes of amphibolites near the bottom, and, finally, a younger intrusion of granodiorite. This succession was named the Boner schistose group by early miners and has been observed everywhere in Swat, broadly domed by a coarse-grained granite intrusion. This doming was followed by severe thrusting, which resulted in the slicing and repetition of the deposits; at least four such episodes have been noted. In the region of the Mingora mines, the schists are almost vertical.

Consequently, the talc schist that hosts the emerald is intruded by a series of serpentinized ultramafic dikes and, as a result of the thrusting, has been repeated at least four times. The uppermost slice seems barren of emeralds, presumably because it lacks the quartz veins that characterize the lower beds, interlinked with pockets of calcite. The quartz and calcite combination becomes more abundant in the lower portions. It is speculated by the author and Dr. M. Weibel, on

the basis of the author's thin sections, that the quartz-calcite-beryl mineralization is hydrothermal, originating from a granodiorite which accompanies the talc schist along its entire prospected length. The chromium necessary for coloration of the emerald probably was incorporated in these ascending solutions as they passed through the ultramafic rocks that have now been altered into serpentinites.

Within the mineralized zones, emerald occurs in pockets that are associated with veins consisting of quartz, calcite, and talc. Emeralds found in the quartz are usually broken, but those embedded in the adjacent, softer, carbonate-talc schist are normally intact and euhedral. The carbonate in the schist is ankerite; this, because of its iron content, commonly alters to limonite, which fills relict rhombohedral cavities.

In summary, the Swat Valley emerald deposits represent a classic example of schist-type beryl-emerald mineralization in which the beryl and other minerals normally found in an acidic environment have been hydrothermally derived from granitic rocks and deposited in host schists after passage through basic rocks which provide the chromium necessary to color the beryl. The role of strong tectonic movements in deforming rocks and opening passages for ascending hydrothermal solutions is evident.

MINING

Under the Gemstone Corporation of Pakistan, the mines are worked scientifically; each has on staff a geologist and a mining engineer who are responsible for providing continuity and ensuring the success of the operation. With the improvements in mining practices that the Gemstone Corporation has brought about, the mines are now safer for the workers and promise to produce more and better emeralds.

All mines are open pit (figure 4). The three individual pits in the Mingora area, designated Mines 1, 2, and 3, will eventually be joined as the terraces are extended laterally into a single excavation covering the entire hillside. In the mining operation, barren rock is first removed by drilling and blasting; as the productive areas are reached, however, the emerald-bearing rock is dislodged with pneumatic picks to avoid unnecessary breakage of crystals.

The following serve as guides to the productive areas in the Swat Valley:

Figure 4. Highest section of mining complex no. 1. At the top, the last portion of a terrace is being broken down.

A. Broad, sheared zones, red-brown as a result of the leaching of ferruginous minerals, are conducive to emerald mineralization. Emeralds occur embedded in soft white lumps of talc, and quartz veins are always present (figure 5). The crystals are euhedral for the most part and possess a magnificent color (figure 6), but they are rarely larger than one carat.

B. Intruded seams of quartz/dolomite/calcite, with or without pale green talc, occasionally contain emeralds.

C. Contact zones between the talc schists and the mica schists, the serpentinite, and the pale green talc schist (which is harder and more compact in texture) also contain emerald crystals. It appears that cavities and cracks formed between these rock types by tectonic movements permitted the subsequent introduction of hydrothermal mineralized solutions. Quartz and ankerite are abundant in such zones.

Disposal of waste rock remains a problem at the mines; the present system uses mine-carts that are loaded manually. If production is to be increased in the future, modern, mechanized equipment will be essential.

EMERALD RECOVERY AND CUTTING

The emerald-bearing rock is broken up with hand hammers, and the crystals are placed in small, padlocked boxes. These are sent to the sorting house, with the suitable rough then going to the lapidary shops that belong to the Gemstone Cor-

Figure 5. Miners working along a contact zone at the innermost section of a ditch.

Figure 6. Slightly bent and partly broken emerald crystals (the largest is 1.5 cm long) accompanied by schorl crystals in quartz. The yellowish brown part is dolomite (ankerite).

poration. According to quality, the stones are either cut into cabochons or faceted into baguettes, drops, squares, or brilliants. At a glance, the poorer-quality stones can scarcely be distinguished from lesser-quality emeralds from other sources, but the best grades are remarkable for their lively, unblemished transparency and their deep green hue. The best Swat Valley stones easily vie in this respect with fine-quality emeralds from Muzo, Colombia.

PROPERTIES OF SWAT VALLEY EMERALDS

Color. Using DIN color chart 6164, the best comparative colors of the lighter and darker hues are: X_c 15.5; Y_c 25.7; Z_c 14.0, resp. X_c 16.2; Y_c 25.1; Z_c 21.2. The author was shown a 60-ct lot of faceted stones of choice color from which he was able to sort out only 5 ct of inferior quality. The best were of good to excellent quality and outstanding in terms of transparency and vivid, saturated hue. The best Swat Valley stones were reminiscent of fine Muzo material, while the poorer-quality stones resembled more the lifeless, cloudy emeralds of the Transvaal. The intensity of hue is believed to be due to the high content of chromium and iron. Crystals of over one carat are relatively rare, while those of two or more carats are considered extraordinary.

Chemical Analysis. In view of the fact that the principal elements of natural emerald are known, only transition elements that may be responsible for coloration were analyzed by means of the elec-

tron microprobe. Table 1 compares the results for the Swat Valley emeralds with complete and partial analyses of emeralds from other sources.

The quantities of trace elements may be significant in aiding identification of emeralds from specific deposits, and, as is evident from table 1, impressively large amounts of chromium and iron are present in the Swat Valley emeralds, whereas vanadium appears to be entirely absent. There seems little doubt that the chromium and iron are responsible not only for the color but also for the special physical properties, which are described below. The high iron content tends to subdue the fluorescence normally inherent to chromium, while the presence of typically large amounts of MgO (2.6%) and Na_2O (2.1%) is also noteworthy.

Optical Properties and Density. Tests for density, transparency to short-wave ultraviolet radiation, luminescence, and behavior under various filters were conducted on a lot of 70 stones, with results tallying well with observations on preselected larger stones, of which seven were chosen for detailed testing. The latter ranged in weight from 0.51 ct to 2.34 ct and were consistently outstanding in clarity and color. Birefringence was 0.007 for all the stones, all showed distinct bluish green to yellowish green dichroism, all were inert to long-wave (365 nm) and short-wave (253.7 nm) radiation, and opaque under ultraviolet radiation. The minor variations in their properties are furnished in table 2. The fact that only minimal vari-

TABLE 1. Chemical analyses, given in weight percentages, of emeralds from various deposits.

Oxide	Zambia (Miku) 1[a]	Zimbabwe (Sandawana) 2[b]	3[c]	Pakistan (Mingora) 4[c]	Brazil (Salininha) 5[c]	6[c]	Colombia (Muzo) 7[d]	8[d]	9[d]	Mozambique (Morrua) 10[c]	11[c]	12[c]	Tanzania (Lake Manyara) 13[d]	14[d]	15[d]	16[d]
SiO_2	62.23	63.84	65.0	n.d.[e]												
Al_2O_3	15.41	18.06	14.2	n.d.												
Cr_2O_3	0.33	0.60	0.50	0.66	<0.03	0.21	0.9	0.01	0.03	0.24[f]	1.20	1.3	0.12	0.03	0.44	0.10
V_2O_3	n.d.	n.d.	n.d.	0.00	<0.03	0.36	0.9	0.01	0.03	0.07	0.08	0.09	less than 10 ppm			
Fe_2O_3	0.04		0.50	0.9	<0.03	0.31	0.8	0.01	0.03	1.30	1.40	1.40	0.31	0.36	0.86	0.50
FeO	0.07	0.3		n.d.												
BeO	11.9	13.28	13.6	n.d.												
MnO	0.02			n.d.												
MgO	0.75	0.75	3.0	2.6												
CaO	0.31			0.0												
Na_2O	2.63	2.03	2.0	2.1				1.15	0.05				0.59	0.62	0.57	0.67
K_2O	2.89	0.05		n.d.												
Li_2O		0.10	0.15	n.d.				0.06					0.028	0.026	0.032	0.032
Cs_2O	traces			n.d.				0.20					0.265	0.23	0.16	0.23
H_2O+	2.59	1.07		n.d.				1.9	0.5							
H_2O-	0.06			n.d.												

[a]*Analysis by Hickman (1972).*
[b]*Analysis by Martin (1962).*
[c]*Stones 3–6 and 10–12 were analyzed especially for the author by M. Weibel (Professor Doctor at the Federal Institute for Crystallography and Petrology, Zurich, Switzerland).*
[d]*Stones 7–9 and 13–16 were analyzed especially for the author by E. Landais (Doctor at CCR Euratom, Ispra, Italy).*
[e]*n.d. = not determined; blank spaces mean zero weight percent in those stones analyzed especially for the author and are presumed to mean the same for the other analyses reported here.*
[f]*This value is evidently too low, because chromium is unevenly distributed.*

ations occur suggests that the mean values provided below are diagnostic for emeralds from this source.

Refractive indices were determined with sodium light (589.3 nm) on a Rayner spinel-prism refractometer with an extended scale that permitted an exact reading to the third decimal place with an error of ±0.0005. The seven stones mentioned provided mean values of $n_\epsilon = 1.5905$ and $n_\omega = 1.5975$. n_Δ (biref.) = 0.007. The mean data on the 70 specimens are: $n_\epsilon = 1.588$ and $n_\omega = 1.596$. n_Δ (biref.) = 0.007. The birefringence proved to be remarkably consistent in value and at 0.007 is very high for emeralds of gem quality.

Density was measured in ethylene dibromide using a hydrostatic balance. Values between 2.75 and 2.78 were furnished, with a frequency mean of 2.777 g/cm³.

A look at table 3, which compares the constants for Swat Valley emeralds with those reported for emeralds from other sources, confirms that the refractive index, birefringence, and density of the Swat Valley stones are unusually high for emerald. Since these property values appear to be diagnostic, they should be useful for separating

these stones from other emeralds. However, the other optical properties provided in table 2 and discussed below are typical of emeralds from other deposits as well.

The dichroism is distinct, yet not intense, and alternates between bluish green parallel to the c-axis and yellowish green parallel to the a-axes.

On the whole, the absorption spectrum contains normal chromium absorption lines in the red region at 683, 680, 662, 646, and 637 nm, as well as expected iron absorption lines in the blue region at 477.4 and 472.5 nm (figure 7). However, the unusually high iron content results in an additional absorption feature, namely, a band in the blue at 425–430 nm, with absorption maximum at 427 nm, which was first reported by Kane (1980/81) but with no mention of the provenance of the emerald. Since this absorption band was consistently present in the Swat Valley emeralds tested, it is a welcome additional means of distinguishing these stones.

Swat Valley emeralds glow light red to red under the Chelsea filter and glow red to orange in the Stokes fluoroscope (double filter method).

TABLE 2. Physical properties of Swat Valley emeralds.[a]

Stone (ct)	R.I.	S.G.	Absorption[b] (in nm)	Chelsea filter	Stokes fluoroscope (double filter)	Inclusions
0.51	1.598 1.591	2.75	683 d 662 d 646 d 620–590 w 425–430 d	Distinct reddish to pinkish red	Orange-red	Healing cracks, liquid tubes, liquid films, zoned banding
1.18	1.597 1.590	2.78	683 d 662 d 646 d 630–590 w 425–430.5 s	Pinkish red to reddish	Orange-red to bright red	Two-phase inclusions, zoned banding, step-like growth lines, liquid droplets
1.22	1.595 1.588	2.78	683 s 646 s 637 s 662 s 630–590 w 425–430 d	Distinct pinkish red to reddish	Distinct reddish	Hair-fine, partly hexagonal liquid films; jagged growth defects and two-phase inclusions
1.40	1.600 1.593	2.78	683 s 662 wk 637 d 630–590 w s 425–430.5 s	Pinkish red to reddish; distinct to strong	Reddish; distinct to strong	Healing cracks with two-phase inclusions; fine, oriented tubelets; color zones and zoned banding
1.60	1.597 1.590	2.76	683 s 680 wk 662 d 646–637 s 625–590 425–430.5 s	Distinct reddish	Distinct reddish	Very fine channels; two-phase inclusions in the basal plane
1.87	1.595 (cabochon)	2.77	683 s 680 d 646 d 637 d 630–590 w 425–430 d	Distinct pinkish red to reddish	Weak to distinct reddish	Two-phase inclusions, jagged two-phase inclusions, step-like growth edges
2.34	1.600 1.593	2.76	683 s 662 w 646 d 637 d 625–590 w 477.4 wk 425–430.5 s	Distinct reddish to pinkish red	Distinct reddish	Two-phase inclusions; color banding and zoned structure, step-like growth edges

[a] Birefringence was 0.007 for all the stones; all showed distinct bluish green to yellowish green dichroism; all were inert to long-wave (365 nm) and short-wave (253.7 nm) ultraviolet radiation, and opaque to ultraviolet transparency.
[b] d = distinct, w = wide, s = strong, wk = weak.

They do not react to either short- or long-wave ultraviolet radiation, while short-wave ultraviolet radiation (253 nm) is completely absorbed. The lack of luminescence and the short-wave absorption is due to the high iron content.

Inclusions. Inclusions in these emeralds present peculiarities that are primarily useful in enabling distinction of these stones from synthetic emeralds, but in many instances they also indicate source.

To the unaided eye, the filamental inclusions in the Swat Valley emeralds studied seem similar to the "jardin" of natural emeralds, but the wavy liquid "feathers" somewhat resemble the wispy inclusions commonly associated with synthetic emeralds. Inexperienced persons could easily misinterpret the entire inclusion scene in Pakistan

TABLE 3. Optical constants and densities of emeralds from various deposits.[a]

Country and deposit	n_ϵ	n_ω	Biref.	Density	No. of samples
Australia					
Poona	1.572	1.578	0.005–0.007	2.693	3
Brazil					
Bahia					
Anagé	1.576	1.584	0.008	2.80	1
Brumado	1.573	1.579	0.005–0.006	2.682	3
Carnaiba	1.583	1.588	0.006–0.007	2.72	3
Salininha, Pilao Arcado	1.583	1.589	0.006	2.70	1
Minas Gerais					
Unspecified localities	1.576	1.581	0.005–0.006	2.76	2
	1.572	1.578	0.006	2.705	6
Itabira	1.580	1.589	0.009	2.725	4
India					
Ajmer	1.585	1.595	0.007	2.735	10
Colombia					
Burbar	1.569	1.576	0.007	2.704	1
Chivor	1.570	1.579	0.005–0.006	2.688	12
Muzo	1.570	1.580	0.005–0.006	2.698	11
Mozambique					
Morrua (Melela)	1.585	1.593	0.008	2.73	8
Norway					
Eidsvold	1.590	1.583	0.007	2.759	5
Austria					
Habachtal	1.584	1.591	0.007	2.734	11
	(1.576)	(1.582)	(0.006)		
Pakistan					
Mingora	1.588	1.596	0.007	2.777	70
Zambia					
Miku	1.582	1.589	0.007–0.008	2.738	8
Kafubu (Bank, 1980)	1.592	1.602	0.010	2.77	1
Zimbabwe					
Mayfield	1.584	1.590	0.006	2.72	2
Sandawana	1.584	1.590	0.006	2.75	12
Tanzania					
Lake Manyara	1.578	1.585	0.006	2.72	20
Union of South Africa					
Gravelotte (Transvaal)	1.583	1.594	0.006–0.007	2.75	9
USSR					
Takowaya (Ural, Sverdlovsk)	1.580	1.588	0.006–0.007	2.74	5
U.S.A.					
North Carolina	1.581	1.588	0.007	2.73	1

[a]*These data have been specially checked by the author for this publication. They represent arithmetic medians of the examined specimens.*

emeralds and assume them to be synthetic. The microscope, however, reveals some surprises: filamental inclusions that have not been observed before in other natural emeralds (figure 8).

Remarkable, yet bewildering, are those inclusions that are so familiar to the gemologist who has had experience with Colombian emeralds, especially those from Muzo. Specifically, euhedrons of calcite and dolomite (figure 9) and jagged inclusions oriented parallel to the c-axis have been observed in the Pakistan stones. Here, as in Muzo, the jagged inclusions represent natural primary syngenetic growth defects which trapped part of the hydrothermal solution during crystal growth. If such solution is chemically pure, then upon condensation as a result of lowering temperature and pressure, these inclusions become two-phase, liquid and gas (figure 10). However, if the solution
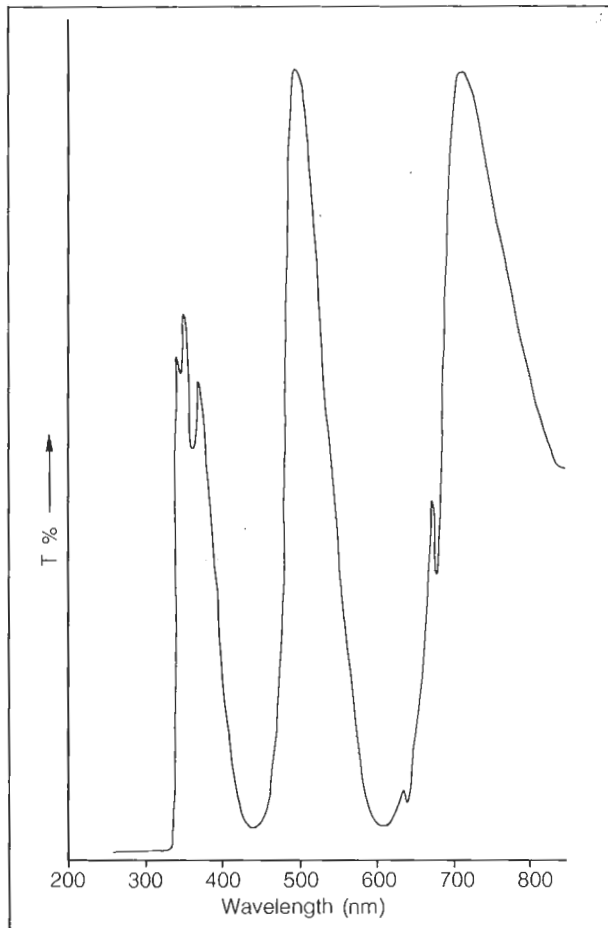
Figure 7. Absorption curve of Pakistan emerald plotted by a Beckman spectral photometer at room temperature. Note the conspicuous amplitude between 425 and 430 nm.

Figure 8. General view of characteristic inclusion suite of Pakistan emerald consisting mainly of primary and pseudosecondary two-phase inclusions. Magnified 20×.

Figure 9. Small group of well-shaped dolomite rhombohedra representing an essential element of the internal paragenesis of Pakistan emerald. Magnified 50×.

Figure 10. Typical jagged, two-phase inclusions with prominent vapor bubbles form another peculiarity of Pakistan emeralds. Magnified 100×.

is not pure, perhaps saline, then a third phase may appear, a solid in the form of a minute crystal. Only one such three-phase inclusion was observed among the Pakistan emeralds examined. These jagged two- and three-phase inclusions are oriented parallel to the c-axis, but isolated fine, wispy two-phase inclusions also occur oriented in other directions.

Fine growth tubes, also two-phase (figure 11), often arise from tiny crystalline obstacles. These tend to accumulate in the direction of the c-axis and sometimes form such dense masses that a cat's-eye effect would result if the emerald were cut en cabochon.

Considerably different in appearance are inclusions that have settled into former cleavage planes parallel to the basal crystal planes or in fractures. One type forms very thin films, in part two-phase, the outlines of which are usually ir-
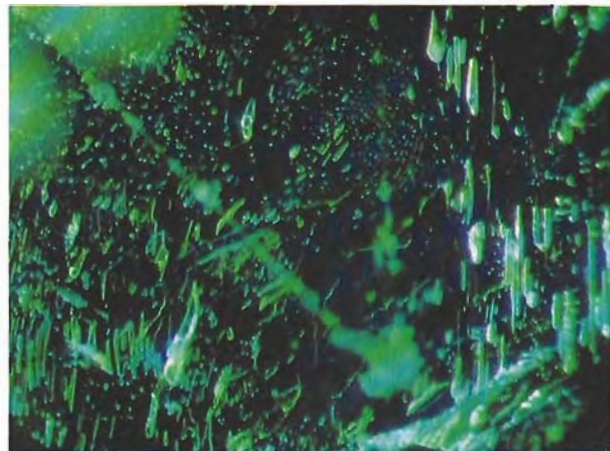
Figure 11. Hair-fine primary growth tubes in parallel alignment to the c-axis of Pakistan emerald. Magnified 50×.
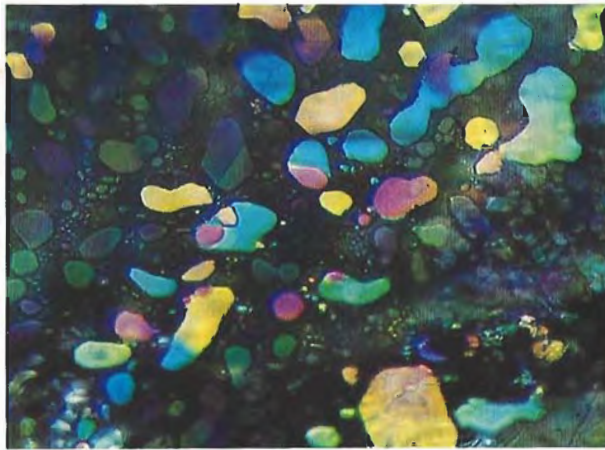

Figure 12. Ultra-thin liquid films displaying interference colors when illuminated vertically. Magnified 50×.

Figure 13. Partially healed fracture with tell-tale pattern of pseudosecondary liquid inclusions. Magnified 40×.
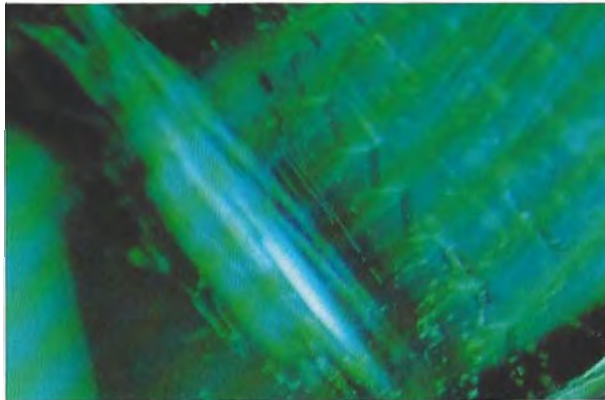

Figure 14. Step-like growth marks constitute an additional "birthmark" of Pakistan emeralds. Magnified 40×.

regular but occasionally form hexagonal contours (figure 12). Slight differences in thickness give rise to various interference colors in which the gas libellae appear in complementary color to the enclosing liquid.

Distinct from these film-like inclusions, which are absolutely diagnostic for beryl from several localities, are the drops of solution that remain in partly healed fractures and that usually form rounded, hose-like, elongated or amoeba-like two-phase inclusions with easily visible libellae. They form webs over flat planes parallel to the basal plane or follow irregularly curved surfaces (figure 13) conforming to the course of former cracks. Directional forces during the healing of such cracks must have had an influence because, interestingly enough, the droplets show not only irregular, but also long drawn-out, hose-like forms

that closely parallel the three crystallographic directions. Despite this parallelism, they do not lie along former prism faces or follow the c-axis. They differ, too, in form and arrangement, from the jagged or tube-like growth defects of primary origin, but betray a striking similarity to the analogous pseudo-secondary syngenetic liquid inclusions of the healing cracks in Colombian emeralds. Certainly, the close resemblance of the inclusions in Pakistan emeralds to those in Colombian emeralds is obvious, and points to similarities in the hydrothermal growth environment. In fact, the inclusion suites in Pakistan emeralds as a whole are unmistakably distinct from those in emeralds of pneumatolytic origin, formed by contact-metamorphic reactions between granitic pegmatites and chromium-bearing metamorphic rocks.

In addition to the internal features just described, which are indeed true inclusions, zoned color-banding, similar to that seen in Gachalá emeralds, and angular accretion steps (figure 14) are often observed. Occasionally, isolated guest minerals mark the sparse internal paragenesis, but these could not be identified either by X-ray or by electron microprobe analyses.

PART II
HUNZA VALLEY CORUNDUM AND SPINEL

Corundum and spinel crystals, many of gem quality, occur in marble outcropping along the flanks of the Karakoram Range, whose peaks tower above the valley in a remote far-north corner of Pakistan. The highest peak over the Hunza Valley is Rakaposhi, at 7,800 m (25,551 ft) above sea level; the highest peak in the entire range is the famous K2, 8,600 m (28,253 ft) above sea level. Little is known about the discovery of this deposit, but it can be assumed that the local inhabitants, as well as the Mir who once governed the valley, must have been aware of these gemstones, which contrast so strikingly with the pale marble that encloses them. Until the construction of the Karakoram Highway in the early 1970s, the valley was so isolated that neither the gemstones nor knowledge of their existence reached the outside. With the new highway, however, tourists began to visit the valley and bring out specimens of ruby. These were first examined and introduced to gemologists by Okrusch et al. (1976).

The marble outcrops are readily visible from the valley floor (figure 16) and easily accessible. They occur below the Mutschual and Shispar glaciers in the district around the villages of Altiabad

Figure 16. View down the Hunza Valley, taken a few kilometers above Karimabad to show the light-colored marble beds intercalated in the metamorphic country rocks.

Figure 15. Lower part of the Hunza Valley, the source recently of many fine corundum and spinel crystals, in the far north corner of Pakistan. Note the terraced fields along the slopes. Mt. Rakaposhi, the highest mountain in the valley (25,551 ft), towers over all.
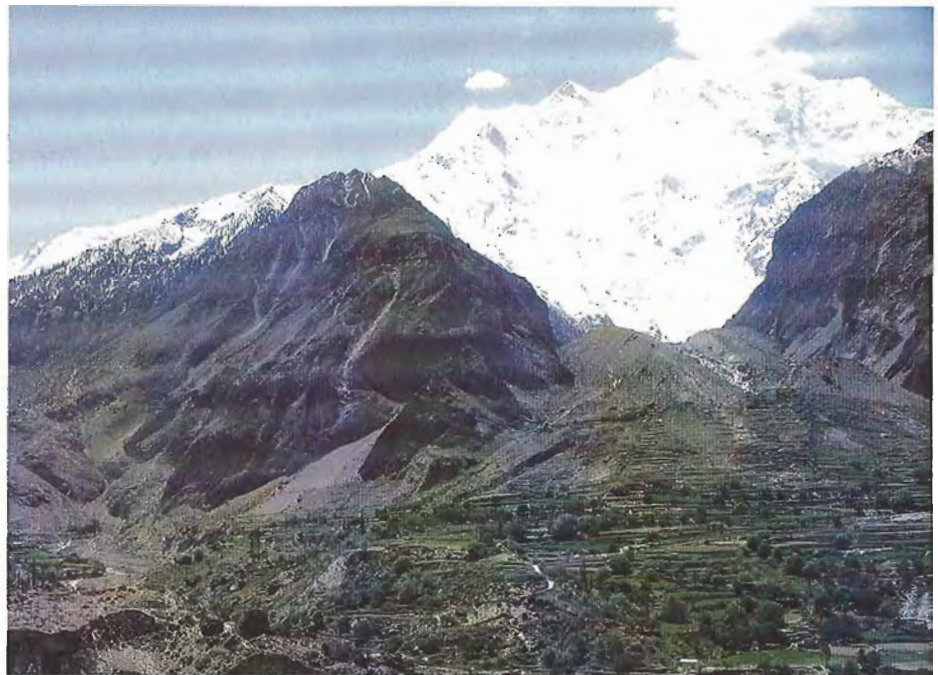
Figure 17. Geologic cross-section showing the intercalation of layers of dolomitic marbles within meta-sediments (garnet-bearing mica schists and biotite-plagioclase-gneisses) in the neighborhood of Karimabad. After a field sketch by A. H. Kazmi.

and Karimabad, previously named Hunza and Baltit, respectively. Only some of the outcrops are presently exploited; the highest is along the southernmost tip of the Shispar glacier, another is on a steep mountainside above a large talus slo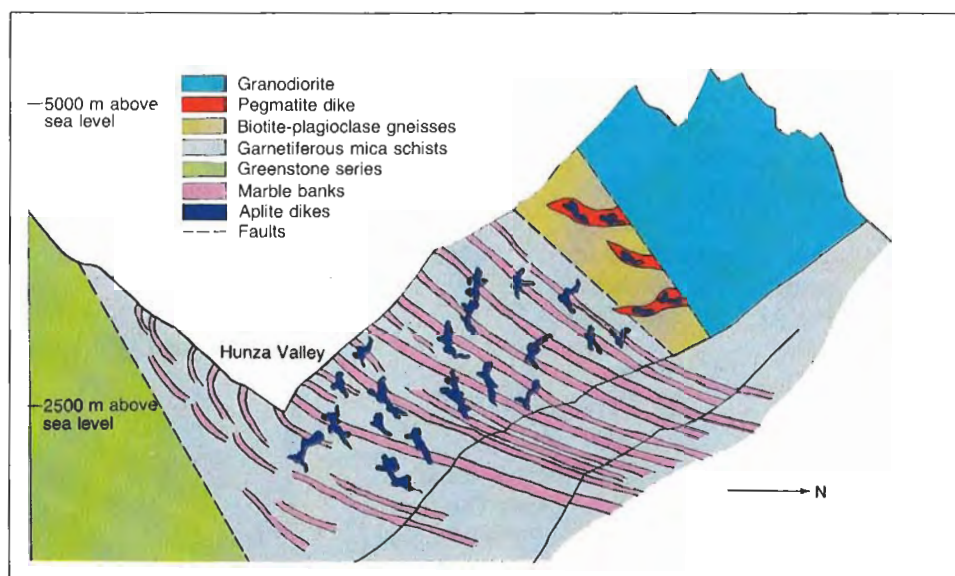pe near Altiabad, and two others are on either side of the bridge behind Karimabad. One of the latter outcrops actually crosses the road, while the other is high above the right bank of the Hunza River in an almost vertical rock face.

GEOLOGY

According to Okrusch et al. (1976), the corundum-bearing marble forms massive, concordant intercalations usually 1-5 m thick (although some go up to 10 m) within garnetiferous mica schists and biotite-plagioclase gneisses. The schists are cut by discordant pegmatite and aplite dikes (figure 17). The series of rocks belongs to the central crystalline zone of the northwestern Karakoram (Gansser, 1964) and is identical to Zone III of Schneider (1959), namely, a variegated sequence of coarse-grained marbles, carbonate-garnet amphibolites, garnet-biotite gneisses, and quartzites. To the north, this sequence is replaced, without sharp boundaries, by biotitic "old gneisses" which merge gradually into the central granite-granodiorite core of the Karakoram (Zone IV).

The emplacement of these syntectonic intrusions and the simultaneous migmatization of the "old gneisses" took place, according to Schneider (1959), at the beginning of the Tertiary and was followed by strong tectonic movements of predominantly vertical tendency. Not affected by these deformations are discordant dikes of lamprophyre and quartz trachyte as well as stocks of granite which cut through Zones III and IV.

The coarse-grained marbles originally consisted of dolomitic calcite sediments metamorphosed by numerous intrusions of granite, aplite, and pegmatite in the Eocene. Geologically, the deposits in the Hunza Valley are very similar to those in Burma. The gem-bearing marble is composed of small to large calcite crystals and is snow-white, grayish (bituminous), or yellowish (sideritic). The gemstones found within the marble are, according to Okrusch et al. (1976), the result of a special metamorphic concentration process that took place at temperatures of about 600°C and pressure of 7 kb.

The mineralogy of the deposits is fairly simple. The corundum occurs as fair- to well-formed crystals ranging from pale to deep blue, and from pink to a fine ruby red (figure 18). Accompanying the corundum are euhedrons of spinel, which are much less abundant here than in the Burma marble. In some places, phlogopite occurs as single crystals or as nest-like concentrations of massed layers that are several millimeters thick. Other associates include amphibole, chlorite, margarite, and muscovite. Large crystals of pyrite also occur, but only in the marble on the right bank of the Hunza River; pyrite is entirely absent in the marble of the opposite bank. A greenish, scaley mineral that often forms the base between the ruby crystals and the enclosing marble, or sometimes enfolds lower parts of the ruby crystals, has been determined by X-ray analysis to be muscovite and

Figure 18. Beautiful group of ruby crystals on white marble from Pakistan. Note the mauve-colored spinel on the left side behind the ruby. The largest crystal is 1 cm high.
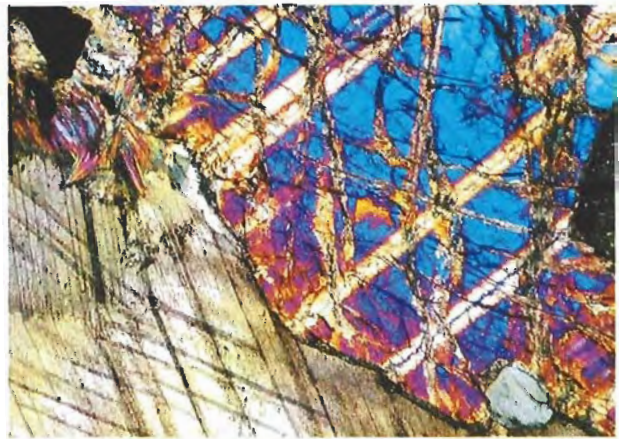

Figure 19. Thin section of corundum-bearing marble. The strong interference colors represent ruby; the striped grains, calcite; the white grain partly enclosed by ruby, apatite; and the black spots are pyrite surrounded by ruby. Magnified 50×.

not fuchsite. It contains minute traces of chromium and vanadium. A detailed description of the mineral parageneses can be found in Okrusch et al. (1976, p. 74). The appearance of the host rock is shown in the thin-section photomicrograph of figure 19.

MINING

The gem-bearing marble is mined in a primitive fashion; the rock is broken up with hammers, hand picks, pneumatic drills, or dynamiting. In a few sites, branching adits have been started into the rock. The marble is then broken up into smaller pieces and the gemmy crystals separated, while those that are obviously unfit for cutting are often left in matrix and sold as mineral specimens. As is common in so many minerals, the smaller crystals tend to be sharper and multifaced, while those that are larger display fewer faces and are generally less well formed.

PROPERTIES OF HUNZA VALLEY CORUNDUM

Color. Ruby is more common than corundum exhibiting blue or violet hues. Most of the red crystals are opaque to translucent, penetrated by numerous fractures, and often marred by large patches of calcite (a characteristic common in the material from Mogok as well). The best that can be done with such crystals is to cut them as cabochons. However, even these specimens may be remarkable for their pigeon-blood hue or for a gamut of tints that range from pale pink to the finest carmine. The best medium hue can be com-

pared with colors 9:5:3 and the corresponding values of X_c 22.5; Y_c 13.5; and Z_c 9.7 on DIN Color Chart 6164.

Other hues that commonly occur can be compared as follows: pink sapphire (11:2:2 = X_c 42.6; Y_c 33.4; Z_c 45.7), purple sapphire (11:4:4 = X_c 17.7; Y_c 11.1; Z_c 19.9), and violet sapphire (11:4:5 = X_c 11.6; Y_c 7.3; Z_c 13.0).

Chemical Analysis. Because of the intense color of the rubies, a microprobe analysis of trace elements was deemed advisable. The results are shown in table 4 along with comparative analyses of rubies from other sources.

As can be seen, the rubies are relatively pure corundum with contents of 97.4% to 99% Al_2O_3. Their magnificent color is due to the variable Cr content, which ranges from 0.15% to 0.81%. Other transition elements detected are FeO (0.01%–0.35%), MgO (0.023%–0.13%) and V_2O_3 (0.02%–0.058%), but these quantities are so small that they have no real influence on color.

Optical Properties. With the Dialdex refractometer, the following mean values were established: n_ϵ = 1.762 and n_ω = 1.770. n_Δ (biref.) = 0.008.

Similar values were found in other hues of corundum from the Hunza Valley and match fairly closely the values established for corundum from other sources. Important pairs of dichroic hues are given in table 5.

The absorption spectrum is normal for corundum, with absorption lines noted at 694.2 nm and

TABLE 4. Chemical analyses, given in weight percentages, of rubies from various deposits.

Oxide	Hunza			Burma				Sri Lanka		Thailand	
	1[a]	2[b]	3[c]	4[d]	5[d]	6[e]	7[e]	8[e]	9[e]	10[e]	11[e]
SiO_2			0.29	0.137	0.542						
TiO_2	0.03		0.0								0.02
Al_2O_3	99.0		97.4	98.8	97.5						
Cr_2O_3	0.81	0.14–0.17	1.30	0.945	1.81	0.07	0.1	0.02	0.10	0.2	0.6
V_2O_3	0.02			0.032	0.058					0.002	
Fe_2O_3	0.03	0.01		0.015	0.025	0.03	0.04	0.01	0.07	0.1	0.35
FeO			0.22								
MgO	0.0		0.13	0.023	0.023						
CaO	0.0		0.02								
MnO			0.02								
NiO			0.01								
Na_2O	0.0		0.04								
K_2O			0.0								

[a]Stone 1 was analyzed especially for the author by M. Weibel (Professor Doctor at the Federal Institute of Crystallography and Petrology, Zürich, Switzerland). Blank spaces throughout the table are presumed to mean zero weight percent.
[b]Analysis by Okrusch et al. (1976).
[c]Analysis by Meyer and Gübelin (1981).
[d]Analysis by Alexander (1948).
[e]Analysis by Harder (1969).

692.8 nm commonly as glowing emission lines, at 668 nm and 659 nm in the red region, and at 476.5, 475, and 468.5 nm in the blue. In the pink, lilac, and violet varieties, the iron absorption lines are absent and the twin chromium absorption lines usually appear in the red end of the spectrum as very fine emission lines. This shows that chromium, although present in lesser quantities, still acts as a coloring agent in the paler red and blue-tinted corundums.

In terms of luminescence, the behavior is consistent with corundum from other localities; that is, the red and red-tinted (pink, lilac, and violet) varieties reveal different quantities of chromium by glowing red in varying strength when exposed to short-wave ultraviolet radiation. For example, ruby glows cyclamen-red at 253.7 nm and red at 365 nm, while the lilac to violet varieties show a dull violet luminescence at 253.7 nm, and glow intense red at 365 nm. Phosphorescence was not found under ultraviolet or X-radiation.

Density. There is little difference in density according to color variety; the value of clean material is 3.995 ± 0.005 variation. As may be expected, the margin of variation will increase with the amount of inclusions in the stone.

Inclusions. The distinguishing features of Hunza Valley corundum lie not in their optical proper-

TABLE 5. Dichroism in corundum from the Hunza Valley.

Variety	Parallel to c	Perpendicular to c
Red corundum, ruby	Purplish red	Orange-red
Pink sapphire	Pale cyclamen-red	Pale yellow
Purple sapphire	Purple	Deep cyclamen-red
Violet sapphire	Purple	Lilac

ties and density but rather in their internal paragenesis. Most of the Hunza Valley rubies are turbid; internally they display numerous cracks, parting planes, polysynthetic twin-planes, and irregular swirl marks similar to those seen in Burmese specimens. Among the solid inclusions that have also been noted, however, are some that may be considered typical and distinctive for this locality.

The most common solid inclusion is calcite (figure 20), which usually occurs as medium to large irregular masses that often occupy large areas of the host. They are sometimes so large that they can be readily recognized by the unaided eye. In some specimens, the calcite forms euhedral crystals in which the rhombohedral twinning is apparent. Dolomite, which is also seen, tends to form resorbed crystals.
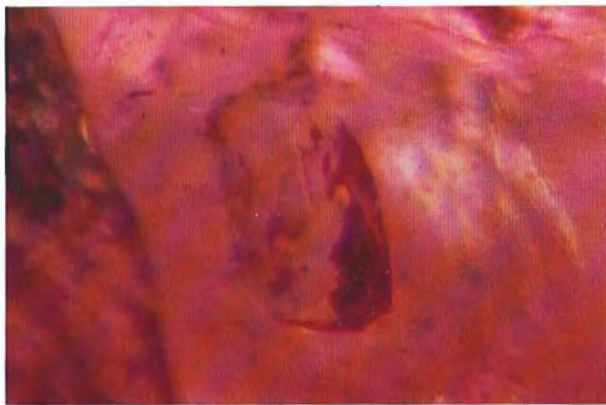
Figure 20. Calcite crystal in a Hunza ruby. Magnified 50×.

Figure 21. Flakes of phlogopite and an angular crystal of pyrite are indicative of rubies from the Hunza Valley. Magnified 20×.

Phlogopite is only a little less abundant than calcite and appears as widely scattered to thickly massed concentrations of red-brown flakes (figure 21). Margarite and chlorite are rarer, and can be distinguished from the phlogopite by appearance, the margarite forming feather-like inclusions while the chlorite is distinctly green. Pyrite, sometimes altered to goethite, may also be present as may be pyrrhotite, rutile, apatite, and spinel. All of these are recognizable because of being well-developed crystals (figure 22). However, rutile "silk" was not found in any of the specimens examined.

PROPERTIES OF
HUNZA VALLEY SPINEL

As in Burma, spinel accompanies the corundum, but the ratio of spinel to corundum is much smaller in Pakistan (1:10) than in Burma (5:1). However, the Hunza spinels, which occur in various colors, surpass the corundum crystals in size; some measure 5 cm or more in diameter. Furthermore, they are often beautifully euhedral (see figure 23).

Color. In many crystals, a high degree of clarity is noted, some being perfectly clear and suitable for faceting. Predominant colors are red, brownish red, plum-red, lilac, violet, and blue. Because the author was able to purchase only plum-red cut gems and to select other color varieties only in the form of crystals or as fragments, the following data were largely determined on the plum-red variety (figure 24). Data on the other color varieties, however, appear in Okrusch et al. (1976).

The color of the plum-red material is comparable to shades 10:2:4 to 10:2:5 on DIN Color

Figure 22. Distinctly shaped, hexagonal crystal of apatite in a Hunza Valley ruby. Magnified 20×.

Chart 6164, with corresponding values of: X_c 19.8, 12.8, and 12.9; Y_c 15.4 and 10.1; Z_c 16.7 and 10.9.

Chemical Analysis. A pale red fragment and a plum-red cut gem were examined on the electron microprobe and found to contain the principal components Al_2O_3 and MgO in normal proportions. As shown in table 6, trace elements are present in usual quantities, although the variations in amount from one stone to the next lend themselves to some interesting conclusions about the influence of the specific trace elements on the color of the stone.

For example, the reddish specimens are influenced in color by the presence of chromium or

Figure 23. Attractive group of red spinel crystals from the Hunza Valley on white calcite marble. The largest crystal is 1 cm high.

Figure 24. Two idiomorphic crystals of plum-colored spinel protrude from white calcite marble from the Hunza Valley. The larger crystal is 8 mm high.

chromium plus iron, while iron appears to be mainly responsible for the blue in no. 5. It is possible that vanadium exerts some influence on color in the plum-red material, but unfortunately this element was not determined in specimens 3, 4, and 5.

Optical Properties. A Topcon refractometer was used to measure refractive indices, providing a range of values from 1.715 to 1.720, with a frequency mean of 1.716.

Of the brightly glowing emission lines common to spinel, only the strongest, at 685.5 nm, appeared in the plum-red spinel, as an ultra-fine line. When the stone was rotated, this line proved elusive, disappearing and reappearing alternately

as emission line and absorption line according to the position of the facets in the light source. On the other hand, the pale red fragments produced three emission lines in the red region, at 685.5, 684, and 675 nm.

The pale red spinel glowed clear pink when exposed to either short-wave or long-wave ultraviolet radiation, but the plum-red specimen showed no reaction to short-wave ultraviolet radiation and glowed only a dull red to long-wave ultraviolet radiation.

Density. Varying according to the refractive indices of the stone, measured values fell in the range 3.585 to 3.614, the mean being 3.599.

TABLE 6. Chemical analyses, given in weight percentages, of spinels from the Hunza Valley.

Oxide	Plum-red spinel 1[a]	Pale red spinel 2[a]	Wine red spinel 3[b]	Grayish red-violet spinel 4[b]	Cornflower blue spinel 5[b]
Al_2O_3	72	72	71	72.18	72.04
MgO	27	28	27.67	28.21	25.66
Cr_2O_3	0.10	0.25	0.41	0.09	0.19
V_2O_3	0.25	0.4	n.d.	n.d.	n.d.
FeO	0.7	0.15	0.39	0.48	1.88
MnO	<0.01	<0.01	0.02	<0.01	0.00
TiO_2	<0.01	0.02	<0.01	<0.01	0.00

[a]Stones 1 and 2 were analyzed especially for the author by M. Weibel (Professor Doctor at the Federal Institute for Crystallography and Petrology, Zürich, Switzerland).
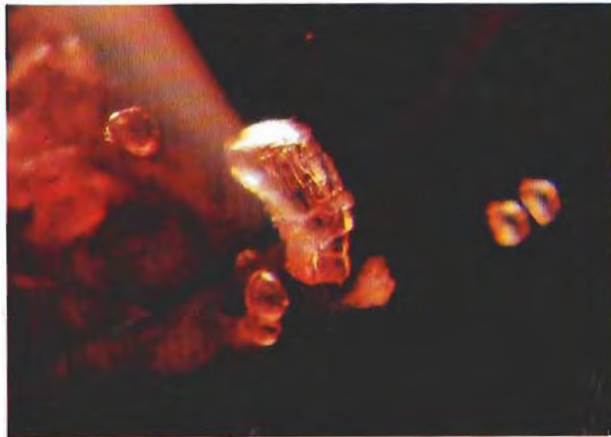[b]Stones 3–5 were analyzed by Okrusch et al. (1976).

Figure 25. Strongly resorbed and etched fragment of dolomite characterizes the interior of a plum-colored spinel from the Hunza Valley. Magnified 35×.

ily included and therefore suitable only for cutting as cabochons, the majority of the smaller specimens are devoid of inclusions visible to the naked eye and consequently lend themselves well to faceting. Many samples are of such high quality that the Swat Valley emeralds readily vie with the finest Muzo emeralds and the Hunza Valley rubies compare favorably with the best Burma rubies.

Both the Hunza and Swat valleys qualify as areas of remarkable gem occurrences with considerable commercial potential. The current efforts of the Gemstone Corporation of Pakistan to provide continuity in the mining and marketing of this material offer great promise for the future importance of these localities.

Inclusions. Spinel crystals of various colors were observed in thin section under the microscope. Large prismatic crystal inclusions of a green amphibole were recognized, as were fine, needle-like rutile inclusions. The amphibole, which also appears as a macroscopic companion to corundum, spinel, and pyrite, showed weak pleochroism and extinguished obliquely between crossed polaroids. The rutile, which consistently settled epitaxially on the octahedron faces, distinguished itself by straight extinction. Growth and intergrowth of calcite and dolomite are also common and look exactly the same as in corundum. Surprisingly, the plum-red cut spinels of gem quality showed a totally distinct inclusion suite. Such stones were either absolutely clean or they contained idiomorphic euhedral or resorbed crystals of either dolomite (figure 25) or Ca-apatite, similar to those commonly observed in spinels from Sri Lanka (Zwaan, 1972; Gübelin, 1973).

Unlike Okrusch et al. (1976), the author could not find tourmalines in the Hunza Valley. Apart from this, he collected some samples of an emerald-green mineral described as chrome-diopside by the members of the Gemstone Corporation of Pakistan who accompanied him. However, a qualitative analysis with the electron microprobe showed this mineral to be pargasite.

CONCLUSION

While most of the larger specimens of emerald, ruby, and spinel described in this report are heav-

REFERENCES

Alexander A.E. (1948) Spectrochemical and spectrophotometric analyses of rubies and sapphires. *Journal of Gemmology*, Vol. 1, pp. 4–8.

Bank H. (1980) Sehr hochlichtbrechender Smaragd aus Sambia. *Zeitschrift der Deutschen Gemmologischen Gesellschaft*, Vol. 29, No. 1/2, pp. 101–103.

Gansser A. (1964) *Geology of the Himalayas.* Interscience Publishers, London, New York, Sydney.

Gübelin E.J. (1968) Gemmologische Beobachtungen am neuen Smaragd aus Pakistan. *Der Aufschluss*, Sonderheft 18, pp. 110–116.

Gübelin E.J. (1974) *Internal World of Gemstones*, 1st edition. ABC-Editions, Zurich, Switzerland.

Harder H. (1969) Farbgebende Spurenelemente in den natürlichen Korunden. *Neues Jahrbuch für Mineralogie, Abhandlungen*, No. 110, 2, pp. 128–141.

Hickman A.C.J. (1972) *The Miku emerald deposit.* Economic report no. 27 of the Republic of Zambia, Ministry of Mines and Mining Department. Geological Survey, Salisbury.

Hussain S.Q. (1980) Geological report on Swat emerald deposits (unpublished report of the Gemstone Corporation of Pakistan).

Kane R.E. (1980/81) Unexpected absorption spectrum in natural emeralds. *Gems & Gemology*, Vol. 16, No. 12, pp. 391–392.

Martin N.R., Siddiqui S.F.A., King B.H. (1962) A geological reconnaissance of the region between the lower Swat and Indus rivers of Pakistan. *Geological Bulletin of Panjab University*, Vol. 2, pp. 1–13.

Meyer H.O.A., Gübelin E.J. (1981) Ruby in diamond. *Gems & Gemology*, Vol. 17, No. 3, pp. 153–156.

Okrusch M., Bunch T.E., Bank H. (1976) Paragenesis and petrogenesis of a corundum-bearing marble at Hunza (Kashmire). *Mineralium Deposita* (Berlin), No. 11, pp. 278–297.

Qasim J.M., Khan Tahirkheli R.A. (1969) The geology of the lower part of Indus Kohistan (Swat), West Pakistan. *Geological Bulletin of the University of Peshawar*, Vol. 4, pp. 1–13.

Schneider H.J. (1959) Tektonik und Magmatismus im NW-Karakoram. *Geologische Rundschau*, Vol. 46, pp. 426–476.

Zwaan P.C. (1965) Apatite crystals in a Ceylon spinel. *Journal of Gemmology*, Vol. 9, No. 12, p. 434.

THE GEMOLOGICAL PROPERTIES OF CHATHAM FLUX-GROWN SYNTHETIC ORANGE SAPPHIRE AND SYNTHETIC BLUE SAPPHIRE

By Robert E. Kane

Recent rumors in the trade and inquiries to the various offices of GIA's Gem Trade Laboratory, Inc., concerning the commercial availability of faceted flux-grown synthetic blue sapphires prompted the writing of this article. Blue as well as orange flux-grown synthetic sapphires are now commercially available from Chatham Created Gems, Inc., in limited quantities as rough crystal groups and single crystals; they have not yet been marketed as faceted gems. In this article, the author examines the gemological properties of Chatham flux-grown synthetic orange sapphires and blue sapphires.

ABOUT THE AUTHOR

Mr. Kane is gem identification supervisor of GIA's Gem Trade Laboratory, Inc., Los Angeles, California.

The synthesis of transparent corundum in virtually every color known to occur in natural corundum has been accomplished by the Verneuil technique (also known as the flame-fusion process) and successfully marketed since the early 1900s (Nassau, 1982). Synthetic ruby manufactured by other methods, including the flux process, has also been commercially available for many years now. The synthesis of flux-grown blue sapphire, however, was first accomplished only eight years ago, by Chatham Created Gems, Inc., and has not yet reached the same level of sophistication as flux-grown synthetic ruby. Because of problems with synthesis, flux-grown blue sapphire to date has been marketed in the trade only on a small scale, in the form of rough crystal groups and single crystals. Flux-grown blue sapphires have not been sold as faceted gemstones by the Chatham firm (Thomas Chatham, personal communication, 1982), although a few stones reportedly have been cut by purchasers of the rough and may be seen, though very rarely, by the gemologist.

Recently, Chatham was successful in synthesizing orange sapphire by the flux method. This material, too, is being sold only as crystal groups or as an occasional single crystal (Thomas Chatham, personal communication, 1982). Although we know of the synthesis of flux-grown orange sapphire, and other colors, by J. P. Remeika in the early 1960s (Nassau, personal communication, 1982), these samples were grown for industrial use only.

The purpose of this article is to present the gemological properties of the Chatham flux-grown synthetic orange and synthetic blue sapphires, as well as means of distinguishing these synthetics from their natural counterparts. The author's intent is to provide the gemologist with the information necessary to conclusively identify flux-grown synthetic orange and synthetic blue sapphires should they become widely available commercially as cut

Figure 1. Exceptional examples of Chatham flux-grown synthetic orange sapphire (rough crystal group, 39.86 ct; faceted stone, 1.32 ct) and flux-grown synthetic blue sapphire (rough crystal group, 11.59 ct; faceted stone, 0.39 ct).

stones. The author conducted this study with 31 Chatham flux-grown orange sapphire crystal groups and single crystals (ranging in weight from 3 to 40 ct) and with 18 Chatham flux-grown blue sapphire crystal groups and single crystals (ranging in weight from 7 to 55 ct), several hundred flux-grown blue sapphire single crystals (weighing from 1 to 2 ct each), and 11 faceted flux-grown blue sapphires (weighing from 0.37 to 2 ct each). Sample material is illustrated in figure 1, including a Chatham flux orange sapphire faceted by Bill Kerr of GIA for this study.

DIFFICULTIES OF SYNTHESIZING FLUX-GROWN ORANGE SAPPHIRE AND BLUE SAPPHIRE

Even though Chatham has not perfected the synthesis of blue sapphire by the flux method after nearly eight years of working on this project, they have had much greater success with the synthetic blue sapphire than they did with flux-grown ruby in the early years of its synthesis (Thomas Chatham, personal communication, 1982). Several different manufacturers have commercially synthesized ruby by the flux technique since the late 1950s; however, many years of experimentation were required to bring synthetic flux ruby to the state that we know it today.

The major difficulties encountered in the manufacture of the orange and blue varieties of flux-grown synthetic corundum derive from the fact that addition of slight amounts of the coloring agent impurities needed to create such colors causes disturbances in crystal growth. Each vari-

ety has a unique set of problems. For example, the addition of iron and titanium to grow blue sapphire by the flux method causes extreme color zoning. Chatham states that they have attempted to alleviate color zoning by trying to control the speed and direction of crystal growth, which is directly related to the clarity of the material. This often results in many of the crystals being heavily included. At this time, Chatham has not solved all of the problems with the synthesis of flux blue sapphire. They currently are concentrating their efforts on eliminating the disruptions in the crystal structure to improve clarity.

Chatham states that they first synthesized orange sapphire by the flux method in 1981. As with the synthetic blue sapphire, Chatham presently sells only limited quantities of the orange material and only as rough crystal groups.

GEMOLOGICAL CHARACTERISTICS OF FLUX-GROWN SYNTHETIC ORANGE SAPPHIRE AND BLUE SAPPHIRE

Even though Chatham has been experimenting with the flux growth of synthetic blue sapphire since 1974, very little descriptive information concerning this synthetic has been published in the gemological literature, with the exception of some brief observations presented by Scarratt (1977) and Koivula (1981a). The following discussion examines in detail the gemological characteristics of the Chatham flux-grown orange sapphires and blue sapphires. These characteristics, many of which are the same for both colors, are summarized in table 1.

TABLE 1. The gemological properties of Chatham flux-grown synthetic orange sapphires and synthetic blue sapphires.

Chatham flux-grown synthetic sapphire	Refractive index and birefringence	Pleochroism	Luminescence			Absorption spectrum	Specific gravity	Inclusions
			Long-wave U.V. radiation	Short-wave U.V. radiation	X-rays			
Orange	1.762–1.770 0.008	Strong pink-orange and brownish yellow.	Variable: intensity ranges from strong to very strong; overall fluorescent color ranges from orangy red through reddish orange to yellowish orange, with zones of chalky yellow.	Intensity ranges from very weak to weak; same fluorescent colors as long-wave.	Variable: intensity ranges from strong to very strong in most cases, with some areas being inert to very weak; overall fluorescent color ranges from reddish orange to orange, may exhibit zoned areas of chalky yellow. No phosphorescence.	Absorption lines at 475, 476.5, 468.5, 659.2, 668, 692.8 and 694.2 nm, and broad absorption blocking out all of the violet and some of the blue, all of the green and yellow, and a small area in the orange portion of the visible spectrum. Not diagnostic.	4.00 ± 0.003[a]	Various forms of flux; platinum; dense, white, cloud-like areas; transparent crystals; fractures; healed fractures; color zoning.
Blue	1.762–1.770 0.008	Strong violetish blue and greenish blue.	Variable: uneven reaction, inert to very strong; fluorescent colors patchy, ranging from chalky greenish yellow to chalky reddish orange to yellowish-brownish green to sulfur yellow.	Variable: uneven reaction, inert to strong. The following fluorescent colors may be observed: chalky greenish yellow, dull yellowish green, dull chalky greenish white, chalky reddish orange, and strong yellow.	Variable: uneven reaction, inert to moderate; overall fluorescent color fairly consistent chalky yellowish white. No phosphorescence.	Weak diffused band centered at 451.5 nm. Not diagnostic.	4.00 ± 0.03[a]	Various forms of flux; platinum; dense, white, cloud-like areas; transparent crystals; fractures; healed fractures; various forms of color zoning; thin, white-appearing needles.

[a]*Crystal groups with applied ceramic glaze are often lower, near 3.85. Platinum inclusions in crystals without applied ceramic glaze may raise S.G. above 4.03.*

Visual Appearance. As the Chatham synthetic sapphire crystals are examined with the unaided eye, several observations can be made on both varieties. Color, transparency, and clarity are the most obvious properties noted, although other unusual characteristics also come to light.

With regard to color, the overall hue of the flux-grown orange sapphires varies from orange to reddish orange in moderate to vivid saturation. Color zoning is often seen within the individual crystal groups and single crystals. There are areas of yellowish orange, orangy yellow, pinkish orange, and orangy pink.

Strong color zoning is evident in nearly all of the flux-grown blue sapphire crystals. The zones range from near colorless through light blue and medium blue to extremely dark blue (almost black). Many of the crystals have heavily included areas that appear white to the unaided eye. In some of the crystal groups, some small crystals will be nearly colorless and others will be zoned with areas that are near colorless or differing shades of blue.

With regard to transparency and clarity, both the orange and the blue flux-grown synthetic sapphires range from transparent to translucent, often within the same crystal. Some blue crystals were opaque. The translucency in both is due to the many areas that are heavily included. The opacity in the blue crystals results from the dark, almost black, color. The clarity to the unaided eye ranges from areas that appear to be free from inclusions (except color zoning) to areas that are very heavily included.

Further examination with the unaided eye reveals a transparent, near-colorless glossy coating on the backs of many of the crystal groups. This is most evident at crystal junctures, where the coating has accumulated. When a pen light is used for horizontal illumination, gas bubbles may be observed in the coating.

Microscopic examination confirms the presence of a coating and the occurrence of many spherical gas bubbles at some of the crystal junctions (figure 2). Chatham states that a liquid silica-based ceramic glaze is applied to the backs of the crystal groups and the crystals fired in a kiln at 1000°C. This practice was started several years ago on some synthetic ruby crystal groups to strengthen those that were thin and fragile. Chatham now routinely applies a ceramic glaze to all of the synthetic orange and blue sapphire
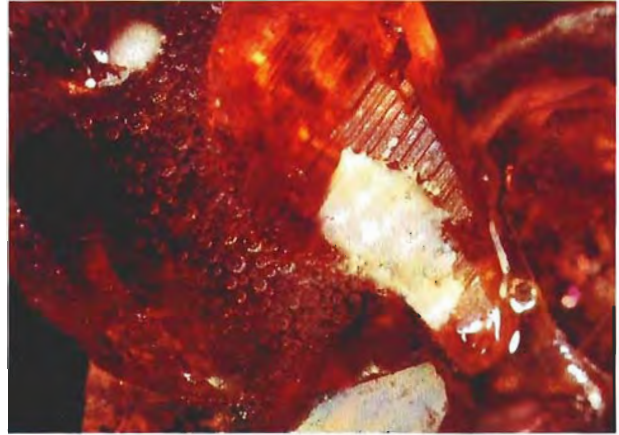

Figure 2. Dense concentration of spherical gas bubbles in the silica-based ceramic glaze applied to the back of this Chatham flux-grown synthetic orange sapphire crystal group. Oblique illumination accentuates the termination of the glaze near the edge of the crystal group. Magnified 10×.

and synthetic ruby crystal groups that they market. Chatham does not, however, put this ceramic glaze on single crystals (Thomas Chatham, personal communication, 1982).

Further examination with the microscope confirms that the ceramic glaze is found mostly on the backs of the crystal groups; occasionally, however, it is seen on the sides. The glaze often seeps between crystal faces and into surface fractures, where spherical and elongated flat gas bubbles may form. These bubbles may look like inclusions within the crystal, but they actually occur only between crystal faces or in fractures. In some of the thinner crystal groups, such gas bubbles in the back are visible from the front. The transparent glossy coating appeared to be essentially the same on both the orange and the blue crystal groups, with the exception that some of the synthetic blue sapphire crystal groups had glazed areas with an opaque, white, burned appearance. This is in contrast to the relatively consistent, transparent, near-colorless appearance of the coating on the synthetic orange crystal groups.

Refractive Indices and Birefringence. Refractive indices were obtained using a GEM Duplex II refractometer in conjunction with a sodium light source. In preparation for testing, one of the flux-grown orange single crystals was faceted. This faceted stone and the faceted synthetic blue sap-

phires were determined to be uniaxial negative with a refractive index of $\omega = 1.762$ and $\epsilon = 1.770$, and a corresponding birefringence of 0.008.

Pleochroism. A calcite dichroscope was used to determine this property. In the flux-grown orange sapphires, the dichroic effect was observed as strongly distinct colors of pink-orange and brownish yellow. The synthetic blue sapphires revealed dichroism in distinct colors of violetish blue and greenish blue. As would be expected, the dichroic colors of both the synthetic orange and synthetic blue sapphires varied depending on the color of the crystal and how much color zoning was present in the area being examined.

Luminescence. Exposure to long-wave ultraviolet radiation of the 31 flux-grown synthetic orange sapphire crystals studied revealed variable fluorescence, from strong to very strong. The overall color of the fluorescence ranged from orangy red (almost pure red) through reddish orange to yellowish orange. All of the crystals had an opaque, dull appearance. Most of the crystals had zones of moderate to strong chalky yellow fluorescence. The crystals that were predominantly orange seemed to have more yellow fluorescent zoning than did the crystals with redder hues.

The fluorescent chalky yellow zones were observed on both sides of the flux-grown orange sapphire single crystals and crystal groups. The ceramic glaze on the crystal groups did not fluoresce and did not appear to affect the fluorescence in any way. These yellow zones were observed to range from being confined to one or two small areas to comprising almost 80% of the crystal.

Exposure of the flux-grown orange sapphires to short-wave ultraviolet radiation revealed essentially the same variable fluorescent reaction. The zoning and color of the short-wave ultraviolet fluorescence was the same as the long-wave fluorescence. The major difference was the intensity of the short-wave fluorescence, which ranged from very weak to weak.

Exposure of the flux-grown orange sapphires to X-rays also revealed a variable fluorescence. The intensity ranged from strong to very strong in most cases, with a few crystal groups exhibiting strong to very strong fluorescence around the edges and inert to weak centers. The overall color of the X-ray fluorescence ranged from reddish orange to orange. Some of the crystal groups and single crystals had zones of moderate chalky yellow X-ray fluorescence that seemed to correspond to the chalky yellow zones of long-wave and short-wave ultraviolet fluorescence. No visible phosphorescence was observed after X-ray excitation.

Almost all of the flux-grown synthetic blue sapphires exhibited a very patchy, uneven reaction to long-wave ultraviolet radiation. Some areas were inert, while others ranged in intensity from very weak to very strong.

In the material examined by the author, many of the extremely dark blue areas were inert; the moderately dark blue areas exhibited a very weak, dull, yellowish-brownish green; the medium-blue to near-colorless areas glowed a weak to strong greenish yellow; the colorless and heavily flux-included areas fluoresced the same greenish yellow, but much more so than the other areas; some of the clean, near-colorless areas fluoresced a weak chalky reddish orange; and the whitish, burned (coated) areas fluoresced a very strong sulfur yellow. Because of possible optical irregularities and unobserved inclusion centers, as well as the obstruction of some areas within the crystal groups, these observations of corresponding areas of color and fluorescent reactions cannot be considered conclusive at this time, but may be viewed as good indications of the synthetic nature of the material.

Exposure of the synthetic blue material to short-wave ultraviolet radiation also revealed a very patchy, uneven reaction. Some areas were inert, while others ranged in intensity from very weak to strong. The color of the fluorescence varied widely, with the following hues observed: chalky greenish yellow; dull yellowish green; dull, chalky, greenish white; chalky reddish orange; strong yellow; and chalky whitish blue (observed in several small, near-colorless fragments).

Exposure of the flux-grown synthetic blue sapphires to X-rays also revealed a patchy reaction. Some areas were inert, and others ranged in intensity from very weak to moderate. The X-ray fluorescence was a fairly consistent chalky yellowish white. There was no visible phosphorescence after exposure to X-rays.

As Webster noted (1975), some natural blue sapphires will change to a "dirty amber colour" when exposed to X-rays. This color change is not permanent; the original color returns after about 3½ hours' exposure to sunlight or even much more rapidly when the stone is heated to a tem-
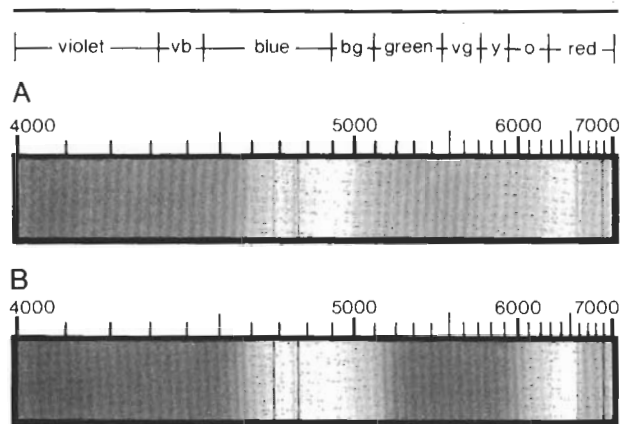
Figure 3. Drawings of absorption spectra for (A) Chatham flux-grown synthetic orange sapphire and (B) Chatham flux-grown synthetic ruby, as observed on a direct-vision spectroscope (in Å) at room temperature.
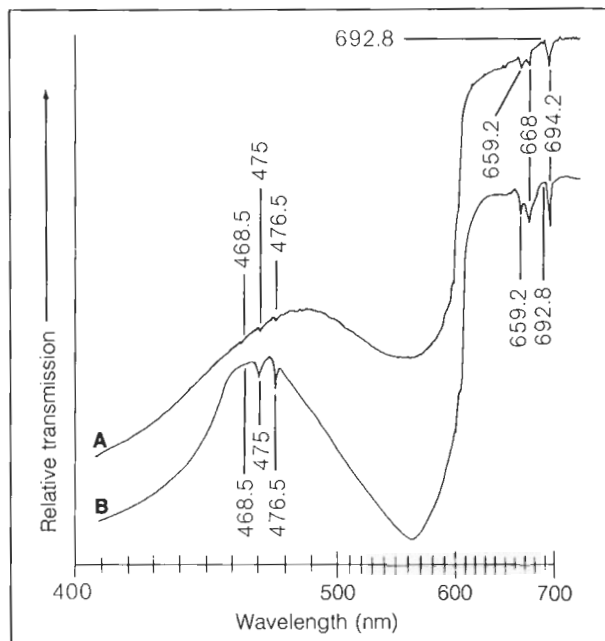

Figure 4. Visible-light spectral transmission curves for (A) Chatham flux-grown synthetic orange sapphire and (B) Chatham flux-grown synthetic ruby, as documented by the automatic recording spectrophotometer at 60 K.

perature of about 230°C. Scarratt (1977) reported that when a few Chatham flux-grown blue sapphire crystals were exposed to X-rays, "the colorless and some of the pale blue areas photocoloured to varying depths of green or yellow, depending on the length of exposure." He also indicated that the induced colors were not permanent. Unfortunately, neither Webster nor Scarratt stated the length of exposure time required for the X-rays to produce such a color change. The Chatham synthetic blue sapphires examined by the author displayed no change in color after exposure to X-rays for 5 to 10 seconds.

Absorption Spectra. The visible light absorption spectra of the 31 synthetic orange sapphire crystals were examined with the GEM spectroscope unit. The observed spectra exhibited essentially the same transmission and absorption features as the diagnostic absorption spectrum described by Liddicoat (1981) for natural and synthetic ruby, purple sapphire, and dark "padparadscha" sapphire. The absorption features, however, are much weaker in the Chatham product. Figure 3 illustrates the absorption spectra for (A) Chatham flux-grown orange sapphire and (B) Chatham flux-grown ruby as observed in the GEM spectroscope at room temperature.

The characteristic spectrum for the Chatham flux-grown orange sapphire has two major transmission areas, one in the blue and one in the red. Within the blue transmission area are three sharp narrow lines: one at 468.5 nm and a very close doublet at 475 and 476.5 nm. The line at 475 nm is extremely faint and difficult to observe. In the

red portion of the visible spectrum is the typical chromium absorption that is often associated with corundum. There are very faint, narrow lines at 659.2 nm and 668 nm, along with two stronger, yet narrow, lines very closely spaced at 692.8 nm and 694.2 nm.

In addition to these areas, there is a broad absorption blocking out all of the violet and some of the blue, all of the green and yellow, and a small area in the orange portion of the visible light spectrum. All of the synthetic orange sapphires exhibited this absorption spectrum. The thicker specimens exhibited a stronger spectrum than did the thinner crystals.

Using a modified Zeiss PMQ$_3$ recording spectrophotometer, Stephen Hofer, of GIA's Department of Research, confirmed this absorption spectrum. Figure 4 shows the visible-light spectral transmission curves for the Chatham flux-grown orange sapphire (A) and the flux-grown ruby (B), as documented by the automatic recording spectrophotometer.

The absence or presence of this spectrum cannot be considered diagnostic at this time. Although orange sapphires are quite rare in nature, when they occur in the same color as their Chatham synthetic counterpart, they may exhibit an absorption spectrum very similar if not iden-
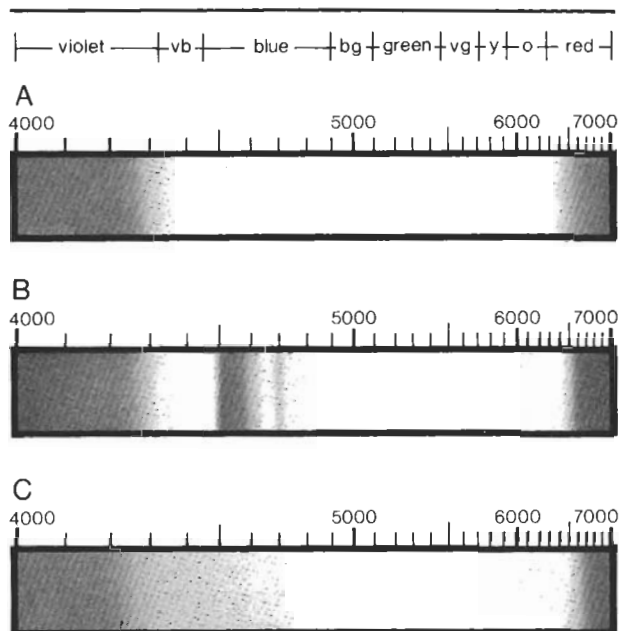
Figure 5. Drawings of absorption spectra for (A) Chatham flux-grown synthetic blue sapphire, (B) natural dark blue sapphire, and (C) Verneuil synthetic blue sapphire, as observed on a direct-vision spectroscope (in Å) at room temperature. Absorption spectrum A may be observed in some natural medium blue sapphires, and absorption spectrum C may be observed in light blue unheated natural sapphires as well as in medium blue heat-treated natural sapphires.
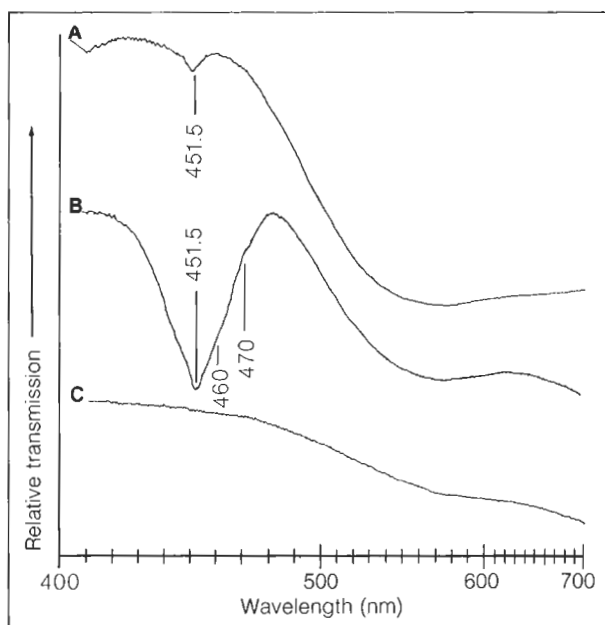
Figure 6. Visible-light spectral transmission curves for (A) Chatham flux-grown synthetic blue sapphire, (B) natural dark blue sapphire, and (C) Verneuil synthetic blue sapphire, as documented by the automatic recording spectrophotometer at 60 K. Some natural medium blue sapphires exhibit the same visible-light spectral transmission curves as A, and some light blue unheated natural sapphires and medium blue heat-treated natural sapphires may exhibit a lack of absorption features as in C; the curve, however, may vary.

tical to the one that is characteristic of the Chatham product.

However, they may also show distinct differences. The natural color of orange sapphires is often attributed to a combination of iron and chromium, both of which are also found in the Chatham synthetic orange sapphire. If iron only appears in the spectrum, it may be observed in bands centered near 450, 460, and 470 nm (Liddicoat, 1981) that will not appear in the Chatham synthetic. Natural orange sapphires may also show chromium bands only, or perhaps no perceivable absorption features at all. These natural, unheated sapphires are often brownish orange, yellowish orange, or orange, and not reddish orange. To complicate matters even further, an orange color that may be slightly different (often brownish orange or yellowish orange) from the color of the Chatham flux-grown sapphire may be produced in natural sapphires by heat treatment or irradiation (Crowningshield and Nassau, 1981). These treated stones often will exhibit a featureless visible-light absorption spectrum.

Spectrographic examination of the visible-light spectra of the Chatham flux-grown blue sapphires also was performed with the GEM spectroscope unit. Most of the stones showed a very faint diffused band slightly above 450 nm. The band was quite vague and difficult to see in many of the stones. Figure 5 compares the absorption spectra for (A) Chatham synthetic blue sapphire, (B) natural dark blue sapphire, and (C) Verneuil synthetic blue sapphire, as observed on the GEM spectroscope unit at room temperature. Again using the modified Zeiss PMQ$_3$ recording spectrophotometer, Hofer confirmed the presence of this absorption band and showed it to be centered at 451.5 nm (figure 6).

The presence or absence of the 450 nm band can no longer be considered diagnostic in and of itself. For many years it was accepted that virtually all natural blue sapphires exhibit an absorption band centered at 450 nm that might be accompanied by two additional weaker bands

centered near 460 and 470 nm (Anderson and Payne, 1955). However, the absorption bands in the blue portion of the visible spectrum in natural blue sapphire are due to iron in the ferric state; these bands decrease considerably in intensity with the decrease in iron content (Webster, 1975). Accordingly, there are natural sapphires that owe their color to titanium and iron that will not show any 450 nm band when examined with a standard hand-held type of spectroscope. There are also heat-treated blue natural sapphires, quite prevalent in today's market (Abraham, 1982), that will not exhibit the 450 nm band (Crowning-shield and Nassau, 1981; Nassau, 1981).

However, the combination of the 450, 460, and 470 nm bands, commonly known as the 450 complex (Webster, 1975), has not been observed in any synthetic blue sapphires as of yet and can still be considered diagnostic of natural blue sapphires.

Specific Gravity. The specific gravity values for both the orange and the blue flux-grown synthetic sapphires were determined by means of the hydrostatic technique, using a Voland diamond balance along with the necessary specific gravity attachments. As would be expected, the applied ceramic glaze affected the specific gravity values. The lower specific gravity of the ceramic glaze, which was determined to be 3.088*, lowered the values of some of the glazed crystals from the expected values for corundum. The specific gravity of the flux-grown orange crystals with the applied ceramic glaze varied considerably, from 3.865 to 3.994. Several single crystals of flux-grown orange sapphire, which did not have the applied ceramic glaze, showed minor variations in density between 3.986 and 4.032 (within the accepted values for corundum).

The synthetic blue sapphire crystal groups that had the applied glaze ranged in value from 3.848 to 3.987. Faceted material and single crystals that did not have the applied glaze showed minor variations in density from 3.974 to 4.055. Platinum inclusions may increase slightly the specific gravity of flux-grown synthetic corundum.

The presence of a large number of gas bubbles in the glaze will undoubtedly lower the specific gravity of this material.

Inclusions. As with essentially all other synthetic corundum, especially synthetic ruby, the most important means of identifying flux-grown synthetic orange sapphires and blue sapphires is their characteristic inclusions. Microscopic examination of the Chatham synthetic orange and synthetic blue sapphire crystals and faceted synthetic blue sapphires revealed a wide variety of inclusions. Most of these can be considered diagnostic of synthesis. However, some of the inclusions in the flux-grown blue sapphire—for example, very thin, white-appearing needles and straight and "hexagonal" color banding—could be quite confusing if used as the sole source of identification. If all of the inclusions observed, however, are carefully examined and considered in the identification, the Chatham flux-grown orange sapphires and blue sapphires should not present any great problems for the gemologist.

Many easily identifiable and diagnostic inclusions are characteristically found in the orange and blue Chatham synthetic sapphires. To date, the following inclusions have been observed in both: various forms of flux; platinum; dense, white, cloud-like areas; transparent crystals; fractures; healed fractures; and color zoning. Observed in the synthetic blue sapphire and not in the synthetic orange sapphire were thin, white-appearing needles.

Flux. Residual, unmelted flux typical of flux-grown synthetics was prevalent in nearly all of the Chatham flux-grown orange and blue sapphires examined. Several forms were observed. "Fingerprints" of flux that ranged from transparent and near colorless to opaque and white were seen in tightly arranged, thin, mesh-like patterns and loosely arranged, wide, flat, mesh-like patterns that frequently intersected one another (figure 7). The opaque, white "fingerprints" were usually observed in very high relief (figure 8). The transparent and near-colorless patterns were often observed in very low relief and may be more visible at certain viewing angles and lighting conditions than at others.

Most characteristic of the flux inclusions were white, wispy veils (figure 9), usually very fine in texture though occasionally moderately thick, that were seen in high relief. In many of the flux-grown blue sapphire crystals, the wispy veils were in such densely concentrated areas that they ap-

Figure 7. Transparent and nearly colorless, wide, mesh-like patterns of flux intersected by tightly arranged white "fingerprints" of flux in a Chatham flux-grown synthetic orange sapphire. Magnified 30×.
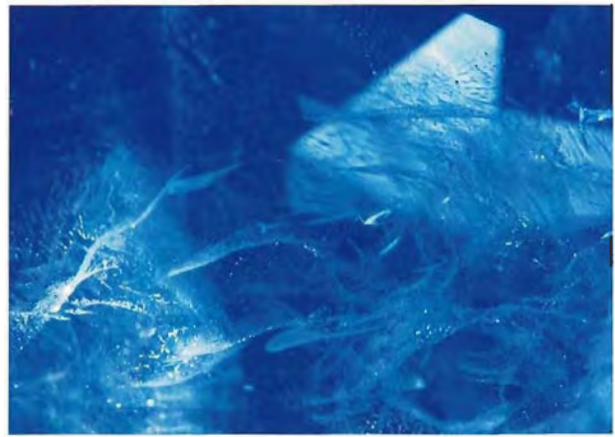

Figure 9. White, wispy veils of flux, fine in texture, betray the synthetic origin of this Chatham flux-grown blue sapphire. Note the thin, white-appearing needle in the upper left of this photomicrograph. Magnified 15×.

Figure 8. "Fingerprint" of white flux observed in high relief with straight-sided, angular, cloudy white zoning in a Chatham flux-grown blue sapphire. Magnified 25×.

peared very white to the unaided eye. Opaque white veils that are not wispy in appearance, but are somewhat flat and curved, also were observed in both the synthetic orange and synthetic blue sapphires. They ranged from fine to moderate in texture. What has not been observed in any of the flux-grown orange and flux-grown blue sapphires are flux veils or "fingerprint" patterns that are as thick and globular as the very coarse flux "fingerprints" often thought to be typical of this type of synthesis and characteristically seen in some Kashan and Chatham synthetic rubies.

Another type of flux that was observed, although not as frequently as the ones discussed above, occurred as opaque globules that ranged from white to yellowish brown and from small to

extremely large (see figure 10). They were present as nondescript droplets or in somewhat angular forms with rounded corners. This type of inclusion was found to be more prevalent in the blue than in the orange material.

Platinum. Perhaps as characteristic as the several forms of flux inclusions is the presence of platinum. Chatham claims, as do other manufacturers of synthetic gemstones (Knischka and Gübelin, 1980) that they can control the formation of metallic inclusions during the growth process. The ability to repress or completely eliminate metallic inclusions is supported by the fact that many synthetics contain very few if any of these inclusions. For example, the Kashan synthetic rubies and pink sapphires contain virtually no platinum inclusions, although platinum inclusions were reported in some of the early material. However, platinum inclusions were quite prevalent in all 31 of the Chatham flux-grown orange sapphire crystals and in most of the Chatham flux-grown blue sapphire crystals and faceted stones that were examined. They are extremely diagnostic when present. Carol Stockton, of GIA's Department of Research, used the scanning electron microscope–energy dispersive spectrometer (SEM-EDS) system to perform chemical analyses on randomly selected metallic inclusions in both the Chatham flux-grown orange and flux-grown blue sapphire, and confirmed their identity as platinum.

Platinum inclusions may result from the flux process. For a substance to occur as an inclusion, the constituents of the inclusion must be present
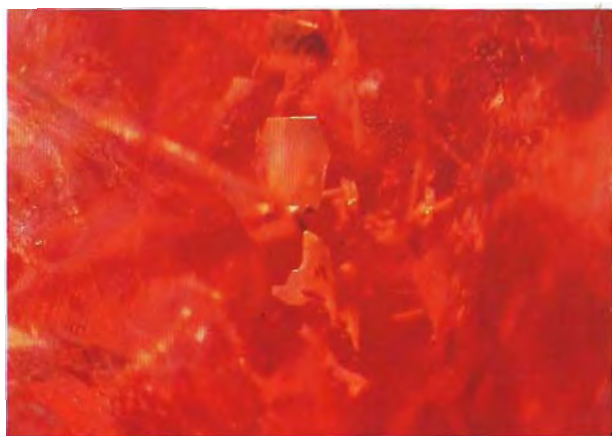
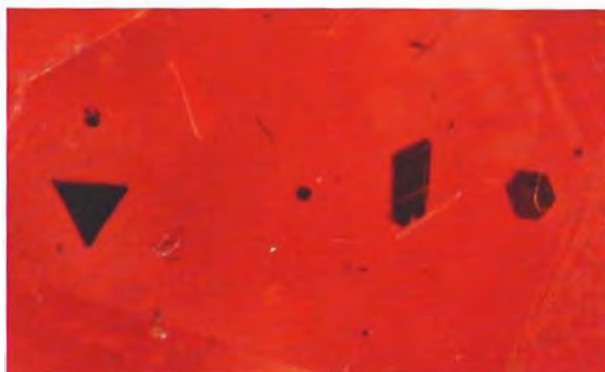Figure 10. Opaque white globules of flux in a Chatham flux-grown synthetic orange sapphire. Magnified 20×.

Figure 11. Very thin flakes of platinum included in a Chatham flux-grown synthetic orange sapphire. The platinum appears black because of the ultra-thin nature of the flakes and the lighting conditions. Slight changes in illumination often reveal the shiny metallic appearance usually associated with platinum. Magnified 60×.

Figure 12. The shiny metallic appearance of platinum is very evident in this large, thick, angular platinum inclusion in a Chatham flux-grown synthetic blue sapphire. Magnified 35×.

in the growth environment. With this type of synthesis, crystals are grown in a metallic, often platinum, crucible. Under the conditions necessary for flux growth, everything in the growth environment will go into solution, at least to some extent. Among the noble metals, platinum is probably the most nearly immune to this; under certain conditions, however, some of the platinum will go into the solution and may become part of the growing crystal.

In the Chatham synthetic orange sapphire and blue sapphire crystals, the platinum inclusions were observed to occur in several different forms: large, irregular flakes that ranged from thin to very thick, thin hexagonal and triangular platelets that occurred frequently in very symmetrical forms but sometimes in distorted forms, spikes, splinters, and small thin flat needles, as well as in other geometric and nondescript forms. These platinum inclusions range from very small to quite large (see figures 11 and 12).

Despite the diversity of forms in which the platinum occurs, this metallic inclusion provides the gemologist with a diagnostic and easily identifiable characteristic. Platinum inclusions occur only in synthetic gem materials and never in natural gemstones. When platinum occurs as an inclusion it is always opaque and may be black or shiny and metallic appearing (again, see figures 11 and 12). Differences in illumination and viewing angle often change the appearance from a shiny platinum color to black or vice versa.

In most of the synthetic orange sapphire crystals examined, the platinum inclusions were randomly oriented throughout, with the addition of a distinct "phantom" layer of growth near the
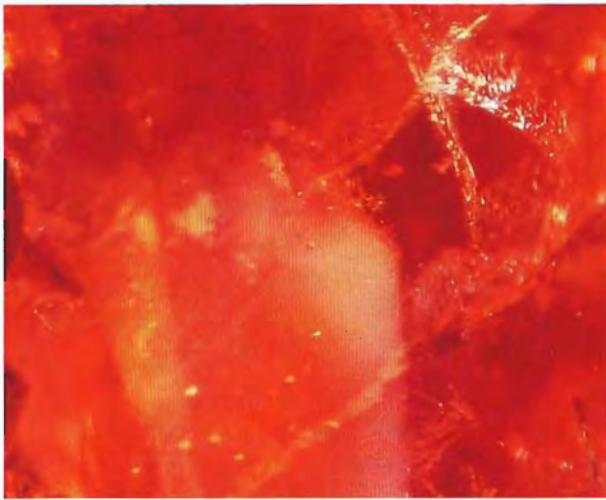
Figure 13. This cloud-like area in a Chatham flux-grown synthetic orange sapphire is composed of a dense concentration of minute, white, dust-like particles in association with larger forms of flux and bordered by pink color zoning. Magnified 30×.

Figure 14. Transparent included crystal and ultra-thin flakes of platinum in a Chatham flux-grown synthetic orange sapphire. Magnified 70×.

outer edges of many of the crystals. This layer of growth is seen easily with overhead illumination, and the boundaries of the growth layer are also readily apparent. Within this growth zone there is an excessive amount of platinum, much greater than is found anywhere else in the crystals. This would indicate a change in environment toward the end of the growth process. Although these thin growth zones would probably be cut away during faceting, this interesting characteristic was observed in many of the flux-grown orange sapphire crystals studied.

Such a layer of growth was also observed in some of the flux-grown blue sapphire crystals studied, but only very rarely; this, too, would probably be removed in faceting. The main difference between the platinum inclusions in the flux-grown orange sapphires and those in the flux-grown blue sapphires is that the platinum in the synthetic orange sapphires examined was found to be relatively consistent in abundance in all of the crystals, whereas it varied considerably in the flux-grown blue sapphires studied. Specifically, some of the synthetic blue sapphires had virtually no platinum inclusions, others had only several extremely large platinum inclusions, and still others were moderately to very heavily included with platinum.

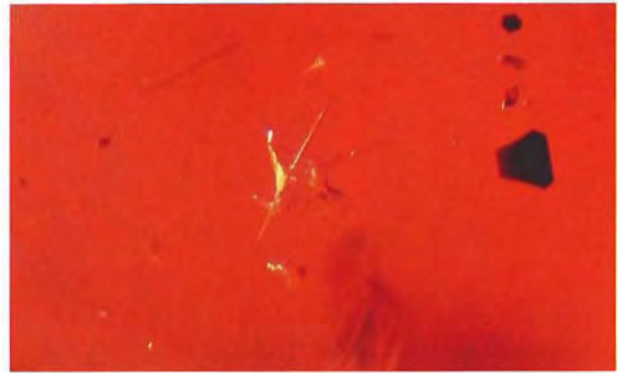*Dense, Cloud-Like Areas.* Many of the Chatham synthetic crystals, both orange and blue, studied contained randomly oriented areas of very dense white clouds composed of minute, dust-like particles. The nature of the clouds was not resolvable at 120× magnification. Other inclusions, such as very small particles of platinum and globules of flux, were sometimes randomly oriented within these cloud-like areas (figure 13). The clouds in the Chatham flux-grown orange and blue sapphires are quite reminiscent of clouds observed in many natural blue sapphires, some Burmese rubies, some Chatham synthetic rubies, and some of the Knischka synthetic rubies (Knischka and Gübelin, 1980), as well as in other gemstones.

Transparent Crystals. Included in many of the synthetic orange sapphire crystals were transparent, near-colorless, "ghost-like" crystals, many of which were very small, typically ranging in length from 0.025 mm to 0.10 mm, although some were much larger. Because of their very low relief, these small crystals often were very difficult to see with dark-field illumination and became easily visible only under certain lighting conditions, such as fiber-optic illumination, and with certain viewing angles. Consequently, these crystals are very difficult to photograph. Figure 14, however, does show one crystal that had a higher relief and a slightly different nature.

In some of the synthetic blue sapphires, transparent, near-colorless crystals were also observed. Some of the crystals are very similar to those observed in many of the flux-grown orange sapphires, in that they are low in relief and have a "ghost-like" nature. More commonly they are seen in a higher relief and are readily apparent. Some are hexagonal tabular crystals with very angular faces and easily visible straight and angular growth striations on several crystal faces (figure
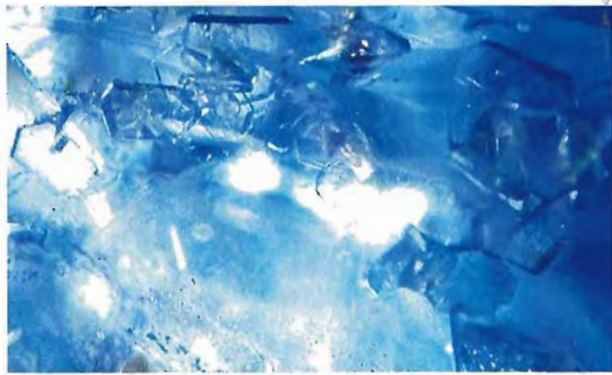
Figure 15. A cluster of transparent, colorless hexagonal tabular crystals included in a Chatham flux-grown synthetic blue sapphire. Magnified 35×.

15). The crystals are observed to occur singly, in groups of several, or in clusters of a dozen or more.

The transparent crystals observed in both the synthetic orange and synthetic blue sapphires are very similar in nature, but not in shape, to transparent, near-colorless crystals seen in some Chatham flux-grown rubies (Kane, 1981). The crystals in both the orange and the blue Chatham synthetic sapphires are often tabular with rounded corners, although the crystals in the Chatham synthetic blue sapphires may be hexagonal and tabular with very sharp angular corners. In contrast, the crystals observed in some Chatham synthetic rubies are angular and not tabular, with rounded corners.

One of the transparent crystals included in the Chatham flux-grown blue sapphire shown in figure 15 reached the surface. X-ray diffraction analysis, performed by GIA's Chuck Fryer, revealed a pattern almost identical to that of chrysoberyl ($BeAl_2O_4$). The lines in the pattern were the same as for chrysoberyl; however, the spacing was slightly different. Chatham states that when experimenting with the synthetic blue sapphires, they would often add many different elements and combinations of elements to the basic aluminum oxide formula (Al_2O_4). These synthetic blue sapphires were part of a group to which they had added heavy concentrations of beryllium, which explains the presence of these inclusions. At the time this article is being written, further research is being undertaken to identify the small "ghost-like" crystals mentioned above.

Fractures. Several fractures and healed fractures were observed in the Chatham synthetic orange

Figure 16. Yellow, orange, and pink irregular zoning borders a thick platinum inclusion in a Chatham flux-grown synthetic orange sapphire. Magnified 20×.

sapphire and blue sapphire crystals. They cannot, however, be considered diagnostic of synthesis, since they are similar in appearance to those seen in natural sapphire. Many of these fractures and healed fractures were iridescent and reflective at certain viewing angles when examined with either dark-field or oblique illumination.

In addition to those fractures observed within many of the flux-grown blue sapphire crystals and faceted stones, many fractures were found to occur between the crystals within a group. Many of these fractures were also very iridescent. The presence of these fractures between crystals, and the fact that crystal groups without a ceramic glaze were fragile and broke easily, indicates a poor cohesion.

Color Zoning. Color zoning of pink, orange, and yellow was observed in many of the crystal groups and single crystals of the flux-grown synthetic orange sapphires. Zoning occurred both confined to individual crystals within a group and in large sections of the crystal group. The same type of zoning may also be seen in single crystals. This color zoning may be straight or irregular; it does not appear to have a definite repetitious pattern (see figure 16).

Color zoning was also quite prevalent in nearly all of the Chatham flux-grown blue sapphire crystals and faceted stones that were examined. The color zoning was observed in a number of differ-
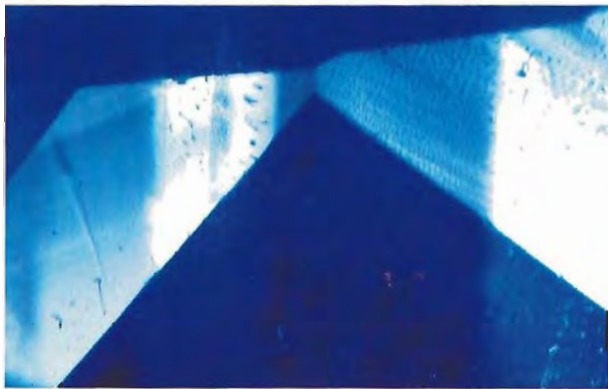
Figure 17. Straight-sided "hexagonal" zoning, colorless and blue, reflects the original growth and structure of this Chatham flux-grown synthetic blue sapphire. Magnified 35×.

Figure 18. Straight and "hexagonal" parallel, cloudy white zoning in a Chatham flux-grown synthetic blue sapphire. Note the needle-like appearance of this zoning confined to one area in the upper center portion of this photomicrograph. Magnified 20×.

ent forms, some of which may be confusing to the gemologist. The zoning ranged from colorless to extremely dark blue. The following forms were noted: straight parallel zoning, straight-sided angular patches (figure 17), dark blue zoning arranged in "hexagonal" patterns with two to five sides (the sixth side of the hexagonal pattern was probably present in one crystal that was examined, but was obscured from view by an adjacent crystal), straight and "hexagonal" parallel cloudy white zoning (figure 18 and, again, figure 8), and irregular curved dark blue areas.

Some of the color-zoned areas reflected the growth and structure of the synthetic host crystal, while others appeared to be randomly oriented. Most of the zoning was easily visible with dark-field illumination. These zoned areas were even more readily apparent with the use of diffused illumination. A very simple method of obtaining diffused lighting is to place a piece of white tissue paper or a thin sheet of translucent white plastic between the stone and the light source, which can be dark-field or transmitted illumination. Diffused lighting also reveals areas of zoning that are not visible with dark-field illumination. Figure 19 shows the effect produced when flux-grown synthetic orange sapphire and blue sapphire are immersed in methylene iodide and viewed over diffused illumination.

Thin, White-Appearing Needles. Observed in some of the synthetic blue sapphires and not in the flux-grown orange sapphires, were extremely thin, white-appearing needles (figure 20). They may be somewhat short or very long, extending through most of the stone. They are usually observed singly or in groups of just a few, and were

not seen to intersect as they often do in natural blue sapphires. They could, however, very rarely intersect one another. Most likely, they would not be observed in the quantity that is often seen in natural blue sapphires.

These needles were observed not only alone but also as a gradual extension of platinum spikes and splinters. Even though the appearance of the needles was not reminiscent of platinum, the gradual extension off other platinum inclusions suggested that they were in fact platinum. One of the faceted synthetic blue sapphires contained an extremely thin, white-appearing needle that broke the surface. Chemical analysis performed by George Rossman and Randy Heuser, at the California Institute of Technology, on an SEM-EDS system confirmed that the needle was platinum.

Extremely thin, parallel, white-appearing needles were also observed in close association with the cloudy white zoning (again, see figure 18). Needles found in this form do not appear to be related to platinum inclusions.

CONCLUDING THOUGHTS

As with most other synthetic corundum, the gemological properties of the Chatham flux-grown synthetic orange and synthetic blue sapphires overlap with the properties of their natural counterparts, with the exception of inclusions. Thus, microscopic examination can provide the definitive means of identification. Among the many inclusions that are often observed, various forms of flux and platinum provide the gemologist with the most easily identifiable and diagnostic characteristics as proof of synthesis. Some inclusions,
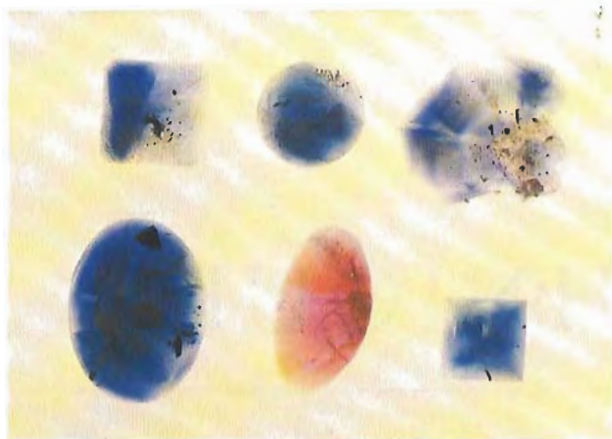
Figure 19. Immersion in methylene iodide and diffused illumination accentuate the "hexagonal" straight and irregular color zoning in a faceted Chatham flux-grown synthetic orange sapphire and four faceted stones and one rough crystal of Chatham flux-grown synthetic blue sapphire (ranging in weight from 0.39 ct to 1.80 ct).
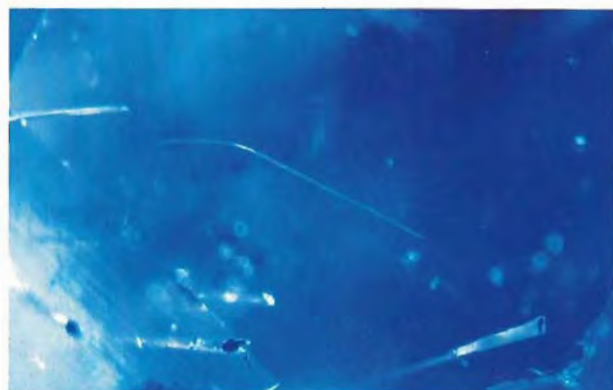

Figure 20. Thin, white-appearing needle of platinum in a Chatham flux-grown synthetic blue sapphire. Such thin platinum needles may be observed in straight or curved forms. Magnified 35×.

such as straight and angular color zoning and thin, white-appearing needles could prove quite confusing if the gemologist were not aware of their possible presence.

It is difficult to determine when and if the Chatham flux-grown synthetic orange and syn-thetic blue sapphires will become commercially available as faceted stones, since many of the crystals currently being produced are heavily in-cluded and color zoned. As changes and advances in crystal growth are made, the properties of the Chatham flux-grown synthetic orange and syn-thetic blue sapphire may change. Many, however, will remain essentially the same, and a complete understanding of and knowledge of these proper-ties will be of great value to the gemologist.

REFERENCES

Abraham J. (1982) Heat treating corundum: the Bangkok op-eration. *Gems & Gemology*, Vol. 18, No. 1, pp. 79–82.

Anderson B.W., Payne C.J. (1955) The spectroscope and its application to gemmology. *The Gemmologist*, Vol. 25, No. 302, pp. 158–162.

Crowningshield R., Nassau K. (1981) The heat and diffusion treatment of natural and synthetic sapphires. *Journal of Gemmology*, Vol. 17, No. 8, pp. 530, 532, 533.

Kane R.E. (1979) Developments and highlights of GIA's lab in Los Angeles—synthetic rubies. *Gems & Gemology*, Vol. 16, No. 7, pp. 206–208.

Kane R.E. (1981) Gem trade lab notes—synthetic ruby. *Gems & Gemology*, Vol. 17, No. 3, pp. 163–165.

Knischka P.O., Gübelin E. (1980) Synthetische rubine mit edelsteinqualität, isometrischem habitus und holer zahl unbeschädigter kristallflächen. *Zeitschrift der Deutschen Gemmologischen Gesellschaft*, Vol. 29, No. 3/4, pp. 155–185. Editor's note: An abbreviated English version of this article appears in this issue of *Gems & Gemology*.

Koivula J.I. (1981a) Brief notes on Chatham synthetic flux sap-phires. *Gems & Gemology*, Vol. 16, No. 12, pp. 410, 411.

Koivula J.I. (1981b) Photographing inclusions. *Gems & Gem-ology*, Vol. 17, No. 3, p. 135.

Liddicoat R.T. Jr. (1981) *Handbook of Gem Identification*, 11th ed. Gemological Institute of America, Santa Monica, CA.

Nassau K. (1981) Heat treating ruby and sapphire: technical aspects. *Gems & Gemology*, Vol. 17, No. 3, pp. 121–131.

Nassau K. (1982) Colored synthetics and imitations. In *In-ternational Gemological Symposium Proceedings 1982*, Gemological Institute of America, Santa Monica, CA, pp. 141–150.

Scarratt K. (1977) A study of recent Chatham synthetic ruby and synthetic blue sapphire crystals with a view to the identification of possible faceted material. *Journal of Gem-mology*, Vol. 15, No. 7, pp. 347–353.

Webster R. (1975) *Gems: Their Sources, Descriptions, and Identification*, 3rd ed. Butterworth & Co., Hamden, CT.

NOTES
· AND ·
NEW TECHNIQUES

A REPORT ON THE NEW WATERMEYER SPLIT-FACET DIAMOND CUTS

By William C. Kerr

Basil Watermeyer has introduced a new technique in diamond cutting that virtually eliminates the "bow-tie" effect commonly seen in the standard oval, marquise, and pendeloque cuts. It has also been adapted to the Barion emerald cut to provide even greater fountaining of light. The author describes these cuts and his experience with them using cubic zirconia. He also discusses their applicability to colored stones.

In November 1981, Basil Watermeyer, of Johannesburg, South Africa, sent GIA a report on his latest work on diamond cuts, in which he described his efforts both to eliminate the "bow-tie" effect commonly seen in the oval and marquise cuts, and to improve brilliance and dispersion in these and other cuts. Using cubic zirconia, the optical properties of which make the material a very suitable diamond simulant, this cutter fashioned stones very similar to the drawings supplied by Mr. Watermeyer and subsequently published in the second edition of his book, *Diamond Cutting* (1982). The results showed that these new cuts come closer than any of their predecessors to attaining the goals stated above.

The cuts described in Mr. Watermeyer's report were obtained using his new "split-facet" technique. On the oval and marquise cuts, the usual large center facet has been split into, or replaced by, two facets, so the pattern has a 10-fold symmetry rather than the usual eight-fold symmetry.

On the pendeloque, extra facets have been added near the point. Mr. Watermeyer has also modified the longer versions of the Barion emerald cut, with the split-facet technique applied to the pavilion of the stone.

Because the drawings provided contained no specific elevation angles and rotational placements to suit the crown and pavilion views given, the author determined the missing data on the basis of his own experience. The changes in design represented by Mr. Watermeyer's cuts, though dramatic in what they accomplish, are not so foreign from standard patterns that an experienced cutter cannot determine the additional details and reproduce them adequately.

Perhaps it should be pointed out that any cut used for diamond can be adapted to other gemstone materials with different optical properties simply by choosing a set of angles that makes the best use of the optical properties of that material. Consequently, these new cuts should be applicable to, and equally successful in, most colored gemstones even though their optical properties are lower than those of diamond.

The purposes of this article are: (1) to briefly discuss the "bow-tie" effect and suggest changes a gem cutter can make to minimize this undesir-

ABOUT THE AUTHOR

Mr. Kerr, a gemologist and experienced gem cutter, is originator and instructor of the faceting program at the Gemological Institute of America, Santa Monica, California.

able condition, (2) to present drawings of Mr. Watermeyer's cuts and explain how they differ from the usual standard cuts, and (3) to show photos of stones (cubic zirconia) fashioned from Mr. Watermeyer's drawings for the reader's evaluation.

THE "BOW-TIE" EFFECT

The eye perceives the "bow-tie" in an oval or marquise cut (diamond or colored stone) as a reflection of light in the midsection of the stone that differs greatly from smaller reflections seen toward the ends of the stone. Whenever the length of a stone is appreciably greater than its width, this unequal internal distribution of light occurs. The gem cutter's task is to find a pattern of facets to fit the shape or outline of the stone and to create a pattern of reflections that is uniform throughout. Brilliance must have the same intensity level, and the size of the reflections should blend smoothly with the shape of the stone.

An infinite number of light rays fall on the crown of a faceted stone, from as many directions, at any given time. To most of us it is a matter of conjecture as to what percentage of these rays are taken into the stone, distributed well, and then returned to the eye of the observer. "Clocking" the crown facets, and more particularly those on the pavilion *parallel to the long direction* of a faceted stone, creates a problem. The word *clocking* refers to the rotational placement of the facets about a circle, or as the clock hands move around the dial. Light rays entering are bounced back and forth across this narrow dimension. They either return through the midsection of the crown or leak through the same area of the pavilion. When these center facets are larger (and they invariably are) than those toward the ends, the oh-so-ubiquitious "bow-tie" confronts the observer.

To correct or diminish the "bow-tie" effect, suppose the cutter avoids any parallelism of facets near the stone's midsection and clocks the facets in a more gradual curving pattern in the center part of the stone. The standard marquise cut usually has wide center facets of much greater surface area than those closer to the ends. By replacing the two wide center facets, which are directly opposite each other, with perhaps eight or more "fanned out" facets near the middle of the stone, we find that the light is now better distributed and directed toward the ends rather than concentrated or trapped near the center. This approach produces a more attractive stone without the problems inherent in the more standard patterns. The Watermeyer cuts successfully follow these principles to both diminish the "bow-tie" effect and increase the brilliance of the stone.

THE SPLIT-FACET OVAL CUT

In discussing the "bow-tie" effect common to the standard oval-cut stone, Mr. Watermeyer has stated (personal communication, 1982) that elimination of the "bow-tie" was actually achieved about 30 years ago, but that diamond cutters persisted in leaving broad "base" curve facets that again introduced it.

Mr. Watermeyer's drawings of his split-facet oval are reproduced in figure 1. In these drawings, no main bezel facets (only two star facets) parallel the long axis of the oval. Thus, no trapped side-to-side reflections occur. The split-facet oval has 10 main bezel facets, whereas the standard oval cut has eight. The pavilion view shows eight main facets clocked to align with eight main facets on the crown, but the usual two pavilion end main facets have been replaced with two sets of four girdle-like facets. The side or profile view, in
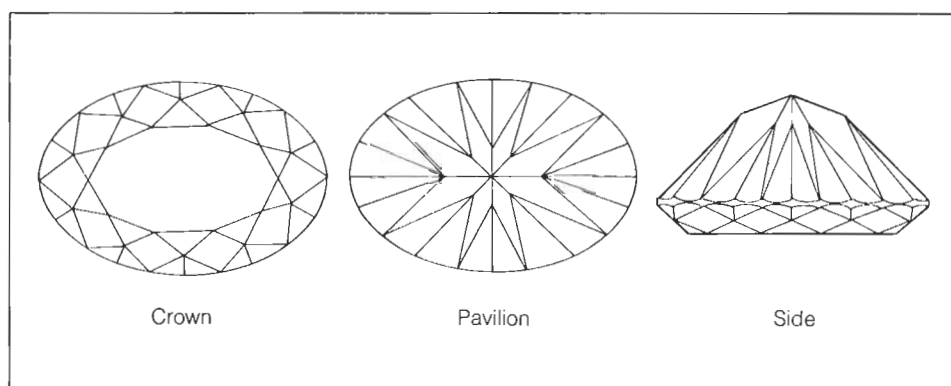

Crown   Pavilion   Side

Figure 1. The Watermeyer split-facet oval cut (total number of facets = 70, including culet). Drawings ©1981 by Basil Watermeyer.

Figure 2. Left = standard oval cut in cubic zirconia, 10.44 ct (note the "bow-tie" effect); right = Watermeyer split-facet oval cut in cubic zirconia, 11.34 ct. Photo by Tino Hammid.

addition to picturing how the pavilion aligns with the crown, shows that the six center girdle facets do not reach the actual culet ridge on the split-facet oval as they do on the standard oval. Last, four of the eight pavilion main facets are larger than the others.

Figure 2 shows cubic zirconia fashioned in the standard oval cut (left) and in the Watermeyer split-facet oval cut (right). The "bow-tie" effect so apparent in the first stone is virtually absent in the second. It should be noted that a longer oval is much less efficient in using the light that falls on it than one that more nearly approaches the round brilliant shape. The Watermeyer oval cut is particularly effective with the more difficult elongated stones.

THE SPLIT-FACET MARQUISE CUT

The marquise cut is essentially an oval shape with pointed ends. The cutter knows that irregular shapes with sharp corners usually turn out to be less efficient, and more light is lost than in

those patterns that have more symmetry. Two views by Mr. Watermeyer of the split-facet marquise cut appear in figure 3. The crown view again shows a 10 main or bezel facet pattern with no parallelism of facets except for the two center stars. Pavilion facets match (align with) crown facets except at the ends. Notice that the pavilion main facets near the center of the cut are smaller
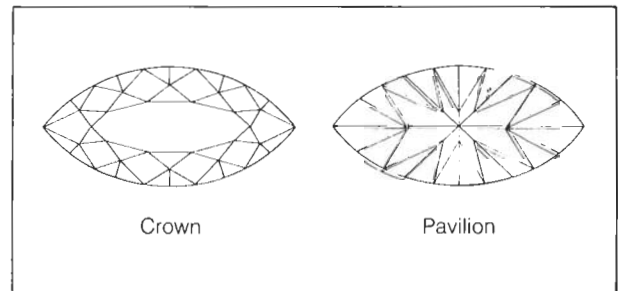

Crown   Pavilion

Figure 3. The Watermeyer split-facet marquise cut (total number of facets = 70 including culet). Drawings ©1981 by Basil Watermeyer.

Figure 4. Left = standard marquise cut in cubic zirconia, 7.51 ct; right = Watermeyer split-facet marquise cut in cubic zirconia, 7.74 ct. Photo by Tino Hammid.
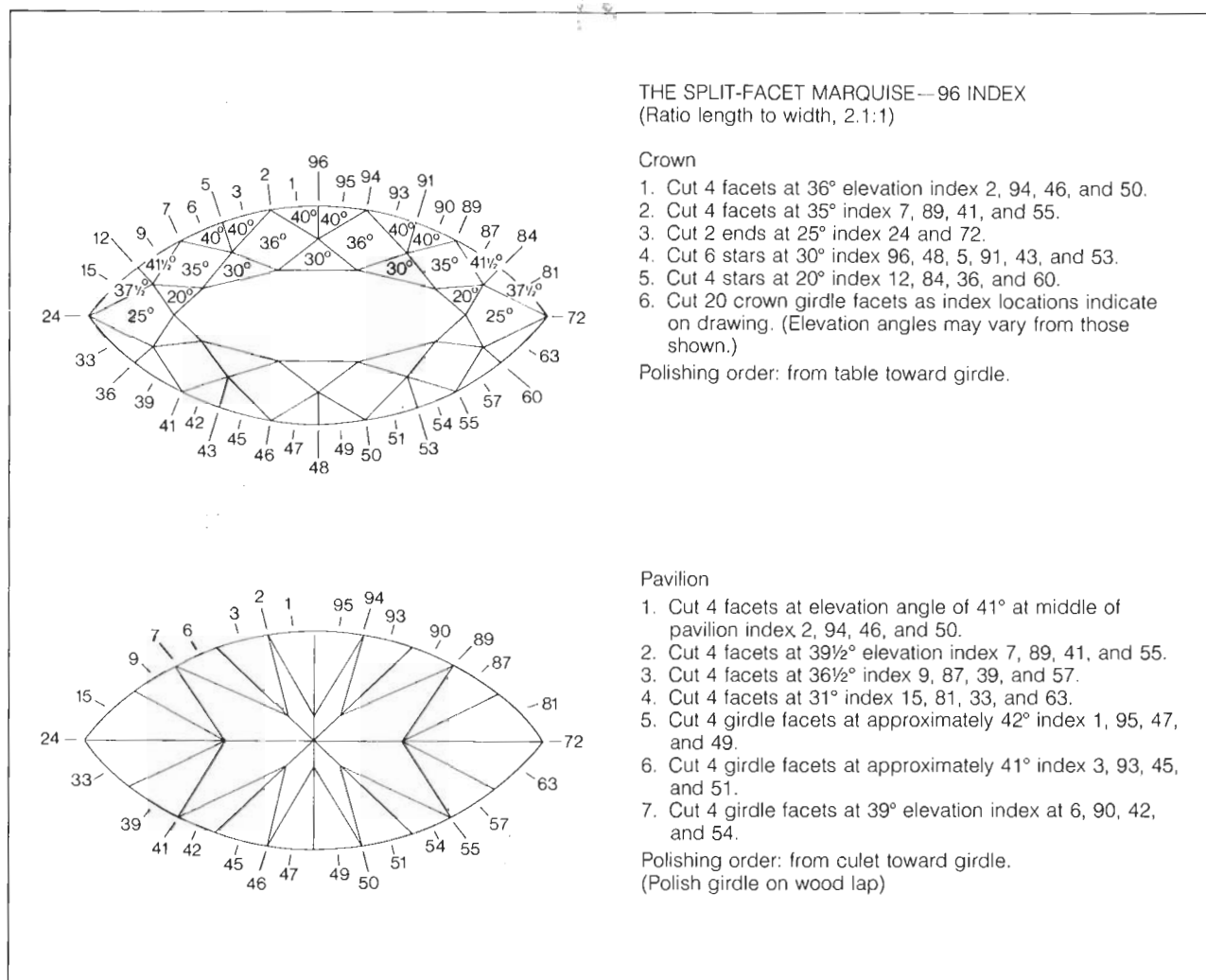
THE SPLIT-FACET MARQUISE—96 INDEX
(Ratio length to width, 2.1:1)

Crown

1. Cut 4 facets at 36° elevation index 2, 94, 46, and 50.
2. Cut 4 facets at 35° index 7, 89, 41, and 55.
3. Cut 2 ends at 25° index 24 and 72.
4. Cut 6 stars at 30° index 96, 48, 5, 91, 43, and 53.
5. Cut 4 stars at 20° index 12, 84, 36, and 60.
6. Cut 20 crown girdle facets as index locations indicate on drawing. (Elevation angles may vary from those shown.)

Polishing order: from table toward girdle.

Pavilion

1. Cut 4 facets at elevation angle of 41° at middle of pavilion index 2, 94, 46, and 50.
2. Cut 4 facets at 39½° elevation index 7, 89, 41, and 55.
3. Cut 4 facets at 36½° index 9, 87, 39, and 57.
4. Cut 4 facets at 31° index 15, 81, 33, and 63.
5. Cut 4 girdle facets at approximately 42° index 1, 95, 47, and 49.
6. Cut 4 girdle facets at approximately 41° index 3, 93, 45, and 51.
7. Cut 4 girdle facets at 39° elevation index at 6, 90, 42, and 54.

Polishing order: from culet toward girdle.
(Polish girdle on wood lap)

Figure 5. Planned program for cutting cubic zirconia to the Watermeyer split-facet marquise design.

in area than those farther out. This results in better distribution of light and in greater uniformity in the size of the pavilion reflections. The photograph in figure 4 shows the far superior split-facet marquise cut on the right. Again, the "bow-tie" effect is easily seen in the standard marquise on the left.

Figure 5 presents a working drawing for cutting the Watermeyer split-facet marquise with a 96-index gear wheel on a modern faceting machine. Angles of elevation are marked on the appropriate facets, and "clocking" index numbers indicate the relative rotational placement of the facets. This illustration represents this cutter's interpretation of the drawings reproduced in figure 3. It was developed while actually cutting the Watermeyer marquise shown in figure 4. The angles given are for cubic zirconia. This cutter sees

no reason why Watermeyer's split-facet technique cannot be used on many of the colored stones by changing the angles for the crown and pavilion facets to suit the lower refractive indexes of such stones.

THE SPLIT-FACET PENDELOQUE (PEAR) CUT

Figure 6 details the 10 main (bezel) facet design of Mr. Watermeyer's split-facet pendeloque. As most cutters are aware, the standard pear or pendeloque usually has an eight-fold symmetry. One familiar with these shapes will note two extra main facets near the sharp point on the Watermeyer cut. Like the marquise, the pendeloque presents the cutter with a great challenge: to maintain uniform brilliance throughout the stone. Basil Watermeyer's design for this shape fully
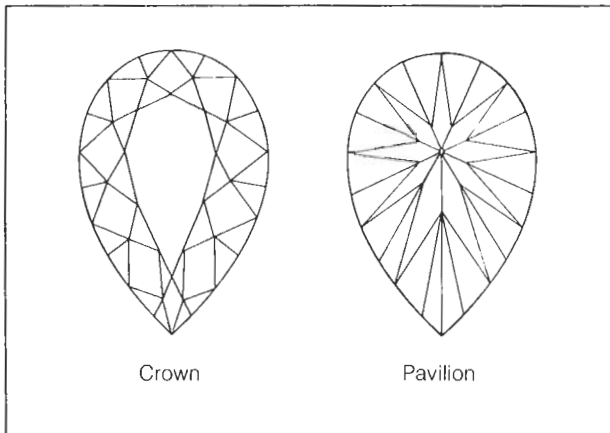
Figure 6. The Watermeyer split-facet
pendeloque cut. The same techniques used on
the marquise can be adapted to the
pendeloque. The increased scintillation is most
apparent in long shapes. (Total number of
facets = 71,* including culet.) Drawings ©1981
by Basil Watermeyer.

Figure 7. The Watermeyer split-facet
pendeloque cut in cubic zirconia, 10.85 ct.
Photo by Tino Hammid.

meets this challenge. Note from the drawing of
the crown in figure 6 that the main facet on the
point is very small and there is no pavilion facet
directly opposite it. Mr. Watermeyer's pende-
loque pattern cut in cubic zirconia is shown in
figure 7.

THE SPLIT-FACET TECHNIQUE
APPLIED TO THE
BARION EMERALD CUT

The Barion emerald cut, also developed by Mr.
Watermeyer, has straight sides with the pavilion
break facet (the one nearest the girdle) called the
"half-moon." The triangular, or "round bril-
liant"–like, facets extending to the culet meet

this pavilion break facet near the girdle, thus
maintaining the straight-line shape. All versions
of the Barion emerald cut have a three-step crown
combined with this unique pattern of triangular
facets on the pavilion. Mr. Watermeyer has ap-
plied the split-facet technique to the pavilion of
the medium-length emerald shape as shown in
figure 8. Only two extra facets are added. On the
long emerald shape, point corner halves of the
standard cut are inserted to maintain a symmet-
rically balanced faceting sequence. For the extra-
long shape, a second wing is introduced to main-
tain a continuous flow of scintillation as well as
a balanced faceting sequence.

The extreme closeness (with regard to rota-
tional placement) of facets to adjacent facets on
the pavilion, plus the fractional elevation angle
changes from the center of the stone toward the
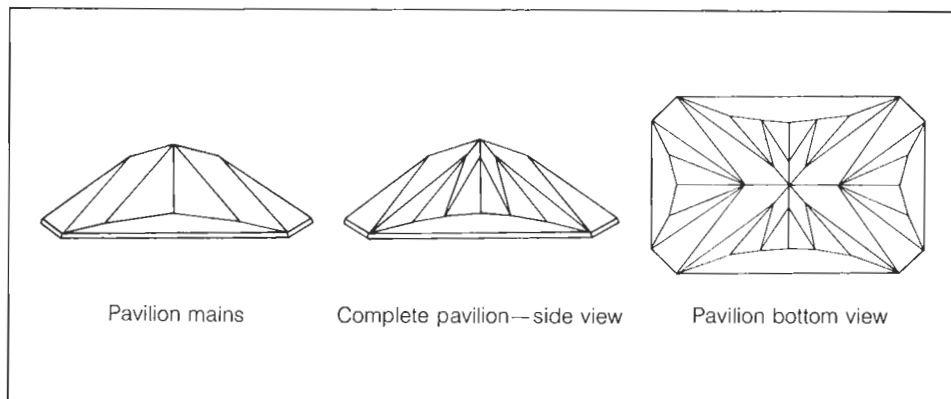ends, of these same facets, are responsible for the

Figure 8. The Barion
emerald cut (here, for a
medium-length stone),
with the split-facet
technique applied. The
proportions recommended
by Mr. Watermeyer for a
medium-length stone are
length/width = 18%/60%.
Crown (not shown) is a
standard 3-step pattern
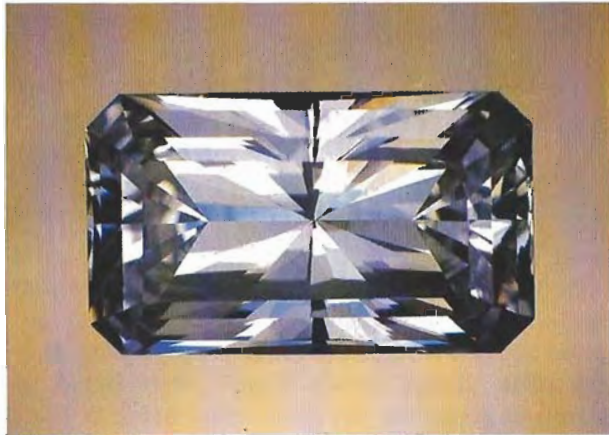common to all emerald
cuts. Drawings ©1981 by
Basil Watermeyer.

Figure 9. Barion emerald cut in cubic zirconia, 18.79 ct. Photo by Tino Hammid.

lively "fountaining" of light that Mr. Watermeyer has achieved (figure 9). To the experienced cutter, this statement concerning the pavilion facets is a revelation of some magnitude regarding faceting techniques. The gem enthusiast who is not a cutter should have little difficulty recognizing the superior "life" this stone displays. It should be noted, though, that because the facets are so close to one another both in elevation and in clocking, the pavilion of the Barion emerald is very difficult to cut.

CONCLUSION

Mr. Watermeyer's new split-facet technique represents an important breakthrough not only in diamond cutting but also in the cutting of the so-called colored stones. Harder stones (8 and above on the Mohs scale) such as corundum, spinel, topaz, and even beryl should easily adapt to these designs. Harder polishing laps, such as the ceramic lap, used in conjunction with one-quarter micron diamond abrasives, should produce exceptionally beautiful colored stones in these fascinating new designs.

REFERENCE

Watermeyer B. (1982) *Diamond Cutting*, 2nd ed. Centaur Publishers, Johannesburg, South Africa.

SHADOWING: A NEW METHOD OF IMAGE ENHANCEMENT FOR GEMOLOGICAL MICROSCOPY

By John I. Koivula

The shadowing technique employs an opaque, black, nonreflecting light shield that is inserted gradually into the transmitted light path of a gemological microscope between the subject and the light source. Shadowing takes advantage of even very slight differences in refractive index between a gemstone host and its inclusions, casting shadows in certain areas of an inclusion scene and passing light to the microscope objectives in other areas of the image. Thus, shadowing produces a three-dimensionality that seems to lift the inclusion from its surroundings, revealing it in vivid contrast against the now-subdued background of the host. This increase in contrast adds much greater detail to growth zones, included crystals, color zones, and the like, thus greatly aiding the gemologist in his work with the microscope.

Shadowing was developed through a desire to study more closely the apparently "straight" and "angular" growth and color zones that often occur in flux-grown synthetic rubies. The theory is that if these synthetic rubies were grown in a low-pressure, flux-type environment, the apparently straight and sharply angular color zoning seen under normal dark-field and transmitted light conditions might reveal slight, very subtle growth undulations on their otherwise overall straight surfaces. Such growth undulations would prove that the host rubies were synthetic. Although the absence of such growth undulations does not necessarily prove that the ruby is natural (some flux synthetics can show color-growth zoning that appears to be perfectly straight), if color zone undulations are present, the ruby is synthetic.

Microscope techniques used outside the realm of gemology, such as modulation contrast, phase contrast, and interference contrast (McCrone and Delly, 1973; McCrone et al., 1979) employ interference rings, slits, and the like to increase image contrast. However, these various systems, as they currently exist and are often used in the biological sciences and petrography, are not practical for gemological application. The cost of such equipment is very high, and the systems are designed to be used on prepared biological slides and thin sections, where depth of field and working distance are not important factors, and where magnification ranges much higher than those required in gemology are commonly used.

Gübelin (1957) was successful in adopting phase-contrast microscopy to gemology, but, again, the equipment is expensive. The problem that persisted was how to obtain the desired effect of enhanced contrast while retaining the depth of field and long working distance of the gemological microscope without a great expense.

With some experimentation, the author found the key to the solution in the other, even more expensive contrast-enhancement systems. They all incorporate slits, rings, beam splitters, and the like that are built into what is known as a substage condenser. The condenser fits between the light source and the subject, and interferes with the direct passage of light to the subject itself. The main body of the condenser is merely a housing for the convenient control of the phase rings, variable slits, and the like. Remove the housing, and we have certainly cut the cost of such a system. Keeping in mind only the principle of light-path interference, the author in a sense stripped away the condenser housing and started to experiment with an array of various shapes and sizes of opaque, flat, black light shields (see figure 1).

THE TECHNIQUE

The first opaque light shield used was a 6 × 2-cm rectangular piece of flat, black, 16-gauge steel sheet (again, see figure 1); next was the movable black dark-field light shield, and then the iris dia-

---

ABOUT THE AUTHOR

Mr. Koivula is the senior staff gemologist in the Gem Identification Department of the Gem Trade Laboratory, Inc., Santa Monica, CA.
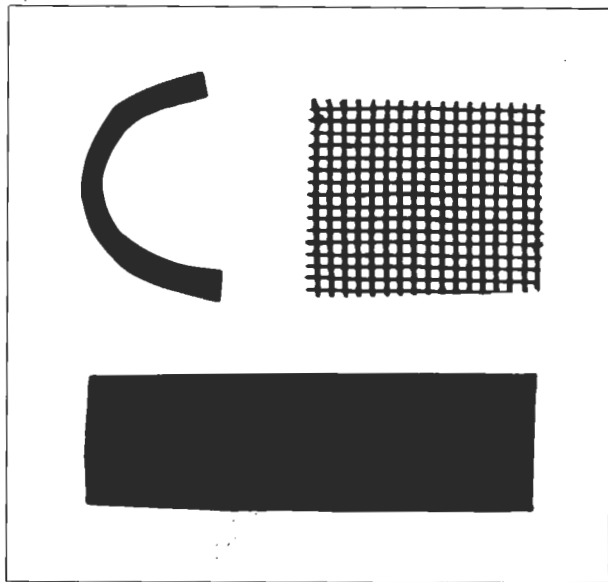
Figure 1. Three opaque light shields used to develop the author's shadowing technique. The crescent-shaped shield provided the best contrast enhancement and control of directionality.
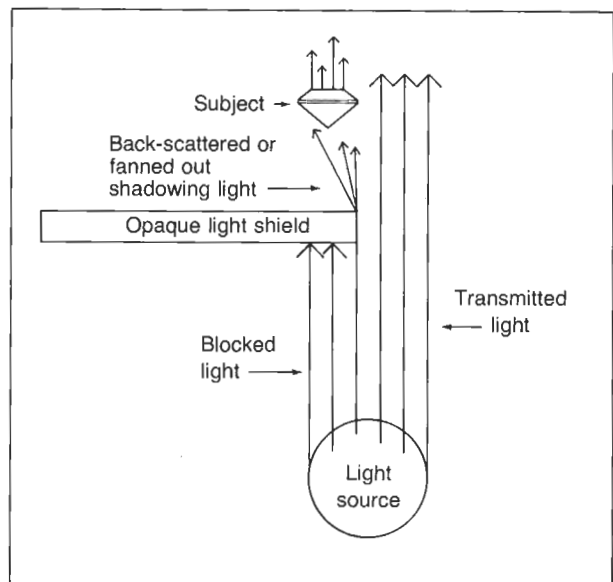

Figure 2. An exaggerated diagram showing the back-scattering of light as the opaque light shield is gradually inserted into the transmitted light path.

phragm of the Gemolite microscope (Gem Instruments, Santa Monica, CA). All increased contrast in the inclusion subject to a similar, limited extent. At low magnification, 10× to 20×, the area of enhancement was quite small, approximately 10% or less of the entire field of view. With higher magnification, the contrast-enhanced area increased proportionately.

The principle behind the light shield is relatively simple. As the edge of the opaque light shield is slowly inserted into the light path, it interferes with the direct upward passage of light, causing it to be diffracted and scattered at the edge. This fanning out of the light (see figure 2) literally causes a transmission of light in certain portions of the inclusion subject while other areas appear to be darkened or shadowed, greatly increasing contrast in and around the inclusion. Theoretically, any inclusion that has a refractive index different from that of its host can be shadowed. However, facets and facet junctions, which often act as mirrors or prisms, can and do greatly reduce the effect of shadowing.

At the interface of the inclusion and its host, in the presence of shadow-scattered light, two things take place to produce the contrast-enhanced image that we see. The scattered light travels through the host unimpaired until it contacts an inclusion of different optical density. Portions of the light are then reflected away from the microscope objective and the observer's eyes,

causing those areas that reflected the light to appear dark. Conversely, areas that allowed the light to be transmitted into and refracted through the subject to the observer's eyes appear light. This effect, as illustrated in figure 3, gives rise to the

Figure 3. Simplified theoretical situation illustrating the effect of both reflection and refraction transmission of the back-scattered light as it contacts an included crystal with a refractive index different from that of its host.
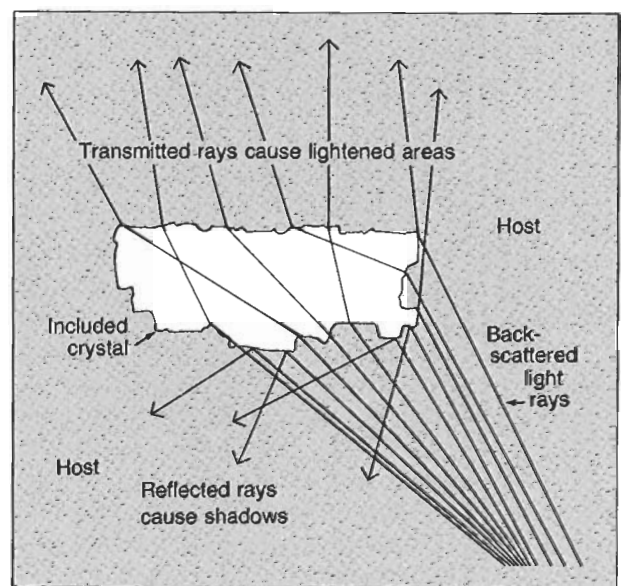
increased contrast we observe with the shadowing technique.

DIRECTIONALITY AND ITS CONTROL

When color or growth zones, as in flux-grown synthetic rubies, are the object of study, a problem of directionality arises, particularly if the zones are in essentially parallel straight lines. The author noted that as the opaque edge of the light shield was inserted in the light path, little or no shadowing took place if the color zones ran perpendicular to the edge of the light shield. If, however, the color zones ran parallel to the edge of the shield, then maximum shadowing took place.

This problem of directionality was overcome somewhat by varying the shape and size of the opaque light shield used. A curved arc, measuring only about 1 cm in diameter (see figure 1), proved quite effective in reducing directionality and increasing contrast. A 1×1-cm² section cut from an old screen door (again, see figure 1) also proved effective in reducing directionality, but the shadowing effect and resulting increase in contrast was somewhat subdued. The curved arc, because it is not as directionally dependent and therefore is easier to control, worked equally well on inclusions such as crystals and on zoning.

SETTING UP FOR SHADOWING

With a standard gemological microscope such as the Gemolite, shadowing can be achieved in the following manner. The iris diaphragm of the microscope is first opened and the dark-field stop (light shield) is rotated out to produce a transmitted light mode in the microscope. The subject to be studied is placed in a stone holder or similar device and oriented so that light is being transmitted through the area of the gemstone that will be shadowed. Then the area of study is brought into sharp focus. Next the shadowing device is very slowly brought into the transmitted light path while the user looks at the image through the microscope. The shadowing shield can be inserted into the light path at any point between the light source and the subject. The author has placed the shadowing shield in the well of the microscope directly on top of the transmitted light diffuser and moved it with a pair of tweezers. He has also placed the shield on a glass slide directly below the subject, almost touching it, with equally good results.

As the shield is inserted, a dark shadow edge will begin to appear at the edge of the microscope's field of view. This is the out-of-focus image of the shadowing shield as it begins to emerge into the field of view. As it gets nearer the inclusion subject the shadowing will begin to take place until, at a particular point, the inclusion seems to almost instantly become three-dimensional, as if it were lifted from the host and placed on its surface. For the beginner, in the initial stages of experimentation with shadowing, the author suggests that perhaps the fixed-position dark-field light stop and/or the built-in iris diaphragm of a microscope like the Gemolite will be much easier to control than free-moving light shields such as those illustrated in figure 1.

With the iris diaphragm, simply stopping it down below the subject and partially blocking the transmitted light will produce a somewhat limited shadowing effect. The built-in dark-field light stop shield can also be used for shadowing either by itself or in combination with the iris diaphragm simply by rotating it gradually into the transmitted light path, producing a dark-field illumination/transmitted light combination. The limitation of both the built-in iris diaphragm and the dark-field stop, however, lies in the fact that they are actual parts of the microscope and cannot be moved about freely to find the optimum direction for shadowing.

The two critical steps in setting up for shadowing are (1) proper initial orientation of the subject, so that light is transmitted through the area to be shadowed; and (2) the slow, careful insertion of the light shield into the light path below the subject while observing the effect through the microscope.

RESULTS

In the opinion of the author, the image enhancement provided by the shadowing technique far outweighs the difficulties encountered in the discovery and early development of the method. In the initial study done on color and growth zones in flux-grown synthetic rubies, the obvious difference between the shadowed image and the unshadowed image, as illustrated in figure 4, was amazing. Slight growth undulations in the otherwise straight color zones became quite apparent in the shadowed view on the right. Without shadowing, as on the left, these same features were invisible.
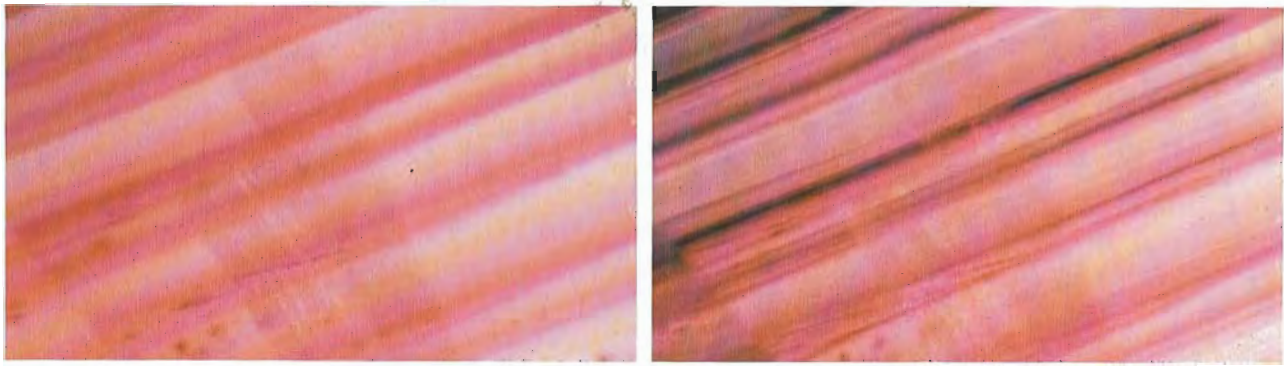
Figure 4. The growth undulations and slight curving seen in the shadowed color zones of this flux-grown ruby on the right are not seen in the unshadowed image shown on the left. Magnified 60×.

The author next experimented with transparent included crystals, and found that shadowing worked equally as well. He also determined that the shadowed image of most included crystals could be further enhanced by the use of shadowed polarized light. The three views in figure 5 vividly illustrate the transition from the unshadowed transmitted light image (far left) through the shadowed transmitted light image (center) to the shadowed polarized light image (far right) of these muscovite mica crystals included in beryl.

Other gemstones studied by the shadowing technique also responded favorably. For example,

swirl marks (schlieren), an important characteristic of glass (figure 6), can be greatly enhanced by shadowing, as can curved striae, the hallmark of flame-fusion synthetic rubies (figure 7).

CONCLUSION

Shadowing increases contrast in an inclusion scene with no ·visible loss of resolution, so the quality of the image is greatly enhanced. When viewing a crisper, sharper, more detailed image, the gemologist is less likely to overlook important internal features in a gemstone. Growth and color zones in both natural and synthetic gems

Figure 5. These muscovite mica crystals included in a Brazilian colorless beryl illustrate the effective use of shadowing on transparent included crystals. The view on the left shows the crystals as they appear in transmitted light without shadowing; the center photo shows the same inclusion shadowed. The view on the right shows the crystals illuminated by polarized light in combination with shadowing. Note the great amount of detail revealed in the two shadowed views. Magnified 80×.
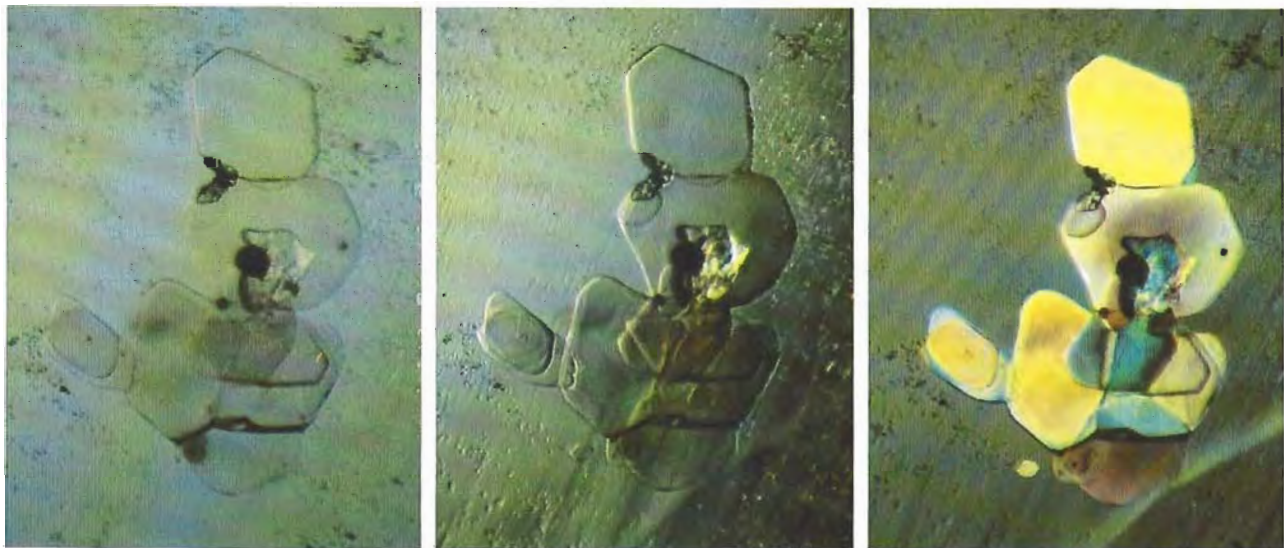
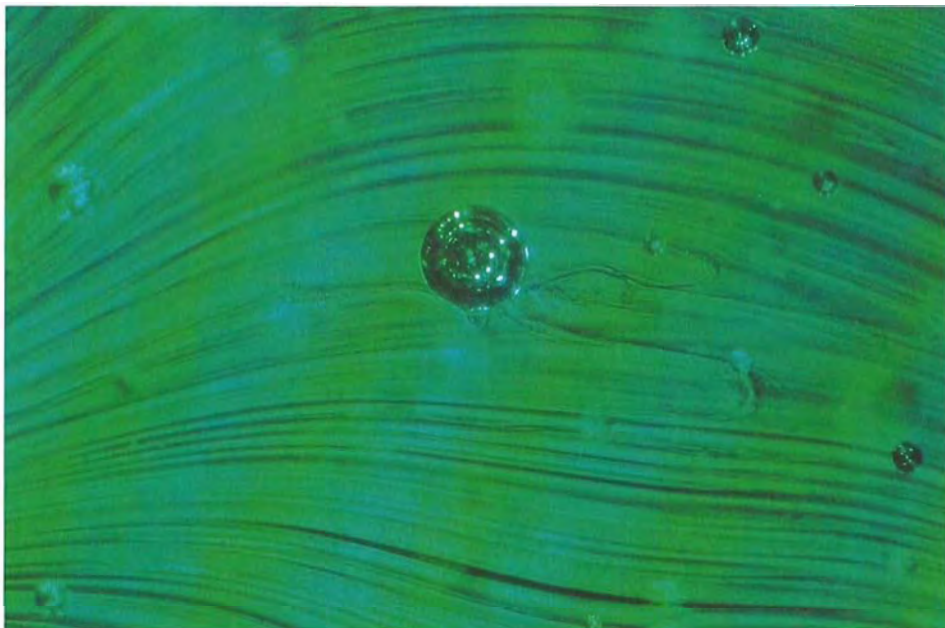*Figure 6. Swirl marks (schlieren) in a green glass appear in sharp contrast under shadowing conditions. Magnified 50×.*
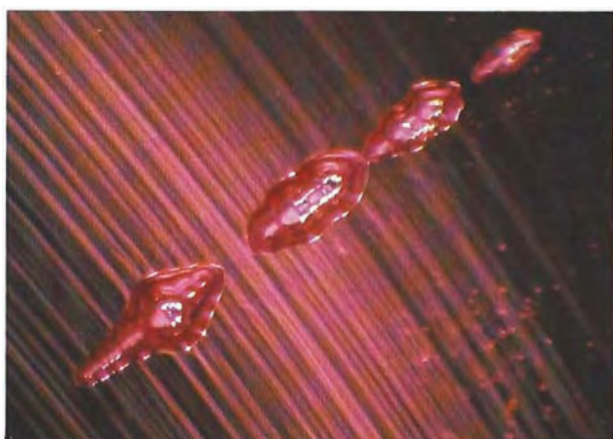

Figure 7. Curved striae, an important internal feature found in synthetic flame-fusion corundum, also respond to the shadowing technique. Here they are shown with typical gas bubbles as well. Magnified 100×.

are more readily studied, curved striae in flame-fusion rubies and sapphires will often take on a bold, three-dimensional appearance, and included crystals of all different types will look as if they have been taken from their host and laid on its surface.

Shadowing is a micro-technique that is both difficult to master and of admittedly limited application. Learning to use the shadowing tech-nique takes both time and a great deal of patience. It requires a gemologist who not only is a skilled microscopist but who also has a sound knowledge of both light interference and reflection and re-fraction for the initial set-up of the host and in-clusion subject.

In spite of these drawbacks, the technique of shadowing adds yet another new dimension to gemological microscopy and further increases the flexibility and available methodology, to the gem-ologist, of the standard gemological microscope. For those gemologists who wish to increase the contrast of an inclusion or study in greater detail otherwise vague and ill-defined internal images while, at the same time, expanding their own abilities with the microscope, the shadowing technique will undoubtedly prove useful.

REFERENCES

Gübelin E.J. (1957) Application of phase contrast microscopy in gemmology. *Journal of Gemmology,* Vol. 6, No. 4, pp. 151–165.

McCrone W.C., Delly J.G. (1973) *The Particle Atlas: Volume 1, Principles and Techniques.* Ann Arbor Science Pub-lisher, Ann Arbor, MI.

McCrone W.C., McCrone L.B., Delly J.G. (1979) *Polarized Light Microscopy.* Ann Arbor Science Publishers, Ann Ar-bor, MI.

NEW SYNTHETIC RUBIES MADE BY PROFESSOR P. O. KNISCHKA

By E. J. Gübelin

A new synthetic ruby, developed by Professor P. O. Knischka using a method of gradient technique (not yet disclosed) through supercooling and saturation, has distinct crystallographic and gemological characteristics. Particularly notable are the great number of faces on the finished crystals and the identifying inclusions.

Professor Paul Otto Knischka, an Austrian engineer, has been successfully producing synthetic rubies by a new method that he invented. This material is distinctive from other synthetic rubies in various features such as crystal forms, optical properties, and inclusions.

Although it is known that these new synthetic rubies are grown from a melt, Professor Knischka thus far has revealed only that they are crystallized synthetically by an as yet undisclosed method of gradient technique through supercooling and supersaturation. The finished crystals (figure 1) display flat brilliant growth faces with mineralogically significant indices. The great number of faces has heretofore not been observed. In addition, the elementary nuclei can be grown to macroscopic mono-crystals, twins, or multiple complexes, as well as clusters.

The crystallographic and gemological characteristics discussed below were determined by careful study by the author in his private laboratory, and through consultation with Professor Knischka. The reader is referred to a prior publication (Knischka and Gübelin, 1980) for information on the other properties of this material. The product, which is not yet commercially available, will eventually be marketed under the trademark ꟼK (Paul Knischka's initials with the "P" inverted).

CRYSTALLOGRAPHY

One of the most interesting features of these new synthetic rubies is the pseudocubic habit that

Figure 1. "Knischka" synthetic ruby crystal cluster, 10 mm.

some of the crystals adopt, although not all exhibit an isometric habit. Those that do normally show six forms: c (0001), $\underline{r}$ (10$\overline{1}$1), • (10$\overline{1}$9), d (01$\overline{1}$2), γ (01$\overline{1}$5), and n (22$\overline{4}$3), repeated several times.

These are forms that also occur in natural corundum, yet natural ruby seldom possesses more than 20 faces, whereas these new rubies by Professor Knischka develop a great number of crystal faces, some of which are extremely rare. In more recent productions the number of faces reached 38 (figure 2) and even 42 on one mono-crystal.

ABOUT THE AUTHOR

Dr. Gübelin is a certified gemologist in Meggen, Switzerland, and honorary professor at the University of Stellenbosch, South Africa.
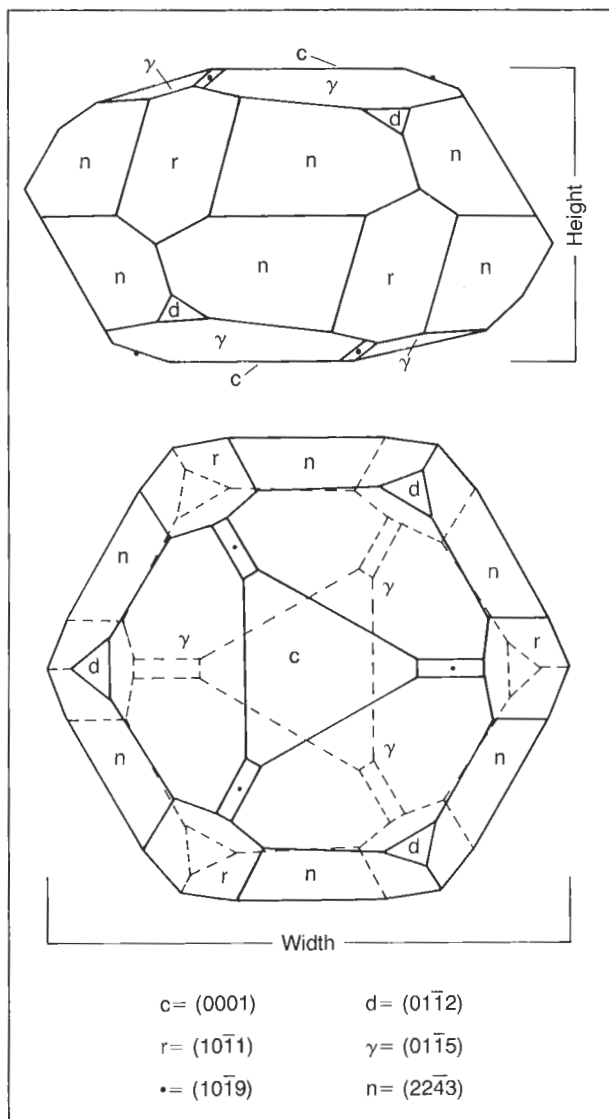
Figure 2. Isometric synthetic ruby by Professor Knischka, with 38 faces. H/W quotient = 0.47. Top = lateral view; bottom = overhead view.

c = (0001)	d = (01$\bar{1}$2)
r = (10$\bar{1}$1)	γ = (01$\bar{1}$5)
• = (10$\bar{1}$9)	n = (22$\bar{4}$3)

Figure 3. Absorption spectrum (200–800 nm) of a "Knischka" synthetic ruby.

GEMOLOGICAL CHARACTERISTICS

The new synthetic rubies call for increased care on the part of the gemologist. In order to gain a proper account of this significance, a thorough examination was carried out with several cuttable crystals whose smooth crystal faces allowed comprehensive gemological tests, as well as with some cut samples.

Appearance. It is as difficult to see a difference in the appearance of this stone compared to natural ruby from various locations as it is to see a difference compared to synthetic rubies grown by other methods. The difference is greatest at first
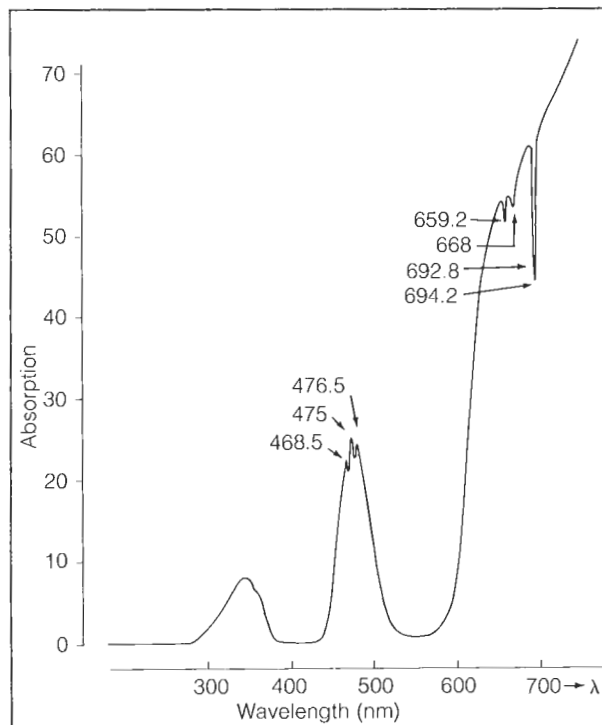
sight between these and Burma rubies, whose luxurious pigeon-blood red was not duplicated in the "Knischka" synthetic product examined. The red color of Professor Knischka's synthetic ruby shows a clear violet tinge, and the best material varies on the color samples of the DIN color chart 6164 from 10:7:3 for the redder to 10,5:6,5:4 for the violet-tinged samples.

Spectrophotometric Examinations. The spectral curve for this material, illustrated in figure 3, corresponds in all stages with the normal and familiar curve of natural as well as synthetic rubies between 400 and 750 nm. However, the particular character of the maximum transmission between 250 and 400 nm is indicative that the examined ruby was synthetic.

The observed color range also corresponds to the absorption spectrum observed in the optical spectroscope, which embraces all the transmission maxima known for ruby in the blue and red regions, together with accompanying chromium lines at 659.2, 668.0, 692.8, and 694.2 nm as well as the absorption maxima at 550 and 410 and from 270 nm downwards (again, see figure 3).

A third transmission maximum at the short-wave end of this graph, at 345 nm, is rare with

Figure 4. Integral picture of the interior of a cut synthetic ϗ ruby with cloudy veils. Magnified 10×.
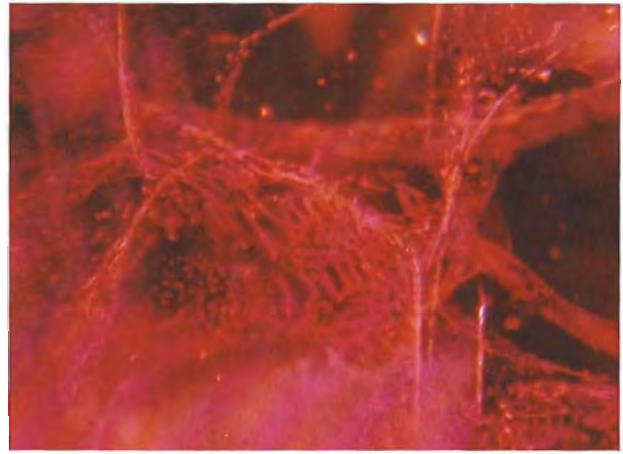

Figure 5. Net-like moisture-banners (healing fissures) which are usually discernible from similar inclusions in natural ruby by their typical pattern. Magnified 25×.

natural rubies but common with synthetic rubies. It would, however, be inadvisable to rely completely on this transmission maximum in the ultraviolet region.

Dichroism. This property is very strongly defined, with the twin colors purple-red and orange-red, but it does not help differentiate this synthetic from natural ruby.

Luminescence. When exposed to short- and long-wave ultraviolet radiation as well as to X-radiation and the "crossed filter" method applied for tests of the property, the "Knischka" synthetic rubies glowed clearly to strongly carmine red. After exposure to X-rays, a weak afterglow of phosphorescence was observed, lasting about seven seconds. This might help differentiate the stone from natural ruby, and is a consequence of the fact that natural ruby contains more iron than its synthetic counterparts.

Refraction and Double-Refraction. Neither the refractive indices nor the birefringence of this synthetic show diagnostically important values or anomalies; that is, they show exactly the same constants as are known for natural ruby: $n_\epsilon =$ 1.760– 1.761, $n_\omega = 1.768$–1.769, $n_\epsilon - n_\omega = -0.008$.

Specific Gravity. The synthetic material shows minor variations in density between 3.971 and 3.981, and can be stated as having an average value of 3.976 ± 0.001 g/cm³.

Inclusions. To the unaided eye, there is nothing to be seen inside the material that might give definite and immediate proof of synthesis. Yet the interiors of several samples showed a broad, phantom-like cloud that varied in size from one sample to the next and was reminiscent of the dust-like clouds in Burmese rubies (figure 4). Viewed with a pocket lens—or, even better, under the microscope—the inclusion scene is revealed in considerable detail, with swirls of color, liquid feathers, negative crystals, black platelets, and two-phase inclusions.

The nature of the turbid clouds could not be determined even with the strongest magnification. The liquid feathers, with their irregular course and net-like pattern (figure 5) are remarkably similar to those in the synthetic rubies by Chatham and are sometimes difficult to distinguish from the fluid inclusions in natural ruby. The negative crystals (figure 6) unmistakably follow the characteristic crystal habit of rubies grown by this method. They perch, usually alone or in small groups, on the ends of long crystalline tubes, and they can be considered identifying features.

Equally characteristic are the small, distorted, hexagonal platelets of platinum or silver that can be observed now and then in synthetic stones but are never seen in natural gemstones. However, the manufacturer of the "Knischka" product states that he can now repress the formation of such platelets during the growth process.

The comparatively large gas bubbles, already visible under low magnification, prove under higher magnification to be the gaseous part of two-phase inclusions, whose contours within the ruby are astonishingly fine, almost to the point of invisibility (figures 7 and 8). These inclusions,
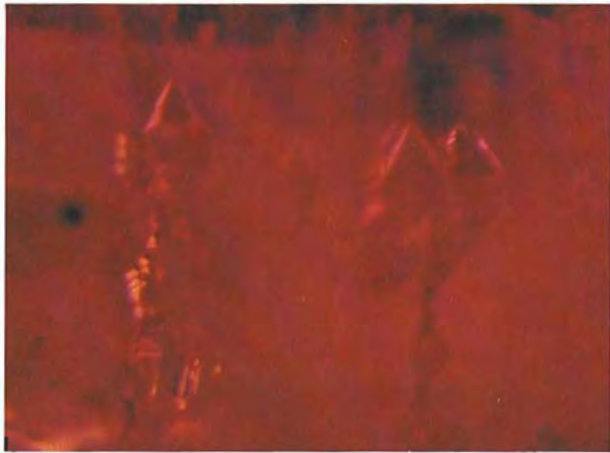
Figure 6. These negative crystals follow the trigonal-dipyramidal habit of the host crystal, terminating crystalline rods. Magnified 25×.
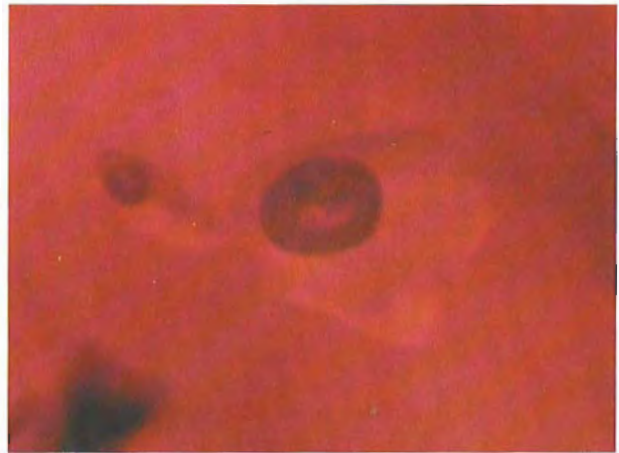

Figure 7. Two-phase inclusion with a large bubble and barely visible form. With a pocket lens or other weak magnification, one would see only the gas bubble. Magnified 64×.

which sometimes appear as negative crystals and sometimes as irregular shapes, must contain a highly refractive substance, the chemical properties of which could only be determined by mass spectroscopy or by the manufacturer's disclosure of the process he has developed. This knowledge, though, is of little importance in the recognition of these synthetic rubies or in their distinction from either natural or other synthetic rubies. However, the distinctive two-phase inclusions in the interior scene of these synthetic rubies are a novelty and can be regarded as an identifying characteristic of Professor Knischka's synthetic rubies.

Although the inclusion assemblage of the synthetic rubies is similar to the internal world of natural rubies, particularly those from Burma, under strong magnification it differs very clearly from that of its natural counterpart. In the same way, these synthetic rubies differ from all other synthetic rubies in the exemplary singularity of their inclusions, and therein lies the challenge to greater care and attention mentioned above.

SUMMARY AND OUTLOOK

These synthetic rubies were grown according to a method as yet undisclosed. Nevertheless, they have characteristics that closely correspond to those of natural rubies as opposed to the curved layers of inclusions seen in synthetic Verneuil rubies influenced by the boule. Only by careful doc-

Figure 8. Complex underlaying of several two-phase inclusions with large gas bubbles and partly crystalline forms. Magnified 64×.

umentation of all the properties and meticulous attention to the detailed characters of the inclusions can one hope to ascertain the synthetic origin of this new product.

REFERENCE

Knischka P.O., Gübelin E. (1980) Synthetische Rubine mit Edelsteinqualität, isometrischem Habitus und hoher Zahl unbeschädigter Kristallflächen. Zeitschrift der Deutschen Gemmologischen Gesellschaft, Vol. 29, No. 3/4, pp. 155–186.

Gem Trade LAB NOTES

CHALCEDONY, Repaired Cameo

Recently brought to the Los Angeles laboratory for identification was a beautiful cameo, measuring 20.5 × 31.6 mm, set in a yellow and white metal antique brooch, with three pearls and numerous diamonds (figure 1). The brooch was represented as being an original Fabergé piece. The cameo had at one time been broken in the upper right corner; the broken portion was reattached with a plastic-type cement of the same color as the cameo. The repaired portion looked very good to the unaided eye and almost restored the cameo to its original appearance.

Figure 1. Brooch set with a 20.5 × 31.6 mm cameo that was damaged and subsequently repaired.

DIAMOND

Fake Crystal

The Los Angeles laboratory recently received the rough specimen shown in figure 2. The client explained that the stone was one of a parcel of about 30 rough diamonds that weighed a total of approximately 60 ct. When one of the client's cutters was placing flats on the crystals in preparation for sawing, he came to a piece that did not respond to the lap as diamond would be expected to. This one was much softer, and thus cut very rapidly. Suspecting it to be a diamond substitute, the client brought the crystal to us for identification. Subsequent testing proved it to be cubic zirconia, fashioned into a
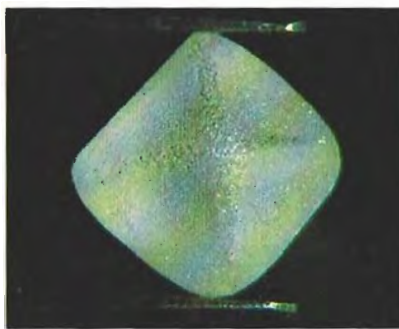
Figure 2. Cubic zirconia fashioned to simulate a rough diamond crystal, 2.68 ct.

2.68-ct slightly distorted octahedral shape with the surface roughened, possibly sandblasted or tumbled, to resemble the skin of a rough diamond.

Rare Inclusion in Diamond

All three labs had the opportunity to examine a 0.47-ct round brilliant–cut diamond with a color-change garnet crystal inclusion that reached the table of the stone. Figure 3 shows the red color of the garnet in the tungsten lamp lighting of the microscope. Figure 4 shows the purplish blue color of the inclusion in fluorescent lighting, approximating daylight. This type of garnet inclusion has been noted in Russian literature, though the source of the stone examined in our lab is not known.

EMERALD

Cat's-eye Emerald

Fine cat's-eye emerald is an attractive rarity. Two such stones, weighing slightly over 5 ct each, were brought into the New York laboratory recently. They were almost a pair, and each had an eye as good as any we have ever seen in this rare material (figure 5).

Manufactured Emerald Specimens

Mineral specimen fakes have been previously described in this publication and elsewhere in the gemological literature. One of the oldest fakes reported is a specimen that is part of a sculpture entitled "Moor with Tray of Emeralds," which dates back to around 1724. The emerald-in-matrix specimen in this statue was traced back to 1581. The specimen consists of 16 emerald crystals, which appear to be of Colombian origin, all manually embedded
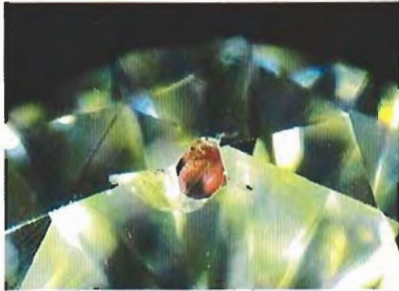
Figure 3. Color-change garnet
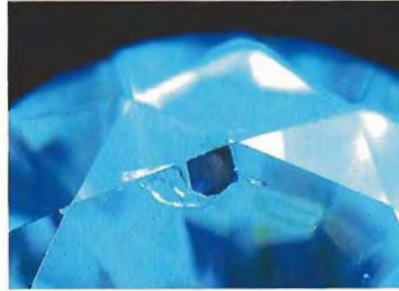inclusion in diamond
under incandescent light.
Magnified 30×.

Figure 4. Color-change garnet
inclusion in diamond
under fluorescent light.
Magnified 30×.

into crude holes carved into the matrix. Similar types of "manufactured" mineral specimens are reportedly quite prevalent in today's market, especially in Bogotá, Colombia.

Often, these fakes are made by carving a depression in a suitable piece of matrix and then attaching the emerald crystal or crystals with an epoxy cement that may or may not be mixed with powdered matrix or related mineral matter. Some of the recent fakes are quite clever and may not be detectable to the unaided eye, often requiring very careful examination with a microscope in conjunction with a hot point. We recently had the opportunity to examine several of these fakes in the Los Angeles laboratory; two of them are shown in figures 6 and 7.

One very successful technique used in identifying these fakes is to remove a small amount of the suspected cement around the base of the crystal with a razor blade. Cement is usually much softer than matrix and may be a different color if it has not been mixed with a powdered matrix. The material on the razor blade is then tested with a hot point to see if it melts or gives off an odor, both indications that the substance is a cement.

The use of ultraviolet light may also be helpful. Most epoxies and glues fluoresce to either long-wave or short-wave ultraviolet radiation (or both, stronger to long-wave).
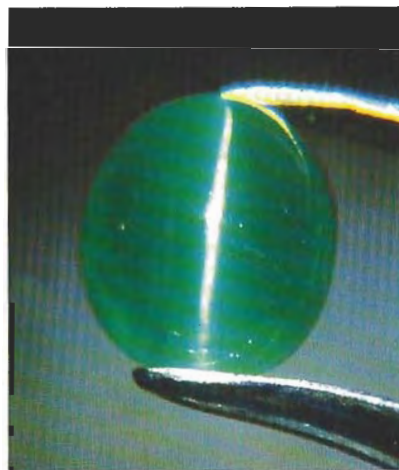

Figure 5. Cat's-eye emerald,
approximately 5 ct.

Another slightly different "manufactured" mineral specimen is shown in figure 8. This one was particularly intriguing: it was composed of many crystals and fragments (both opaque and transparent) of emerald and green beryl ranging from less than 1 mm to 27 mm in length, together with many fragments and crystals of pyrite along with a few other sparsely placed minerals. All were glued with an excessive amount of epoxy onto a base of undetermined composition. The coating of crystals varied in thickness from approximately 2 mm to 10 mm; in a few small areas there was no coating and the exposed base was quite visible. Also intermixed with the applied crystals and epoxy were many gas bubbles and fibers that were perhaps from a brush used to apply the epoxy.

Synthetic Emerald

The New York laboratory recently received two examples of a new French synthetic emerald that is being introduced with the trade name Lennix. The properties of this material are typical of flux-grown synthetic emeralds, that is, low refractive index, low specific gravity, and strong red ultraviolet fluorescence. Under magnification, how-

Figure 6. Emerald crystal glued on matrix. Crystal measures 5.05 × 8.30 mm.

Figure 7. Emerald crystal recessed into a matrix specimen containing numerous naturally occurring smaller beryl crystals. Crystal measures 13.9 × 20.6 mm.

Figure 9. Unidentified opaque black inclusions in synthetic emerald. Magnified 20×.

ever, we noticed several fairly large, black, opaque, irregular, unidentified inclusions (figure 9) in addition to the flux fingerprints commonly seen in synthetic emeralds grown by the flux method.

IOLITE, An Unusual Cat's-eye

The staff at the Santa Monica laboratory had the opportunity to examine an attractive, translucent, grayish blue oval iolite cabochon with a fairly diffuse eye. The 13.91-ct stone reportedly came from India. Iolite, our gemologist readers will recall, is also known as cordierite after the French geologist Cordier, or as dichroite on the basis of its pronounced pleochroism. The properties of this stone were determined as follows: refractive index (spot method) 1.54, with weak birefringence; specific gravity, estimated with heavy liquids, approximately 2.56. A rather faint biaxial figure could be resolved in the polariscope.

Under magnification, the stone showed primarily fine, long, parallel, needle-like inclusions which produced the cat's-eye effect. Unfortunately, the identity of these inclusions could not be determined during the short period of time the cabochon was in the laboratory.

As is to be expected, the absorption spectrum of iolite, which is due to its Fe content, varies with the direction the light passes through the stone. Therefore, two faint lines centered at 490 nm and 590 nm were visible only when the stone was viewed through the long axis.

Figure 8. Specimen manufactured out of beryl and pyrite cemented on a base, 78 × 69 × 39 mm.

JADE IMITATION

Submitted to the Los Angeles laboratory for identification was a translucent green hololith measuring approximately 8.69 mm in outside diameter by 1.53 mm thick (see figure 10). To the unaided eye, and even under magnification, this stone bore a remarkable resemblance to jadeite.
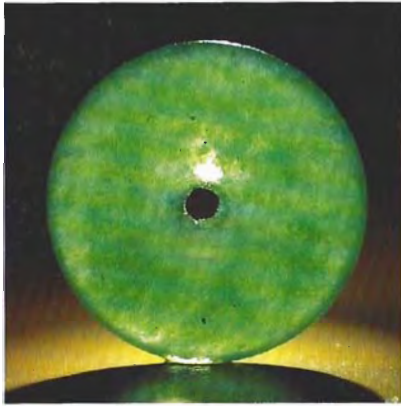
Figure 10. Glass hololith that imitates jadeite. The piece measures approximately 8.69 × 1.53 mm.

Testing, however, proved that it was not. A refractive index of approximately 1.62 was obtained using the spot method. The specific gravity was found to be 3.38 by the hydrostatic method. No absorption spectrum was observed other than a lightly shaded area in the blue and far red regions of the visible spectrum.

The stone was sent to our Santa Monica laboratory where a minute amount of powder was scraped from it for X-ray diffraction. The diffraction pattern revealed an amorphous structure indicative of glass. In appearance, this is certainly one of the most realistic jade imitations we have encountered.

LAPIS LAZULI IMITATION

Submitted to the Los Angeles laboratory for identification was an opaque, dark blue, 11.9-mm round drilled bead (figure 11). The client explained that the bead was from one of many necklaces that he had purchased as lapis lazuli.

When we tested this bead for dye with an acetone-soaked cotton swab, no stain was produced; however, when a solution of 10% hydrochloric acid was used, a very dark blue stain was observed on the cotton. Although the material effervesced to the acid, there was no hydrogen

sulfide (rotten egg) odor, leading us to suspect that the bead was a dyed substance other than lapis lazuli. Since we were unable to obtain a spot refractive index due to the very poor polish of the material, we asked the client to have the bead repolished. We were then furnished with one half of the bead with a polished flat (figure 12), and it was quite obvious that our suspicions were correct. With further testing, the bead was identified as dyed marble. X-ray diffraction confirmed that the material had a calcite pattern.
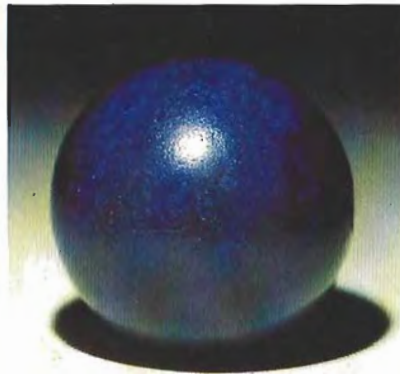

Figure 11. Imitation lapis bead, actually dyed marble, 11.9 mm.

PINK OPAL, a Rare Bird Indeed

The Santa Monica lab received for identification a variegated light pink and gray carved and assembled bird with brown beak and white metal feet (see figure 13). According to the owner of the piece, the material from which the bird had been carved was represented to be opal. Visual examination indicated that only very limited gemological tests could be performed. The textured surface of the opaque bird together with a lack of polish did not allow us to obtain a refractive index or any other optical properties. Because of the size of the carving and the fact that it had been assembled with metal legs, the specific gravity could not be de-

termined either. Under the spectroscope, the material did not show any absorption lines and there was no reaction to ultraviolet light. It became obvious that the material could only be identified by means of X-ray diffraction. Therefore, a minute scraping was taking from the body of the bird for the analysis. The diffraction pattern revealed weak lines for palygorskite and cristobalite, superimposed on a strong amorphous pattern suggesting opal. The palygorskite is a clay mineral frequently encountered in this type of

Figure 12. Cross-section of bead in figure 11 shows depth of dye penetration.

pink opal. When pink opal of this nature first appeared on the market in the mid-1970s, palygorskite was

Figure 13. Pink opal carving, 12 × 10.2 × 5.7 cm high.

identified by means of X-ray diffraction to be present as well.

Conch "PEARL"

The Santa Monica laboratory recently identified a beautiful, oval-shaped, purplish pink calcareous concretion measuring approximately 7.15–8.20 mm in diameter by 9.60 mm long. Figure 14 shows this attractive little "gem," commonly called a conch "pearl," which was found in the Caribbean area. The flame-like structure on the surface of this bead is characteristic of a conch "pearl" and serves to identify it.

SAPPHIRE, Diffusion Colored

The first reaction we had to a group of 21 quite "clean" blue cabochon natural sapphires received in our New York lab was: "Something is suspicious. Why didn't the cutter facet them?" Sure enough, under immersion the color proved to be surface induced, or as we state on reports: "Natural sapphire with color synthetically enhanced by a surface diffusion process." We are definitely against saying "Natural sapphire, treated color," because it is not the
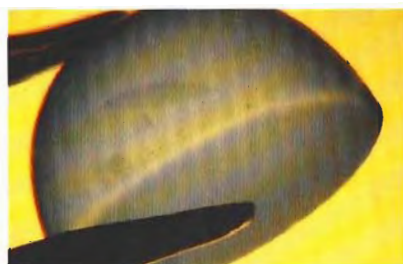

Figure 15. Girdle edge of a diffusion-treated blue natural sapphire cabochon. Magnified 10×.

same as, nor as durable as, plain heat treatment. The evidence of surface diffusion of blue natural sapphire cabochons is best seen at the girdle edge (figure 15).

SPINEL?

An opaque, apparently black, oval faceted stone weighing 15 ct arrived in our New York lab with a note stating that it was cut from a portion of a Mexican meteorite named "The Black Ruby." A vague refractive index could be seen at approximately 1.77. Figure 16 shows a poorly polished brecciated table, which accounted for the hazy R.I. reading. Also as shown in the photo,
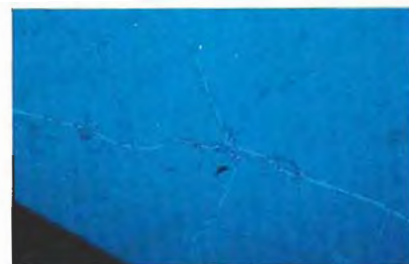

Figure 16. Table of a black spinel? Note the metallic veins in this 15× magnification.
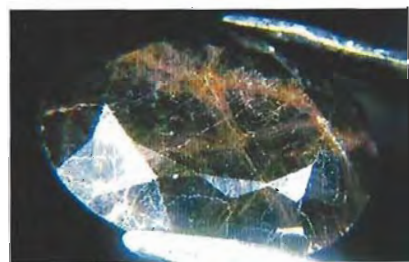
Figure 17. Strong side light on stone in figure 16 shows true color. Magnified 10×.

seams of a bright metallic substance criss-crossed the table, although the stone was not attracted to a magnet. A specific gravity of 3.83 was found, so corundum was ruled out.

With strong side lighting from a pair of fiber optic probes, an entirely different stone appeared (figure 17). The stone now seemed semi-opaque with brown zones outlined by the metallic seams. Unfortunately, we were not permitted to secure powder for an X-ray diffraction to substantiate our tentative identification that the stone is probably not meteoritic, but rather is a variety of spinel.

Figure 14. Conch "pearl" measuring 7.15–8.20 mm in diameter by 9.60 mm long. Note the characteristic flame-like structure.

GEMOLOGICAL ABSTRACTS

Dona M. Dirlam, Editor

COLORED STONES AND ORGANIC MATERIALS

Connoisseurship in pearls. B. Zucker, *Connoisseur*, Vol. 208, No. 837, 1982, pp. 194–197.

Benjamin Zucker briefly discusses some historical pearl events, the beauty of natural pearls, and the birth of cultured pearls. He begins with an account of "the

most beautiful pearl object in the world": a ten-foot by six-foot pearl rug in the palace of Baroda, India. It is made entirely of very well matched pearls that have been woven together, with diamonds sewn into the tassels. He presents this within the context of the history of natural pearl production, reminding us that a natural pearl is a unique gem in that it is found in its completed state. The finest natural pearls are perfectly round, whitish or slightly whitish pink, with fine luster, shiny orient, and good size. Pearls over 10 mm are exceptionally rare. Quality, however, is more important than size.

In the early 20th century, wealthy women wore pearl necklaces that would have been worth millions of dollars at today's prices. In 1930, however, the sky-high prices of natural pearls dropped, brought down by the failing economy and the appearance of cultured pearls on the market. At this point, distinguishing between natural and cultured pearls became an important scientific problem.

K. Mikimoto was a pioneer in the pearl-culturing trade. The author suggests that his particular expertise was in marketing these pearls. Zucker touches on the

Japanese method of culturing pearls, in addition to the standards these pearls must meet. It is interesting to note that the Japanese Chamber of Commerce insists on the destruction of poor-quality pearls.

Kerry Werner

Historic Blue John and other flourites. R. P. Mac Fall, *Lapidary Journal*, Vol. 35, No. 10, 1982, pp. 1998–2016.

Beginning with a brief history of Castleton, England, Mac Fall describes the lead-zinc mines of the region, which are famous for the occurrence of a rare form of fluorite dubbed "Blue John." After speculating on the derivation of the term *Blue John*, Mac Fall describes the formation of this fluorite and theorizes about the cause of its color.

The author then traces this bluish variety of fluorite from its original site through the mining process and the steps taken to work it into articles of decoration and jewelry. Also discussed are the many uses of fluorite in industry and the many production sites in the U.S. and other countries, including the history of some of the more important locations. *RSS*

Recent observations on an apparently new internal paragenesis of beryl. E. J. Gübelin, *Journal of Gemmology*, Vol. 17, No. 8, 1982, pp. 545–554.

Dr. Gübelin has observed some interesting inclusions in beryls from such localities as Afghanistan, Brazil, Kenya, and Switzerland that had never been reported before. Beryls from each of these occurrences had at least one guest mineral in common. In a colorless beryl from Brazil, the association of muscovite, phlogopite, and niobite was observed. Another beryl from Brazil added a manganese-apatite to this association.

An aquamarine from Afghanistan showed a spessartite garnet inclusion with muscovite. An aquamarine from Kenya had inclusions of albite, spessartite, phlogopite, gahnite, niobite, and tourmaline.

Gübelin demonstrates the value of inclusions for determining the origin of gemstones. Niobite is of utmost importance in understanding the paragenesis of the inclusions in the beryls discussed here. The environment of niobite is a manganese (Mn)-rich granitic pegmatite with albite and lithium minerals. This allows a Mn garnet (spessartite) and Mn-rich apatite to occur in the same host crystal. *GSH*

Of taaffeite, painite, charoite, etc. E. Tucker, *Jewelers' Circular Keystone*, Vol. 152, No. 9 (Part II), 1981, pp. 92–98.

Evelyn Tucker describes the most important gemological finds of the last 40 years in this article. With engaging prose, Ms. Tucker traces the natural colored stones discovered since 1942, describing their appearance, interesting facts about their discovery, and their place in gemology. Her carefully referenced discussion includes the popular tsavorite garnet and tanzanite as well as rarer specimens such as liddicoatite, red beryl, and maw-sit-sit. By capsulizing important gemological information, Tucker's article provides a handy reference to developments during this period. *JMH*

Taprobanite, a new mineral of the taaffeite group. R. Moor, W. F. Oberholzer, and E. Gübelin, *Schweizerische Mineralogische und Petrographische Mitteilungen*, Vol. 61, No. 1, 1981, pp. 13–21.

Both the title and the content of this article are somewhat misleading because they suggest that the rare gemstone referred to as "taprobanite" ($BeMg_3Al_8O_{16}$) is a valid new mineral species distinct from taafeite. While the species status of "taprobanite" was initially sanctioned by the International Mineralogical Association Commission on New Minerals and Mineral Names, on the basis of more recent data the commission has since ruled that both "taprobanite" and taaffeite belong to the same species, and that only the original name taaffeite should be retained for this mineral. Nevertheless, this article presents new and valuable mineralogic data on one apparent compositional variety of this very unusual mineral species.

These investigators examined a 204-mg stone cut from a single, hexagonal-prismatic crystal from an unknown locality in Sri Lanka. Their data further confirm the recognized close relationship between taaffeite and spinel. X-ray study of their specimen showed the mineral to be hexagonal, in space group $P6_3mc$, a=5.684 Å, c=18.332 Å, Z=2. The strongest X-ray diffraction lines (39 given) are 2.415 (100) (114), 2.595 (60) (106), 2.043 (60) (205), 4.58 (50) (004), 1.469 (50) (2,0,10), and 1.421 (50) (220), which is consistent with X-ray data reported earlier. In addition, these investigators present a refinement of the crystal model of their material: a structure that consists of a close-packed framework of oxygen atoms arranged in a distinct, eight-layered, stacking sequence. Aluminum atoms fill half of the octahedral sites in this framework, whereas both beryllium (Be) and magnesium (Mg) atoms occur in the tetrahedral sites. They suggest that the closely related crystal structures of taaffeite (and its varieties) and spinel can be described in terms of different stacking sequences of oxygen atoms and by variations in the relative occupancy of sites in the oxygen framework by metal atoms.

The specimen examined has a hardness of approximately 8, apparently lacks cleavage, and has a conchoidal fracture. Its density is 3.588 g/cm³ (calc.) and 3.605 g/cm³ (meas.). It is optically uniaxial negative and is pleochroic—ϵ=1.717 (yellow rose) and ω=1.721 (carmine red). The unusual bright red color of this stone has not been reported previously for taaffeite.

On the basis of analysis by electron microprobe and atomic absorption spectroscopy methods, the tabulated

chemical data, and a calculated chemical formula, the authors suggest that the Be:Mg ratio in their specimen is 1:3., which is quite different from the compositional data for the taaffeite originally described, where the Be:Mg ratio is 1:1. Thus, one can infer that the chemical composition of taaffeite may extend over a variable range (in terms of Be and Mg) intermediate between spinel and chrysoberyl. Further confirmation of this feature must await recognition and examination of additional crystals of this rare gem material.

James Shigley

DIAMONDS

Color centres in diamond. A. T. Collins, *Journal of Gemmology*, Vol. 18, No. 1, 1982, pp. 37–75.
Color centers in diamond are characterized as point defects in the diamond lattice which give rise to optical absorption in the visible spectral region. Dr. Collins presents a comprehensive study of the various color centers that can occur in colored diamonds. Much of the early work on colored diamonds was pioneered by B. W. Anderson using the hand spectroscope; today, however, modern research involves the use of the spectrophotometer.

In a detailed and well-indexed article, Dr. Collins proceeds to describe the various absorption systems in diamond. He emphasizes the inaccuracy of transmission spectra (hand spectroscope) and stresses the absorption measurement as an accurate means of determining the absorption coefficient, that is, how strongly a diamond is absorbing at a particular wavelength. This is a determining factor in deciding whether the diamond has been artificially colored. A brief explanation of the instrumentation and optical system used by the author first acquaints the reader with the intricacies of recording and evaluating spectral data. Dr. Collins then discusses systematically the various types of diamonds and their respective absorption features, beginning with a section on pure diamond and the properties associated with this unique structure of carbon atoms, before turning to impurity-induced color centers and vibronic color centers.

The two major color-causing impurities in diamond are nitrogen (which produces yellow) and boron (which produces blue). The author presents schematic diagrams representing the electron bonds between such atoms in the diamond lattice to help the gemologist better understand the nature of these particular color centers. Other absorption features seen in the visible range in diamond are labeled vibronic centers. These are absorption and luminescence bands that arise when the electron in an optical center is excited (i.e., given energy) and at the same time vibrational energy is transferred to the crystal lattice. Using the clever analogy of a snooker table and a selected arrangement of balls, the author explains the process of the transfer of electronic energy within a crystalline lattice. The transfer of energy from a ground state to an "excited state" corresponds to the electronic transition (absorption) at a color center in a crystal.

Noting the effects of temperature, the author discusses the important vibronic bands individually, concluding with information on the irradiation methods used to alter color in diamonds and the various color varieties of natural and artificially colored diamonds. Among the sections covered are natural pink and mauve diamonds, treated pink diamonds, natural green diamonds, brown diamonds, and miscellaneous absorption lines observed in diamonds.

In the summary, Dr. Collins presents some of his thoughts concerning the future of diamond testing, noting that there are still instances where modern science cannot determine with certainty from the spectroscopic tests whether certain diamonds are treated or natural. This article is a valuable contribution to the science of gemology and is a must for anyone interested in diamonds and their properties.   *SCH*

Famous diamonds of the world (XI): the Regent diamond. I. Balfour, *Indiaqua*, Vol. 30, No. 3, 1981, pp. 119–125.
The most important item in the French crown jewels, the Regent diamond, has played a prominent role in the intrigues of French politics. With one of the most fascinating histories of any of the famous diamonds, it is also one of the last large diamonds found in India.

The Regent diamond was discovered in 1701 in the Partial deposits on the lower Kistna River in India. The 410-ct rough stone was reportedly found by a slave who smuggled it out of the mine by concealing it in a leg wound. The slave was soon deceived by an English ship captain, and the stone was eventually sold to Thomas Pitt, the president of Fort Madras. The new owner had the stone cut to a cushion shape with a weight of 140.5 ct (it is reported to be the best cut of the older famous stones). The Pitt diamond, as it was then called, did not give the owner piece of mind; after several attempts to dispose of it, he sold the diamond to the regent of France, the Duke of Orleans. Now with a new name, the Regent diamond passed first to Louis XV and then to Louis XVI, whose queen, Marie Antoinette, had it reset often. Following the French Revolution, the Regent was stolen from the treasury along with the "Sancy," the "Blue Diamond," and other treasures. Recovered a year later in a Paris attic, the Regent was used as collateral by the new republic in a number of complicated financial transactions.

Napoleon put the diamond to more personal use by mounting it in the hilt of his court sword. Following the death of Napoleon and a brief stint out of the country, the Regent was returned to the Crown; fortunately, it was not included among the many other pieces of the

crown jewels that were sold in 1887. It can now be found in the Galerie d'Apollon of the Louvre.

Ian Balfour has retold an intriguing tale that should engage everyone. Fifteen illustrations, including a recent photograph of the Regent, accompany the text.
FLG

Migrating nitrogen atoms in diamond. G. Davies, *Nature,* Vol. 292, No. 5821, 1981, pp. 288–289.

The author summarizes the current knowledge concerning the migration of nitrogen impurities in diamond by citing key experiments and observations of leading diamond researchers. Aggregation experiments provide a tool for studying the geology and physics of diamond. Most gem-quality diamonds contain impurities of nitrogen, typically about one nitrogen atom per 1,000 carbon atoms. Nitrogen atoms can occur as isolated atoms each replacing a carbon atom (the simplest form), or as groups or clusters of nitrogen atoms referred to as aggregates.

Experiments have shown that in high-temperature treatments of natural and synthetic diamond, the isolated nitrogen will migrate first to form pairs and then to form even larger aggregates. The longer the diamond is held at high temperatures, the farther the aggregation proceeds. This has led diamond researchers to theorize that the state of aggregation in any diamond gives some idea of the length of time it has been heated.

Davies also mentions how each form of nitrogen atoms—isolated, pairs, and triangles—is responsible for the specific absorption of electromagnetic energies. This absorption, if in the range of visible light, will affect the body color of the diamond.

Larger defects, called platelets, seen in some diamonds are also mentioned by Davies. Future experimentation to determine the correlation between nitrogen concentration and the number of platelets is forthcoming in the 1980s. Key experiments to determine the thermodynamics of the migration and aggregation of nitrogen atoms along with accurate calibrations could establish more about the role of nitrogen in diamond.
SCH

Mineral inclusions in zircon from the "Mir" kimberlite pipe (in Russian). A. I. Botkunov, V. K. Garanin, G. P. Kudrjavceva, and M. S. Perminova, *Papers of the Soviet Academy of Sciences,* Vol. 251, No. 5, 1980, pp. 1233–1236.

"Zircon is a rare mineral, but one constantly encountered in many of the kimberlite pipes of Yakutia." The authors of this article continue by describing their survey of numerous zircon nodules from fracture concentrates at the Soviet Union's most famous diamond-producing kimberlite pipe, the Mir, in north central Siberia. Using optical and electron microscopy, as well as computerized electron-probe instrumentation, the team completed detailed studies of both the morphology and the chemical content of various solid inclusions noted in the zircons.

Three major types of inclusions are discussed. Crystals of chrome-spinellide, which occur as distorted octahedrons up to 3 mm, are described as high in titanium but comparatively low in aluminum oxide. Sulfide inclusions, distinguished by admixtures of nickel, iron, and copper, form hexagonal shapes up to 2 mm. Small discs or ellipsoids of calcite reveal slight traces of magnesium.

Detailed analyses, tables, and four photographs support the researchers' conclusion that the crystals of chrome-spinellide and sulfide in the zircon formed before the host material, whereas the calcite inclusions are syngenetic and crystallized out of the kimberlite magma during its ascent. A thorough bibliography is included.
MPR

GEM INSTRUMENTS AND TECHNIQUES

GE develops process to brand codes in diamonds. S. Goldman, *National Jeweler,* Vol. 26, No. 9, 1982, pp. 41–42.

Two employees of General Electric in Schenectady, New York, have developed a way to brand diamonds with the use of an ion implanter. Robert C. DeVries and Roy E. Tuft have recently received a patent on the process, in which a beam of charged ions penetrates the surface of the diamond. These ions create an area on the surface with an electrical conductivity distinct from the rest of the stone. A mask with an individualized symbol may be used to create a specific pattern. The image can then be revealed by giving the diamond an electrostatic charge (e.g., rubbing it with a piece of silk or cotton) and subsequently dusting it with a special powder. The powder adheres only to the charged region, thus exposing the branded pattern. Although this new concept is an excellent way of identifying a diamond without damaging the stone, it is expensive and not without problems. The ion-implanter ranges in cost from $300,000 to $600,000, and the image can be removed by recutting or repolishing the stone. *LCH*

GEM LOCALITIES

Amethyst from the Thunder Bay region, Ontario. D. G. Elliott, *Mineralogical Record,* Vol. 13, No. 2, 1982, pp. 67–70.

Although amethyst has been collected in the Thunder Bay region of Ontario, Canada, since the 1880s, the most recent burst of activity began in 1967 with the opening of the Thunder Bay amethyst mine. The area is approximately 56 km northeast of the city of Thunder Bay; the majority of specimen collecting and mining is confined to a section that measures 40 × 196 km. The amethyst-bearing veins, from 7 mm to 1.2 m wide, occur in vugs that usually range up to 3 m long. An

exceptionally large vug (1.8 × 3 × 5 m) discovered in 1968 produced a crystal 38 cm long, while the largest crystal found in the region to date measures 61 cm.

Ranging from near colorless to dark purple, the amethyst is commonly color zoned parallel to the terminal rhombohedrons, with the crystals occurring primarily in aggregates that usually display only the terminations. Small hexagonal prism faces can often be seen, but they are always poorly developed. Iron-oxide inclusions are very common, as are red inclusions that are presumed to be hematite. Although only a small percentage of the material is gem quality, many of the large crystals found in the Dzuba mine (another amethyst source) have areas of facet-grade material. It is interesting to note that on heating, the Thunder Bay amethyst turns colorless to pale brownish white, in contrast to the Brazilian material which turns bright yellow to yellow-orange.

In a brief description of the geology of the area, Elliott theorizes how amethyst was deposited. In addition to a short bibliography, he incorporates three maps and six photographs of specimens, localities, and typical inclusions.   *SFM*

Burma. V. Kumar, *Jeweler/Lapidary Business*, Vol. 6, No. 2, 1982, pp. 28–30.

Recent articles on Burma, a country that has been known for centuries as a source of some of the world's finest gems, are rare. Kumar begins this update by describing the production and marketing of gems by the government-controlled gem corporation, Maymyo, which handles all gem sales through annual auctions. The author then gives his view of the history of the "Burmese Way to Socialism," concluding that the "production of everything including gems has declined." He cites jade as an example: in the 1950s annual production was 54 tons, by the 1960s it had declined to 35 tons, and in the 1970s production was down to 1 ton. Smuggling is prevalent, and many gemstones leave the country illegally on elephant caravans that travel through the jungle.

Kumar concludes with a description of important Burmese gemstones. The world-renowned Burmese rubies have been found in three localities, the primary source being 90 miles (144 km) northeast of Mandalay near the city of Mogok (visitors are prohibited from entering this area). There is another locality in the Sagyin Hills about 10 miles (16 km) northeast of Mandalay, and a third near Pegu that was exhausted some time ago. Sapphires are found less frequently in the same localities as rubies, along with spinels of various colors.

The world's primary source of fine jadeite is in northern Burma, not far from the Chinese province of Yunnan, near the town of Mogaung. Peridot is also found in the gem-rich Mogok area; some of the stones

from this region have been exceptionally large, yielding cut gems over 200 ct.

Pearls are found in the Bay of Bengal off the southern end of Burma, with the nearest city being Mergui. Pollution of Japanese waters has helped create a shortage of pearls, thus making Burmese pearls more significant in the world market.

Topaz, zircon, chrysoberyl, tourmaline, and other gemstones are commonly found in the gravels of Burma. Although the government has recently loosened its hold on commerce and industry somewhat, it will undoubtedly maintain firm control of gem mining and marketing. Consequently, the gem production of this country will probably remain static for some time.
                                                     SFM

The Pailin ruby and sapphire gemfield, Cambodia. E. A. Jobbins and J. P. Berrangé, *Journal of Gemmology*, Vol. 17, No. 8, 1981, pp. 555–567.

This article is based on the authors' visit to the Pailin gemfield in western Cambodia and their subsequent laboratory work. In the first section, they discuss the geology of the area: the gem deposits are located in basalt bodies that were intruded into fault zones during the Himalayan orogeny of Tertiary times. A thin-section study of these basalt bodies shows them to be porphyritic with a groundmass of analcime and feldspar and phenocrysts of augite, olivine, and feldspar. Since very few gem minerals were found in the primary rock, Jobbins and Berrangé conclude that there was sparse distribution in these rocks, with later concentration the result of weathering and erosion, notably by rivers. Additional work has led the authors to theorize that minerals such as corundum, clinopyroxene, garnet, and spinel were originally formed at a great depth by metamorphism and/or metasomatism and then intruded rapidly with the basic magmas at a later date.

In an interesting section on the gem minerals of this region, the authors point out the virtual absence of colorless, yellow, and green corundum, and describe the color range found in the rubies. A detailed map locates the numerous occurrences in this region. The last two sections report on the various methods of working the deposits as well as the marketing and cutting of the gemstones. The article concludes with the comment that a substantial proportion of the stones produced in Cambodia were being heat treated and cut in Pailin and Bangkok.   *GSH*

The resplendent isle. E. J. Kahn, Jr., *GEO*, Vol. 4, No. 2, 1982, pp. 18–27, 114, 115.

This article is a beautifully illustrated source of general information about the island nation of Sri Lanka. Unfortunately, the author mentions Sri Lanka's gem industry only briefly before turning to some of the country's other industries (tourism and agriculture). He also

presents an overview of Sri Lanka's history, current government, and contemporary social problems. This article would be of interest to anyone seeking general information about this country or planning to visit it. *ET*

Thunder egg deposits of the Wycarbah district, Central Queensland. J. R. Kay, *Queensland Government Mining Journal*, Vol. 82, No. 969, 1981, pp. 566–579.

This article details the gem deposits at the Mount Hay Gemstone Tourist Park southwest of Rockhampton, Queensland, Australia. The material mined from these deposits is given the name *thunder egg*, a term first assigned by the American Indians to the small geode-like bodies of chalcedony or opal that weathered out of the welded tuff of central Oregon.

The author hypothesizes that the formation of the thunder eggs begins with a very viscous acid lava containing microscopic features such as gas bubbles, inclusions, or phenocrysts, which act as nuclei from which crystallization occurs outward in all directions. When the sphere reaches maximum size, a layer of amorphous material forms and prevents further growth except by distention. If the lava contains a high proportion of volatile content, the spheruloids become distended and hollow, thus allowing the still-fluid magma to enter and fill, or partially fill, the cavity. This process is illustrated by a series of drawings.

After solidification of the magma, mineral-bearing fluids deposit minerals such as quartz, chalcedony, or calcite. The final step, deep weathering, enables the easy removal of the spheruloids from the host rhyolite.

In addition to this extensive explanation of the formation of thunder eggs, the author presents the geologic setting of the area and describes the deposit. *GSH*

JEWELRY ARTS

Bob C. Stevens' collection of Chinese snuff bottles. R. Kleiner, *Arts of Asia*, Vol. 12, No. 1, 1982, pp. 61–64.

This article features part of the snuff bottle collection of the late Bob C. Stevens, author of *The Collector's Book of Snuff Bottles*. Color photographs of 15 unusual snuff bottles from the Stevens collection illustrate the article. Each bottle is unique; some are outstanding examples of a particular period, some illustrate an artistic technique, and others are noteworthy because they are made of unusual or rare materials.

Figure 10, a carved coral bottle, is unique because of its age. Although most snuff bottles made of gem materials (such as coral, turquoise, malachite, and aquamarine) were manufactured in the late 19th or

early 20th century, this bottle is attributed to the 18th century on the basis of quality, style, and the color of the material.

Figures 5 and 6 are of the finest quality overlay glass. The small size of the snuff bottle made it an ideal medium for this type of glass. Figure 6, a striking bottle modeled in the form of a cabbage, illustrates the technical skill and imaginative use of material possible with an overlay glass.

Stevens was particularly interested in snuff bottles made from unusual materials. The examples pictured here are of bronze, glass, nephrite, jadeite, agate, coral, fossiliferous limestone, amber, pottery, and even mammoth tooth.

This interesting and informative article with its excellent photographs appears in an issue of *Arts of Asia* that emphasizes snuff bottles in the advertisements as well as in four other articles. *ET*

Optical qualities of carved gemstones. H. Hunt, *Metalsmith*, Vol. 1, No. 4, 1981, pp. 38–41.

This is the first of a three-part series focusing on the unique way that carved stones affect light. This first article is primarily a statement of the author's strong opinions about the visual aesthetics of carved gemstones. Since the carved form is Mr. Hunt's speciality, his bias is understandable. However, his assertion that "there is virtually no way a faceted stone can be satisfactorily integrated into a design" will certainly alienate most jewelry designers and stone faceters. Dogmatism of that sort invites vigorous protest.

The description of the optical effects relates the material and the particular carving form to the resulting play of light and color. Mr. Hunt explains how planned thickness variations and surface texturing develop these effects. Several black-and-white photos give at least a partial illustration of the principles. The discussion of the optics is handled in a loose, nontechnical manner. *BFE*

Optical qualities of carved gemstones: basic tools and techniques. H. Hunt, *Metalsmith*, Vol. 2, No. 1, 1981/82, pp. 19–22.

In the introductory section of part two of this series on carved gemstones and light, the author points out how innovations from the industrial sector, along with the development of diamond abrasives and the increased knowledge of crystal optics, have created new possibilities for the lapidary arts. The bulk of the article summarizes the tools and techniques used in the three basic stages of carving: sawing, grinding, and smoothing.

Sawing blocks out the general form of the carving. For most sawing jobs, Mr. Hunt recommends the silicon carbide separating discs used by jewelers. A small diamond saw may be handy for delicate materials, unusual cuts, and increased speed.

The grinding phase firms up the elements of the design. For lapidary work, the abrasives in the grinding wheel should be bonded by a relatively soft agent. The author recommends the Mizzy wheel. He also mentions the unsuitability of wheels designed to grind metal. Diamond points are used for the final grinding and detailing.

Smoothing, which precedes the final polishing, is the most tedious stage, but it is especially important for the proper execution of transparent carvings. A sequence of diamond grits embedded in certain woods or plastics reduces the scratch pattern from coarse to superfine. Various grades of silicon carbide sandpaper on boards and rods are also mentioned as suitable for smoothing opal, quartz, and moonstone carvings.

Toward the end of the article, Mr. Hunt emphasizes the importance of mastering the basic techniques before moving on to fancy tools and methods. Also, he briefly mentions the different responses of various gem materials to the three stages of carving, including 14 photographs to illustrate the tools and their uses.

BFE

Optical qualities of carved gemstones: carving characteristics. H. Hunt, *Metalsmith*, Vol. 2, No. 2, 1982, pp. 14–17.

In the final installment in this series of articles on carved gemstones and light, the author describes how specific gem materials cause certain effects in carved forms. To demonstrate a relationship between color and form, the author explains how abstract forms that are adapted to the pencil-shaped tourmaline crystals exploit the strong dichroism of the stone. In fact, all the illustrations of carvings throughout this whole series of articles portray abstract or geometric forms rather than pictorial forms like flowers and birds.

Other stones that Mr. Hunt discusses include aquamarine, almandite, peridot, topaz, and the varieties of quartz. He mentions the specific advantages and drawbacks one may encounter in these materials during the carving stages. The closing section of the article explores some of the carving possibilities for synthetic materials.

There are some errors in terminology that may be confusing. Concerning the heat treatment of aquamarine, for example, the author refers to a "blue of about the same hue as the original green." Perhaps he meant to say tone instead of hue? In another instance, almandite is classified as a variety of garnet. He also refers to "veils of tiny bubbles" in topaz. Maybe this should translate to "patterns of two-phase inclusions"? These gemological slip-ups aside, one can still acquire from these articles a heightened awareness of the creative potential in the carved form.

BFE

Thai mother-of-pearl. S. Fraser-Lu and S. Krug, *Arts of Asia*, Vol. 12, No. 1, 1982, pp. 107–113.

This article reviews an exhibit of mother-of-pearl inlaid objects on view last year at the National Museum in Bangkok, Thailand. The exhibit showcased approximately 200 objects, most of which were fashioned during the 19th century, when the art of mother-of-pearl inlay was at its height. It was popular in Thailand at that time to decorate doors, windows, and furniture with inlaid mother-of-pearl, as well as many different containers for household and ceremonial use. These latter vessels were constructed of rattan or wood covered with a thick layer of lacquer and then inlaid with *hoi fai*, or flaming mother-of-pearl, a variety of shell that has a deep luster of pink and green reminiscent of fire opal.

The lavish designs of the inlay follow traditional Thai ornamental motifs, incorporating foliage, animals both real and imaginary, and various deities intermingled in complicated patterns. A Chinese influence can occasionally be detected in some of the subtler designs and in scenic panoramas.

The use of mother-of-pearl to give a feeling of depth and dimension by the subtle arrangement of the shell can be seen in the 16 photographs included. The artisans also cleverly incised the mother-of-pearl to form facial expressions. The screens and panels were the highlight of the show and represented the art of mother-of-pearl inlay at its finest.

Elise B. Misorowski

The utilization of diamond powder—optimum abrasive for the lapidarist. B. A. Cooley and H. O. Juchem, *Indiaqua*, Vol. 30, No. 3, 1981, pp. 105–108.

In part 2 of a series of articles, the authors investigate the use of diamond abrasives in a country with high labor costs; Idar-Oberstein, Germany, one of the largest colored-stone cutting centers in the world, is the example presented. In addition to faceted stones, Idar-Oberstein produces a wide range of artistic articles fashioned from ornamental materials such as chalcedony, marble, lapis lazuli, jade, and the like. Here, the development of specialized cutting equipment, notably equipment that uses diamond abrasives, has increased production by decreasing cutting time, thus making mass production possible.

Diamond-impregnated saw blades are used to saw the gem materials. These blades have a good tool life, give straight, smooth cuts, and may be used to slice very thin slabs of gem material. Many of the saws being used are fully or partially automated.

Cabbing, carving, or cutting can also be accomplished on a variety of diamond-impregnated tools, which include grinding wheels, core drills, carving tips, and flat or curved laps. Polishing is the only process that does not normally use diamond abrasives. The long tool life of diamond abrasives has increased the use of automated cutting equipment. Automatic cabbing and faceting machines are very accurate and highly efficient, and they may cut up to 50 stones simul-

taneously. Twenty-eight photographs document the equipment and techniques used.

In Idar-Oberstein, diamond abrasives are not only practical for cutting hard gem materials, but they have also proved economical as an abrasive for all gem materials. *Dino DeGhionno*

JEWELRY TRADE

Mike Rapaport: prophet or pariah? J. Thompson, *Jewelers' Circular Keystone*, Vol. 153, No. 3, 1982, pp. 52–53.

Mike Rapaport, who publishes the weekly *Rapaport Diamond Report*, has become a very controversial figure on 47th Street. He began publishing his weekly price lists in August 1978, when he saw the need for demand price information. The data are compiled from many sources, including brokers from the New York diamond market, fed into a computer, and then analyzed by Rapaport. While he readily states that the price lists are merely "our opinion of the diamond market," some diamond dealers have accused him of influencing prices. It is true that people in the trade have used the Rapaport lists to guide their buying and selling. As a response to the furor caused by his lists, the Diamond Dealers Club (DDC) has now begun to issue its own price lists. Perhaps different viewpoints gained from the use of other price lists will aid dealers in drawing their own conclusions about what is going on in the trade. *LCH*

SYNTHETICS AND SIMULANTS

Erkennungsmerkmale der neuen synthetischen Rubine (Identifying characteristics of the new synthetic rubies). E. Gübelin, *Goldschmiede Zeitung*, No. 5, 1981, pp. 53–59.

Focusing on the synthetic rubies made by Kashan, Chatham, and Knischka, Dr. Gübelin describes how these "new synthetics" (manufactured within the last 14 years) can be separated from their natural counterpart. He explains that the old rules for determining natural versus synthetic rubies no longer apply and suggests methods of separation based on color, inclusions, reaction to ultraviolet radiation, and absorption spectra.

The emphasis is clearly on inclusions, with 41 fine colored photographs demonstrating typical and confusing inclusions found in synthetic rubies (37 Kashans and 4 Chathams). Describing them as "feathers," "veils," and "net or lace-like fingerprints," he reports that these inclusions have been identified as kryolith (Na_2AlF_6) by X-ray analysis.

Other highlights of the inclusions section are:

1. Fine, "cloud-like" or "hair needle" inclusions are among the most difficult to find and recognize. Some look like rutile needles, but thus far they have been too small to permit analysis. These inclusions are seen best in dark-colored stones; fiber-optic lighting is essential.

2. Fine, well-formed needles of varying lengths appear in the synthetics singly or in groups, and may occur in one or several directions in a plane. This occurrence was formerly used as proof of natural origin!

3. The straight (and sometimes bent) parallel growth striations cause the most confusion in the products of Kashan, because they disappear with the slightest movement of either the microscope or the stone. They resemble the curved striae in the Verneuil synthetics and are easily separated from the lamellar twinning of the natural stones, because the twinning planes extend deep into the stone while the synthetic growth striations disappear with the raising and lowering of the microscope tube.

4. Knischka rubies, not yet available on the market, show clouds of rutile-like needles, negative crystals, two-phase inclusions, and three- to six-sided metallic platelets of silver or platinum.

The author also notes that light red and rose-red stones (which contain titanium) fluoresce more strongly when exposed to ultraviolet radiation than the darker red stones. X-ray fluorescence varies from strong to very strong red and shows some phosphorescence. The phosphorescence, although noticeable, lasts only 3 to 5 seconds; while not intense, it does indicate synthetic origin.

A difference between the synthetic rubies and the natural stones is spectral transmission in the blue region between 465 nm and 478 nm. This characteristic, though not alike in all synthetics, is visible with the gemological spectroscope. In addition, the spectrophotometer shows transmission between 250 nm and 400 nm with a maximum at 335 nm. *BJT/KNH*

Synthetics: in the beginning, there were "reconstructed rubies." E. Tucker, *Jewelers' Circular Keystone*, Vol. 152, No. 9 (Part II), 1981, pp. 84–90.

In this article, Ms. Tucker traces the development of man-made gem materials (primarily synthetic) from the myth of reconstructed rubies to the manufacture of synthetic cubic zirconia. Synthetic growth is categorized by decades from the 1930s through the 1970s, with the exception of diamond simulants, which are discussed in a separate section. Tucker's survey of synthetics demonstrates the advances in technology and the increased sophistication of methods and materials used to simulate natural gemstones. Colored graphics in the article illustrate the changing methods used to manufacture synthetic gemstones. By placing synthetic development into a historical framework, Tucker provides a neat summation of man's attempt to synthesize natural gemstones. *JMH*

GEM AND JEWELRY FACT SHEETS

Edited by Gloria Giunta Ross, 38 pp. with quarterly supplements, American Gem Society, 2960 Wilshire Blvd., Los Angeles, CA 90010, 1981. US$25.00 AGS member, US$35.00 nonmember*

This is an attractive and informative book for the jeweler who may or may not be a gemologist.

The book is printed in red and black on heavy gray paper. The loose-leaf three-ring binder has card-stock index dividers for ready reference. Individual stones are discussed separately on easily removable pages; this is especially helpful when preparing a lecture or an in-store sales meeting. While referred to as a book, the work really is the beginning volume of a service, since updated material will be added quarterly to keep subscribers current on developments in the marketplace.

Basic gemological information is given on 26 of the most commercially popular gem materials. The information includes sources, market, substitutes, synthetics, history and legends, and, most importantly, precautions that should be observed when handling or cleaning the gem. Listings of the various treatments to which gems may be subjected should provide a handy reminder that such practices are quite common today.

Metal-testing techniques are explained in a two-page section. The Tables and Charts section includes birthstones, wedding anniversaries, the relative hardness of commonly encountered gem materials and metals, weights and measurements, diamond simulants and their common trade names, ring sizes and their equivalents in other countries, and the formulas for estimating weights of round and fancy-shape gemstones.

Although the book contains no new information, it does consolidate often-needed information in a convenient form. The book is well suited to people who have little or no gemological training but who need enough product knowledge to make effective sales presentations. It could also serve as a quick refresher for gemologists. A particu-

BOOK REVIEWS

larly interesting feature of the book is that it does not include information about gem identification or separations; this seems to be a wise editorial decision, since nongemologists sometimes get themselves into trouble with testing information. Essentially, the book presents basic, general production knowledge to be used in retail selling.

Whether the service is worth the subscription price will depend largely on the quarterly supplements. The first two supplements have been received by the reviewer. They contain up-to-date information condensed from numerous trade sources and publications, and cover a wide range of subjects, including current market conditions, price trends, sales tips, fashion modes, and the treatment and detection of treatment in gem materials. Most articles that are condensed from other publications are referenced, giving the name and date of the publication so that further information can be located easily.

The editor, Gloria Giunta Ross, a graduate gemologist, has been associated with AGS since 1975 and has written many of their consumer information brochures and other jewelry education materials.

J. B. STREETER
Special Advisor, GIA

THE CAMBRIDGE ENCYCLOPEDIA OF EARTH SCIENCES

Edited by David G. Smith, 496 pp., illus., Crown Publishers, New York, NY, 1982. US$35.00*

Editor David G. Smith presents in a single volume a logically laid out, general review of the major subjects of earth science investigation.

The book is divided into six main parts: The Earth Sciences in Perspective, Physics and Chemistry of the Earth, Crustal Processes and Evolution, Surface Processes and Environments, Evaluation of Earth Resources and Hazards, and Extraterrestrial Geology. Each of these sections is in turn subdivided into one or more chapters, for a total of 27 chapters. The text is complemented by an excellent glossary and a list of additional reading that is broken down by chapters. A thorough alphabetical index completes the volume and puts specific subjects at the fingertips of the reader. The book is beautifully illustrated, with over 500 first-rate color and black-and-white photographs, tables, line drawings, and maps that serve to further elucidate the various geologic principles described in the text.

The volume also contains a great deal of up-to-date information, such as the volcanic eruption of Mt. Saint Helens in western Washington state and current information on the subject of plate tectonics.

In spite of the book's high quality and precisely conveyed information, it must be considered of limited value as a gemological reference. In the text, virtually no information is given on specific gemological topics and, with the exception of one polished section of Baltic amber containing a fly, no fashioned gem materials are illustrated.

With its easily understood text and the high quality of the illustrations, however, this book is an excellent source of readily available information for both the amateur and professional earth scientist. In addition, gemologists, with or without a strong background in earth science, who desire to learn more about the geological processes that produce gems will enjoy and benefit from reading *The Cambridge Encyclopedia of Earth Sciences.*

JOHN I. KOIVULA
*Senior Staff Gemologist
GIA Gem Trade Laboratory, Inc.
Santa Monica*

**This book is available for purchase at the GIA Bookstore, 1735 Stewart Street, Santa Monica, CA 90404.*

GEM NEWS

Stephanie Dillon, *Editor*

DIAMONDS

Belgium/Sri Lanka. The Belgian Administration for Development Corporation is joining with the government of Sri Lanka to establish a diamond cutting and polishing operation in Sri Lanka. Belgium plans to arrange for the import and export of the stones and will provide equipment and technical knowledge. Sri Lanka's contribution will be the land, labor, and plant for the joint venture. The product will be traded through a new sales center to be opened in Antwerp.

COLORED STONES

Brazil. Jack Lowell, of the Colorado Gem and Mineral Company, reports that some good-quality cat's-eye emeralds are being found in the region of Itabira, Minas Gerais, Brazil. Also noteworthy are some very fine greenish blue tourmalines that are being produced near Taquaral, Minas Gerais, as well as the recent mining of some fine, cutting-quality brazilianite.

Pakistan. Dr. Edward Gübelin has provided some additional notes regarding his contribution "Pakistan Enters the Gem Scene" (*Gems & Gemology*, Fall 1981, pp. 180–181). Information he originally received on the Haramosh Valley was ambiguous: the valley does exist, and deposits of aquamarine are currently being mined there as well as on Haramosh Mountain.

In addition, the bright green material known locally as "hunzanite" and originally reported to be chrome diopside has been subjected to quantitative and qualitative analysis by means of the electron microprobe. These analyses (performed by Mr. R. Gubser with the consultation of Professor M. Weibel), in conjunction with gemological examination of the stone, proved that the material was actually the iron-poor amphibole pargasite. This "emerald"-green pargasite occurs in the limestone marbles of the Hunza Valley as an accessory mineral in paragenesis with ruby, spinel, pyrite, and phlogopite. This material is very brittle and does not lend itself to faceting.

Ruby. A new mine in Kenya is producing cabochons of fine color, described as approximating that of Burmese stones; these were first presented at this year's Basel fair.

Inasmuch as Mogok, Burma, is currently producing very few rubies, Thailand is now considered the world's primary source. Alluvial deposits at Bo Rai and Na Wong produce stones of fine quality from depths of 5 to 12 m. Rubies from Bo Rai are commonly of pigeon's blood color, while Na Wong produces deep red-orange stones. Other deposits in Chanthaburi Province produce lower-quality rubies. Bangkok sources estimate that the ruby deposits will be exhausted within 10 to 15 years.

Dr. Peter Keller, GIA's director of education, recently returned from a trip to Thailand and other gem centers around the world. He reports that in spite of political upheavals in Cambodia, numerous miners cross the border daily from Thailand to mine the Cambodian ruby deposits. The majority of the stones are taken back through Bo Rai. Dr. Keller confirmed that the heat treatment of corundum is practiced routinely in Thailand, primarily in Chanthaburi and Bangkok.

ANNOUNCEMENTS

The Walters Art Gallery—600 North Charles Street, Baltimore, Maryland 21201. Telephone: (301) 547-9000. "Egypt's Golden Age: the Art of Living in the New Kingdom" will be on display from October 27, 1982 through January 2, 1983, featuring more than 400 objects used by Egyptian people from 1558–1085 B.C. In the exhibit are jewelry, carved and decorated tools and furniture, containers, cosmetic accessories, and household ornaments. The jewelry includes beads, pendants, earrings, and rings of gold, silver, turquoise, agate, garnet, lapis lazuli, glass, and faience.

"Connoisseurship of Gems," a four-day lecture series, will be held at the Smithsonian Institution, Washington, D.C., November 7–11, 1982. Presented by internationally noted gem expert Benjamin Zucker, the program will include the assessment of gem quality, the history of gem collecting, and examination of the commercial gem market for investment purposes. In addition to Mr. Zucker's many slide illustra-

tions, those attending will also learn from seeing the famous pieces in the Smithsonian collection. Reservations can be made through the Selected Studies Program, Smithsonian Institution—Washington, D.C. 20560. Telephone: (202) 357-2475.

The Tucson Gem & Mineral Society's 29th Annual Show will be held February 10–13 at the Tucson Community Center, 260 South Church Avenue, Tucson. The featured mineral will be cerussite. Educational programs and displays will bring together gem and mineral materials

from all over the world. A gem identification booth will be supervised by a gemologist. Further information is available from the Tucson Gem & Mineral Show Committee, P.O. Box 42543, Tucson, Arizona 85733.

The American Gem Trade Association Fair and Conclave will be held February 5–10 at the Doubletree Hotel, 445 South Alvernon Way, Tucson, Arizona 85711. "Put a little color in your life" is the theme of the association's second annual show, featuring natural, colored

gemstones. There will be seminars, social events, and a business meeting of the association. Further information may be obtained by contacting Chairwoman Maureen Jones, (213) 990-2411, or Manager Don Elwood, (213) 703-8671.

Gems & Gemology welcomes news of exhibits and events of a gemological nature. Please contact Stephanie Dillon, Gemological Institute of America, 1660 Stewart St. Santa Monica, CA 90404. Telephone: (213) 829-2991.